ABSTRACT

AGHAZADEH ARDEBILI, ZAHRA. Analyses of Capacity and Response of Plate Anchors: 2-D and 3-D Modeling with Advanced Constitutive Soil Models. (Under the direction of Dr. Mohammed A. Gabr, and Dr. Shamim Rahman).

Evaluation of the uplift capacity of plate anchors in saturated soils is an important aspect of the offshore foundation of various structures. These anchors are attached to the structures through mooring lines and embedded to a sufficient depth to provide the needed pullout resistance. In most of the literature reviewed, a constitutive model such as Tresca or Mohr-Coulomb has been used in characterizing the anchor response under loading. Previous studies show that analytical and numerical methods (using Mohr-Coulomb and Tresca models) overestimate the capacity of plate anchors. There exists a need to study the anchors pull out capacity using various soil models to understand better the pullout capacity and failure mode development with the progress of deformation level. The first two parts of this study present the results of finite element simulation of a plate anchor in saturated soils (clays and sands) using different constitutive models and soil properties. Mohr-Coulomb, Modified Cam-Clay, and Soft- Soil models are used to represent the clay. Mohr-Coulomb and Hardening Soil Models are used to represent sands. The dilatancy and size effects for the plate anchors in saturated sands are investigated and discussed. The capacity factors (N_c for clays and N_q for sands) of the plate are assessed through the application of displacement control approach using the computer program PLAXIS 2D. The third part of this study investigated the failure mechanism of plate anchors using PLAXIS 3D. Different soil properties and embedment depths are considered, and the results are compared with the available experimental observations in the literature. Also, the effect of a plate's shape on the failure mechanism and break out factor is investigated. Shape factors are presented for square and strip plates at different embedment depths. The results of the 2D and 3D finite element analyses are compared, and preciseness of 2D analysis for this problem is investigated. The last part of this study investigates the effect of bad keying process of Suction Embedded Plate Anchors (SEPLA). SEPLA is a type of plate anchors, which is embedded in the seabed by using a suction caisson. The results show that, Mohr-Coulomb model considers a constant mean effective stress during shearing and yields a higher pullout capacity in comparison with

Modified Cam-Clay, and Soft- Soil models in undrained clays. Modified Cam-Clay and Soft-Soil models provide predictions that are in good agreement with each other as well as experimental data, especially for the axisymmetric condition. In sand, the results of the large deformation analyses using Hardening Soil model are in a good agreement with existing experimental data. A very good agreement is found between the results from Hardening Soil model and those from Mohr-Coulomb model at the shallow depths (H/D<4). At larger depths, Mohr-Coulomb model provides lower capacities in saturated sands. The increase in dilatancy angle increases the capacity by extending the failure zone. The effect of dilatancy angle in the shallow embedment depths and loose sands are negligible. However, this effect becomes significant at larger embedment depths and dense sands. The results show that the size effect is negligible when the friction angle is independent of stress level. When friction angle is changing (decreasing) with the stress level, the larger plate provides smaller breakout factor at a given embedment ratio. The results from the 3-D modeling indicated that the failure mechanism in sands depends on relative density and rigidity of the soil and depth to width ratio of the foundation. In the case where the plate anchor is not rotated ideally during SEPLA keying, a reduction in the final breakout factor is computed, and found to be a function of rotation of the plate.

Analyses of Capacity and Response of Plate Anchors: 2-D and 3-D Modeling with Advanced Constitutive Soil Models

by
Zahra Aghazadeh Ardebili

A dissertation submitted to the Graduate Faculty of
North Carolina State University
in partial fulfillment of the
requirements for the Degree of
Doctor of Philosophy

Civil Engineering

Raleigh, North Carolina

2015

APPROVED BY:

Dr. Mohammed A. Gabr Co-Chair of Advisory Committee	Dr. Shamim Rahman Co-Chair of Advisory Committee
Dr. Brina Montoya	Dr. Akhtarhusein Tayebali

DEDICATION

This dissertation is dedicated to

My mother Shamsi,

My dear husband, Afshin,

and

the memory of my beloved father,

Hossein Aghazadeh Ardebili (1934-2010)

You are profoundly appreciated for all of your love, supports and unflinching commitment to my career pursuit!

BIOGRAPHY

Zahra Aghazadeh Ardebili was born in Ardebil, Iran. She got her bachelor degree in Civil Engineering from K.N. Toosi University, Tehran, Iran in 2004. At the same year, she entered the graduate school at University of Tehran, Tehran, Iran, with an emphasis in Geotechnical Engineering. She worked as a geotechnical- structural engineer in consulting companies for four years, before moving to the state of North Carolina to pursue a Ph.D. in Civil Engineering at North Carolina State University. Her professional interests are on offshore structures foundations, numerical analysis and constitutive modeling of soils.

ACKNOWLEDGMENTS

I would like to express my deepest gratitude to my advisors professor Shamim Rahman and professor. Mohammed A. Gabr for their precious guidance and supports throughout my graduate life at North Carolina State University. Their advice helped me to improve my research skills and complete this research successfully. I would also like to extend my sincere thanks to my research committee members Dr. Brina Montoya, Dr. Akhtarhusein Tayebali and Dr. Min Liu for their valuable advice and supports. I would like to acknowledge my family in Iran for their love and moral supports. I would also like to give heartfelt thanks to Dr. Afshin Karshenas, who more than a supportive husband and best friend, was a part of my graduate life at North Carolina State University. I would like to give my recognition to all civil engineering department staff at North Carolina State University. I am also indebted to all of my friends at Office 402 Mann Hall for their helps and supports.

TABLE OF CONTENTS

LIST OF TABLES

LIST OF FIGURES

Chapter 1 Overview of Dissertation

1.1 Background

Plate Anchor is frequently used as an anchoring system for the structures subjected to uplift pressures such as storage tanks subjected to flooding, offshore structures, and transmission towers. They typically are fixed to the structures and embedded in a sufficient depth to provide enough resistance. The resistance of plate anchors comes from the weight of overlying soil and shear strength of soils around them. The different shapes of plate anchors are shown in Figure 1-1. These anchors can be placed horizontally, vertically or inclined.

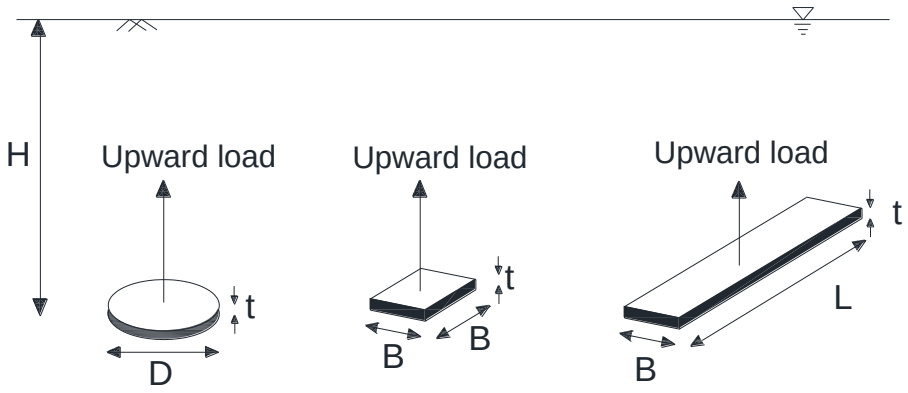

Figure 1-1 Different shapes of the plate anchor, the circular, square and strip plate anchor

Plate anchors are viewed as a foundation system for oil and gas installations in deep water depths. Figure 1-2 shows foundations evolving with increasing water depth. Evaluation of the uplift capacity of plate anchors in saturated soils is an important aspect in offshore anchoring of various structures.

In most of the literature reviewed, simple constitutive models such as Tresca or Mohr-Coulomb have been used in evaluating the plates' pullout capacity. There exists a need to study the pullout capacity of anchors using other advanced soil models and explore

differences in estimated behavior. The traditional models like Mohr-Coulomb model overestimate the capacity in the saturated clay. They do not consider the stress dependent behavior of sands. The mean effective stress has a significant effect on the behavior of sands. Some of the advanced soil models can consider this nonlinear stress dependent behavior. There exists a need to study the anchors pullout capacity using various soil models including nonlinear models to capture the behavior of soils more precisely and specify the best constitutive models for modeling the soil at this problem. There is not a comprehensive finite element study on circular plate anchors in sands to specify the effect of plate's size and the dilatancy angle at different embedment depths. Both of them have significant effects on the capacity as reported before.

Understanding the failure mechanism of plate anchors in sands is an important aspect of plate anchors design. Understanding the effect of plates shape at the failure mechanism and ultimate breakout factor in sands is an important issue, which can be investigated by 3D numerical analysis. Also, the comparison between the results from 2D and 3D numerical modeling can be a valuable study in the numerical analysis of horizontal plate anchors in sands.

Suction Embedded Plate Anchor (SEPLA) is a plate anchor installed on the seabed by using a suction caisson. Since 1988, suction embedded plate anchor SEPLA has been used as an economical and efficient foundation system in the deep water (>1500m) to response the oil and energy development on seabed resources. SEPLA uses the advantage of suction piles (known penetration depth and geographical location) and vertically loaded anchors (VLA) (lower cost and efficiency) while it avoids their disadvantages (large, heavy and costly to handle suction caissons and imprecise positioning for VLAs), (Brown 2011). The installation of the plate anchor is one of the essential aspects of the performance and efficiency of SEPLA. During the keying, anchor loses some of its embedment depth for decreasing this loss, a flap that is another rectangular plate anchor and can rotate is added to the plate anchor. Padeye for propose of connection with chain and also shank are added to the fluke or rectangular plate anchor. The configuration of SEPLA is shown in Figure 1-3 and Figure 1-4. In this mooring system, a suction caisson is used to embed a plate anchor in the seabed, which is slotted vertically into its base. The plate is placed vertically in the soil using this

caisson, and then a mooring chain attached to the plate is tensioned causing plate anchor to move and rotate until become perpendicular to the pullout direction. This process is called installation or keying. The procedure is shown in

Figure 1-5. In the majority of earlier research for SEPLA, an ideal keying procedure is assumed. During the ideal keying procedure, a plate anchors rotate until to become perpendicular to the pull out direction. In this situation, the maximum soil resistance is mobilized. In the reality, reaching to this ideal condition is not feasible always. Therefore, the effect of bad keying in which plates are not completely perpendicular to the pull-out direction is very important in considering a proper safety factor in the design of this kind of foundations. The importance of this study comes from the rapidly developing offshore energy industries.

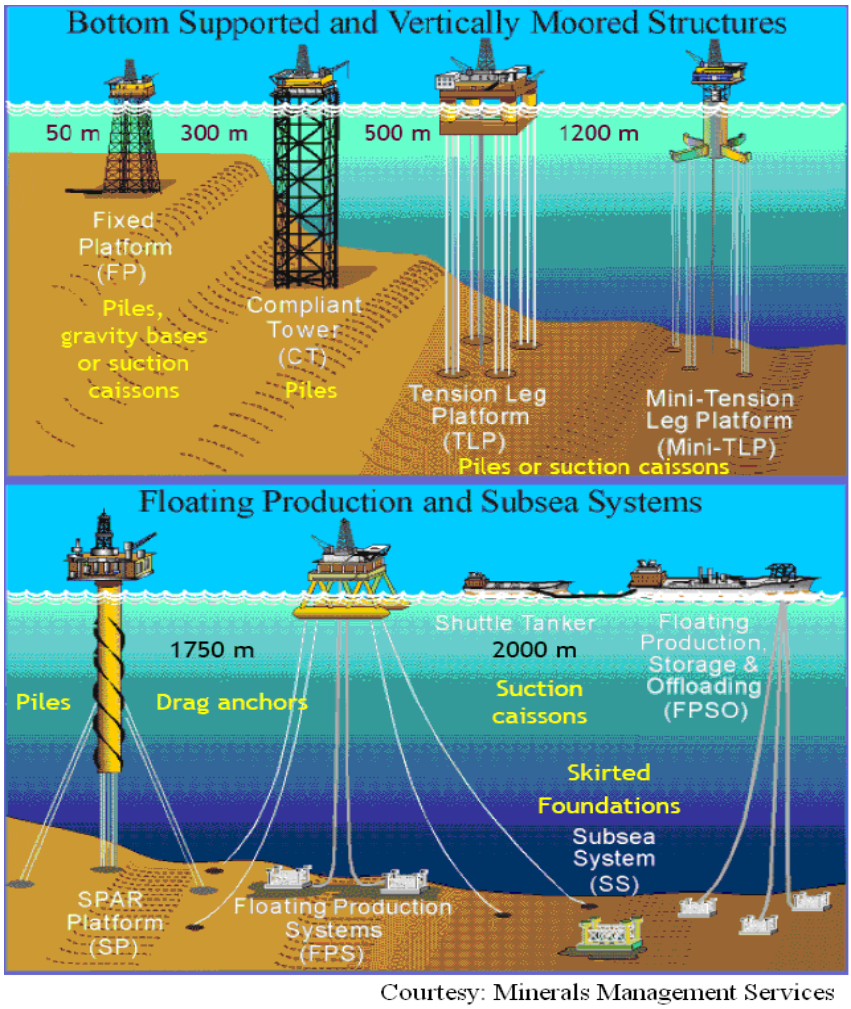

Courtesy: Minerals Management Services

Figure 1-2 Development of deepwater systems from shallow to very deep waters

1.2 Scope of Research

The main objective of this research is to investigate the response and uplift capacity of horizontal plate anchors in clays and sands, shape effect on the failure mechanism in sands, as well as the bad keying effect in SEPLA's capacity. This study will focus on the following parts:

1- Influence of the constitutive models of the soils in the plate anchors in clays and sands including influence of soil properties, embedment depth and size effect.

2- Failure mechanism of different shape of plate anchor (3D modeling) in sands

3- Influence of bad keying of SEPLA on the ultimate capacity (3D modeling).

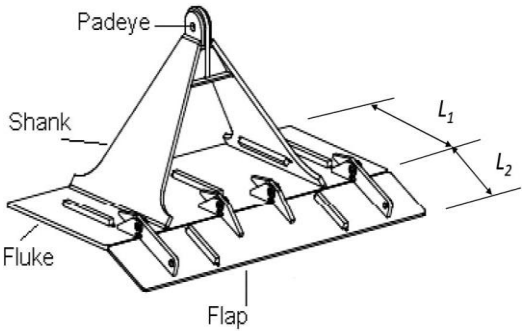

Figure 1-3 Configuration of SEPLA (Yang 2012)

Figure 1-4 Typical SEPLA (Brown, et al. 2011)

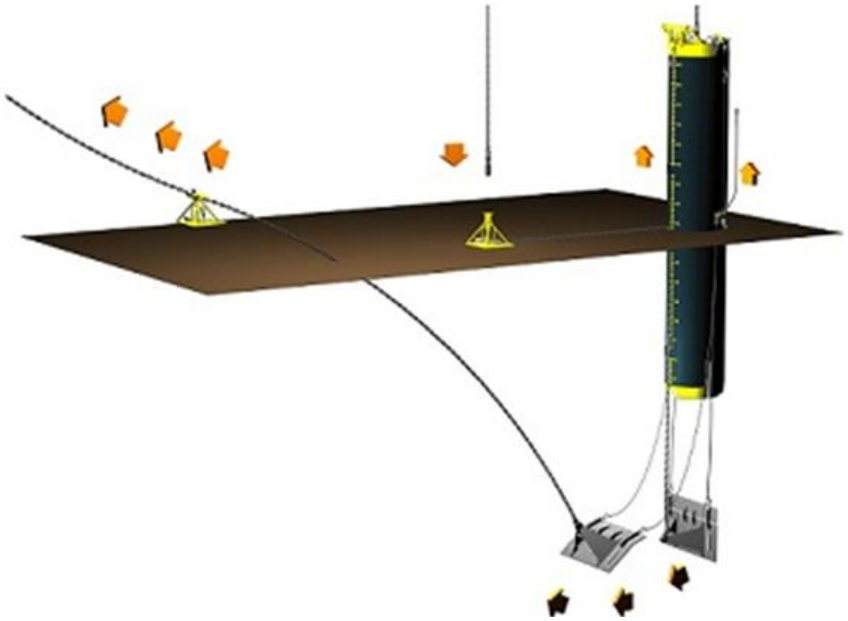

Figure 1-5 SEPLA concept suction installations, caisson retrieval, anchor keying, and mobilized anchor. (InterMoor)

1.3 Dissertation Organization

There are six additional chapters in this dissertation. Chapters 2 through 6 are papers that are published or will be submitted for publication. The author was the lead author of all the papers and responsible for organizing and writing the papers. References are presented at the end of each chapter. Chapter 7 is the summary of the main findings of this research and suggestions for future work.

Chapter 2 is an accepted journal paper. It has a complete discussion on the numerical undrained effective stress analysis of plate anchors in the clay. It includes a discusion on the effect of using different constitutive models on the capacity estimation. Three constitutive models are applied to represent the caly. They are Mohr-Coulomb, Modified Cam-Clay and Soft Soil models. The effect of different soil parameters (stiffness and strength), and embedment depths are also investigated. This paper proposes an optimized procedure for estimating the plate anchors capacity in clays. It is accepted to be published in the International Journal of Geomechanics.

Chapter 3 is a conference paper about the numerical analysis of plate anchors in clay including the total stress analysis and effective stress analysis using different constitutive soil models and plate's sizes. At this paper at the beginning, a total stress analysis using Mohr-Coulomb model is conducted, and the results are compared with existing numerical and lower bound solutions (using Tresca soil model) in the literature. Undrained effective stress analysis is conducted using three different constitutive models including Mohr-Coulomb, Modified Cam Clay and Soft Soil models and results are compared and discussed. This conference paper is published and presented at the Proceedings of the 33rd International Conference on Ocean, Offshore and Arctic Engineering, OMAE 2014, June 8-13, 2014, San Francisco, CA, USA

Chapter 4 is about the numerical analysis of plate anchors in sands. At this chapter, the differences between the results from Mohr-Coulomb and Hardening Soil models are investigated and discussed for the drained analysis of saturated sands. The effect of soil properties especially dilatancy angle, embedment depths and plate's size are investigated. This paper is ready to submit as a journal paper to the International Journal of Geomechanics.

Chapter 5 presents the 3D numerical analysis of plate anchors in sands investigating the failure mechanisms at the different sand densities and embedment depths. It investigates the shape effect including circular, square and strip plates. It also investigates the comparison between the results of 2D and 3D analyses. This chapter will be submitted as a journal paper.

Chapter 6 presents the effect of bad keying in the installation of suction embedded plate anchors. The reduction in the breakout factor, when plates are not perpendicular to the pull out direction, is investigated. This chapter will be submitted as a technical note or a conference paper.

Chapter 2 Uplift Capacity of Plate Anchors in Saturated Clays: Analyses with Different Constitutive Models

This chapter is accepted to be published in the International Journal of Geomechanics. The authors are Zahra Aghazadeh Ardebili,[1] Mohammed A. Gabr[2], and M.S. Rahman[3]

2.1 Abstract

Evaluation of the uplift capacity of plate anchors in saturated clay is an important aspect in the design of offshore foundation systems of various structures. In most of the literature reviewed, simple constitutive models such as Tresca or Mohr-Coulomb have been used in evaluating the plates' pullout capacity. There exists a need to study the pull-out capacity of anchors using other advanced soil models and explore differences in computed behavior. In addition to Mohr-Coulomb (MC) model, two other constitutive models are used herein to represent the soil behavior. These are Modified Cam-Clay (MCC) and Soft Soil (SS) models. A series of finite element analyses are performed using the three constitutive models. Undrained effective stress analyses are conducted to study the response of both strip and circular plate anchors in saturated soils. The capacities of plate anchors are assessed through the application of displacement control approach. The effective stress parameters are correlated with the undrained shear strength and dimensionless breakout factor (N_c) values from the three constitutive models are presented and compared to the lower bound solution, as well as to the data obtained from similar studies and experimental data available in the

[1] Graduate Research Assistant, North Carolina State Univ., Campus Box 7908, Raleigh, NC 27695 (corresponding author). E-mail: zaghaza@ncsu.edu
[2] Alumni Distinguished Undergraduate Professor, North Carolina State Univ., Campus Box 7908, Raleigh, NC 27695.E-mail: gabr@ncsu.edu
[3] Professor, North Carolina State Univ., Campus Box 7908, Raleigh, NC 27695.E-mail: rahman@ncsu.edu

literature. Differences resulting from the characteristics of the three constitutive models are examined and discussed.

Subject: Constitutive models; Anchors; Capacity; Finite element method; Clays.

2.2 Introduction

Plate Anchors are frequently used to support structures such as storage tanks subjected to flooding, offshore structures and transmission towers. These types of structures often induce to uplift loading and the evaluation of the uplift capacity of plate anchors is one of the important issues for robust use of these types of foundation systems. Plate anchors' uplift capacity depends on several factors including embedment depth, plate's shape and soil properties.

The behavior and capacity of plate anchors in clay have been studied over the past six decades (Kupferman 1965). These studies were mostly empirical or experimental (Ali 1968; Das 1980; Das et al. 1994; Kupferman 1965) with few utilizing numerical analyses (Rowe 1978; Equihua-Anguiano et al. 2012). The uplift capacity of a plate anchor in clay is generally reported in literature in terms of dimensionless breakout factor N_c which is a function of the above-mentioned parameters (Das et al. 1994; Merifield et al. 2003; Yu 2000).

Vesic (1965) presented an analytical solution for calculating the ultimate radial breakout stress of an embedded spherical or cylindrical cavity below the surface of a semi-infinite rigid plastic solid. Later, Vesic (1971) presented a solution for plate anchor capacity based on cavity expansion approach. In this method, the weight of soil directly above the plate anchor is added to the ultimate cavity pressure for finding the ultimate capacity of circular and strip plate anchors. Vesic (1971) compared this analytical solution with laboratory test data, performed on circular anchors, in soft and stiff clay. The results showed that the model over predicted the capacity of deep anchors.

Das (1980) proposed solutions for estimating the uplift capacity of the strip and rectangular anchors based on laboratory tests in soft clay. Das et al. (1994) performed laboratory model tests investigating the effect of suction and the presence of soft soil on a circular plate anchor pullout capacity. Rowe and Davis (1982) used finite element analyses to

determine the breakout factors for horizontal circular anchors and vertical and horizontal strip anchors. In this case, Mohr-Coulomb constitutive criterion was used for representing the soil domain. The failure load was defined as the value corresponding to an apparent stiffness of one-quarter of the elastic stiffness (referred to it as k_4 failure). Rowe and Davis (1982) showed a relatively good agreement between their k_4 failure loads and experimental data; in the case of deep anchors their results underestimated the capacity of plate anchors. Yu (2000) presented an expression for calculating the breakout factor of the strip and circular plate anchors based on an analytical solution for cavity expansion in the cohesive frictional soil. Yu (2000) assumed that soil failure occurs when the plastic zone reaches the ground surface, and there is not any outer elastic zone around the plastic flow. Merifield et al. (2003) proposed a three-dimensional lower bound solution for circular, square and strip plate anchors considering Tresca yield criterion for soil. Merifield et al. (2003)'s results showed a good agreement with the experimental data in the shallow depth range (where failure mechanisms propagate to the soil surface). Equihua-Anguiano et al. (2012) performed laboratory testing on circular plate anchors and also performed numerical analysis using Mohr-coulomb soil model under plane strain and axisymmetric conditions. Since their numerical results overestimated their experimental ones, they concluded that for better estimation of plate bearing capacity, using complex constitutive models is necessary.

In summary, Rowe and Davis (1982)'s finite element analysis using Mohr-Coulomb and assuming k_4 failure load underestimates the deep anchors capacity, Merifield et al. (2003)'s lower bound solution using Tresca yield criterion overestimates deep anchors capacity and Equihua-Anguiano et al. (2012)'s finite element analysis using Mohr-Coulomb model, overestimates the bearing capacity of plate anchors. With the utilization of advanced numerical analyses, it becomes important to understand the impact of using a given constitutive model, with the same set of soil parameters, on the estimated anchors' pullout capacity. The objective of work in this paper is to investigate the development of the vertical uplift capacity of circular and strip plate anchors using three different constitutive models: Mohr-Coulomb, Modified Cam-Clay and Soft Soil models. Analyses are conducted using the same set of parameters that correspond to the same soil properties for each constitutive model. The study is conducted using the finite element analyses PLAXIS (2012). Analyses

are performed for plane strain and axisymmetric condition at various embedment ratios *H/B* (*H/D* in the axisymmetric condition) in the range of 2-10. Analyses considered a range of effective friction angles from 15 to 30 degrees and different stiffness parameters ($\lambda = 0.1$, 0.15 and 0.2). Results are presented in dimensionless graphs and are compared with results in the literature by others.

2.3 The Constitutive Models for Soils

Several researchers have presented models depicting the constitutive behavior of soils. The five basic aspects of soil behavior are summarized by Brinkgreve (2005). He explained that a comprehensive soil model should be capable if incorporating the following aspects: (1) influence of water, (2) variable stiffness of soil (which is function of stress level, stress path, strain level, drainage conditions, and anisotropy), (3) plastic deformation, (4) strength (which is a function of loading speed, age, density, undrained behavior, consolidation and anisotropic shear strength) and (5) other aspects such as dilatancy, compaction and stress history.

For the plate anchor analyses addressed herein, the following three models are chosen: i. Mohr-Coulomb, ii. Modified Cam-Clay, and iii. Soft Soil model. These are considered appropriate for modeling soft soils, and their parameters are relatively easy to estimate and correlate with other models. A detailed description and limitations of each model was presented by Brinkgreve (2005).

2.3.1 Mohr-Coulomb (MC)

The Mohr-Coulomb model is one of the most frequently used in analyses because of the simplicity in defining its parameters. It consists of a completely reversible linear elastic stress-strain part and an irreversible perfectly plastic stress–strain part. It is defined as:

$$\tau = \sigma_n' \tan(\phi) + c' \qquad \text{Equation 2-1}$$

$$\sigma = \mathrm{E}\,\varepsilon \qquad \text{Equation 2-2}$$

τ (kN/m^2) is shear strength, σ'_n (kN/m^2) is normal stress, ϕ (°) is friction angle and c' (kN/m^2) is cohesion, E (kN/m^2) is modulus and ε is strain. The yielding functions of Mohr-Coulomb model present a fixed hexagonal cone in the principal stress space.

2.3.2 Modified Cam-Clay (MCC)

The Modified Cam-Clay model (Roscoe and Schofield 1963; Schofield and Wroth 1968; Roscoe and Burland 1968) is based on critical state theory and was developed to model the behavior of normally consolidated clays. In this model, the volumetric behavior is represented by the following logarithmic relation between the void ratio and the mean effective stress:

For isotropic compression:

$$e - e_0 = -\lambda \left(\frac{p'}{p'_0} \right)$$

Equation 2-3

For isotropic unloading and reloading:

$$e - e_0 = -\kappa \left(\frac{p'}{p'_0} \right)$$

Equation 2-4

Where, e is a void ratio, p' (kN/m^2) is mean effective stress, λ is the compression index; and κ is the swelling index. Because of the non-linear and stress (path)-dependent behavior prior to failure, Modified Cam-Clay is a reasonable model for clay and it better describes the deformation path rather than the failure behavior.

2.3.3 Soft Soil Model (SS)

The stiffness in the Soft Soil model is stress-dependent (logarithmic compression behavior) and considers primary loading, pre-consolidation, unloading and reloading situation. The failure criterion of this model is the same as Mohr-Coulomb. It uses a logarithmic relation between mean effective stress and volumetric strain (ε_v^e). The following equations define the soft soil model in the strain stress plane:

For virgin compression:

$$\varepsilon_v^e - \varepsilon_v^{e_0} = -\lambda^* \ln\left(\frac{p'}{p'_0}\right)$$ Equation 2-5

For unloading and reloading:

$$\varepsilon_v^e - \varepsilon_v^{e_0} = -\kappa^* \ln\left(\frac{p'}{p'_0}\right)$$ Equation 2-6

λ^* and κ^* are the modified compression and modified swelling indexes.

2.3.4 Model Parameters and Their Correlations

The parameters needed for developing MC model in PLAXIS are: Young's modulus (E), Poisson's ratio (ν), cohesion (c), friction angle (ϕ) and a non-associate flow rule parameter, which is the dilatancy angle (ψ).The parameters for MCC model are Poisson's ratio in unloading/ reloading (ν_{ur}), Cam-Clay compression index (λ) and Cam-Clay swelling index (κ), tangent of the critical state line (M) and initial void ratio (e_0). SS model is defined in PLAXIS by modified compression and swelling indices (λ^* and κ^*), cohesion (c), friction and dilatancy angles (ϕ and ψ) and Poisson's ratio in unloading/ reloading (ν_{ur}).

For estimating the equivalent parameters, the following equations, (Budhu 2007; Brinkgreve 2005; PLAXIS 2D Manuals 2012) are used and the parameters for each model are chosen such that they are correlated with other model parameters:

$$E' = \frac{3p'(1+e_0)(1-\nu')}{\kappa}$$ Equation 2-7

$$M = \frac{6\sin\phi'}{3-\sin\phi'}$$ Equation 2-8

$$\lambda^* = \frac{\lambda}{1+e_0}$$ Equation 2-9

$$\kappa^* = \frac{\kappa}{1+e_0}$$

Equation 2-10

2.4 Finite Element Effective Stress Analysis

A finite element model is developed in PLAXIS for analyzing the plate anchors in saturated clay. The plane strain condition is assumed to simulate the strip plate anchor, and the axisymmetric condition is used for the circular plate. Figure 2-1 schematically presents the model domains for these two conditions.

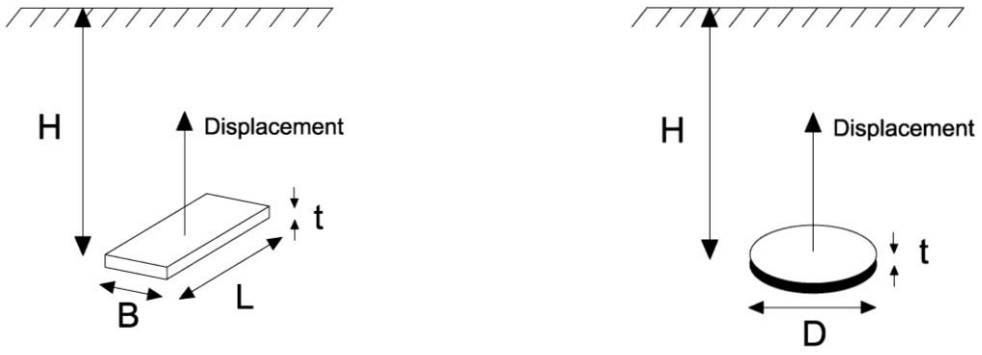

(a) (b)

Figure 2-1 Model domains (a) plane strain condition, (b) axisymmetric condition

The analyses conducted herein are displacement-controlled in which a series of prescribed uniform displacements is applied to the plate top boundary nodes and the corresponding forces are computed. The capacity at the specific embedment depth is defined as the load where the load-displacement graph becomes a plateau, or where the displacement is 10% of the plate width (diameter), whichever occurs first.

For minimizing the boundary effects, large domains are used in the FEM model ($60m \times 50m$) for plane strain and ($30m \times 50m$) for axisymmetric. The diameter of the circular

plate anchor is assumed equal to 2.76 meters (9 feet), and the width of the strip anchor is assumed as 3 meters. The thickness of the plate is considered 0.3 meters (Equihua-Anguiano et al. 2012) in both axisymmetric and plane strain conditions. The plate anchor is assumed as rigid steel with a high stiffness (Young's modulus equal to 200 Gpa). Several depth values (*H*) are considered such that embedment ratio *H/B* (*H/D* in the axisymmetric condition) is in the range of 2-10.

As explained earlier, MCC and SS models are chosen to compare the results with those from MC model. The type of analysis common to the above-mentioned models (in PLAXIS menu) is the undrained effective stress analysis using effective stress parameters. The assumed effective stress parameters are summarized in Table 2-1 Table 1.

Table 2-1 Effective Stress Parameters of Soil

Model Parameters	Assumed Amount
γ_{sat} (kN/m^3)	17
ϕ' (°)	30
c' (kN/m^2)	0
ν_{ur}	0.3
λ	0.1
κ	0.02
ψ (°)	0
e_0	0.5

Table 2-2 shows the correlated parameters of three models. These are calculated based on assumptions outlined in Table 1 and Equation 2-7 to Equation 2-10.

Interface elements are used all around the plate with a rigidity factor of R_i= 0.7, which is the ratio between the shear strength of the soil structural interface and shear strength of the soil. This value is recommended in PLAXIS (2012) reference manual for minimizing

numerical errors. It does not affect the results that much (using R_i= 0.7 gives a result, which is 0.01 less than a similar case with R_i= 1).

Table 2-2 Correlated Parameters

Model	Calculated Parameter
MC	$E = 756 * \text{depth}$ (kN/m^2)
MCC	$M = 1.2$
SS	$\lambda^* = 0.066$ $\kappa^* = 0.013$

The mesh is chosen as a cluster, which has finer elements around the plate. Figure 2-2 shows the mesh and interface elements around the plate anchor for the plane strain and axisymmetric conditions, respectively.

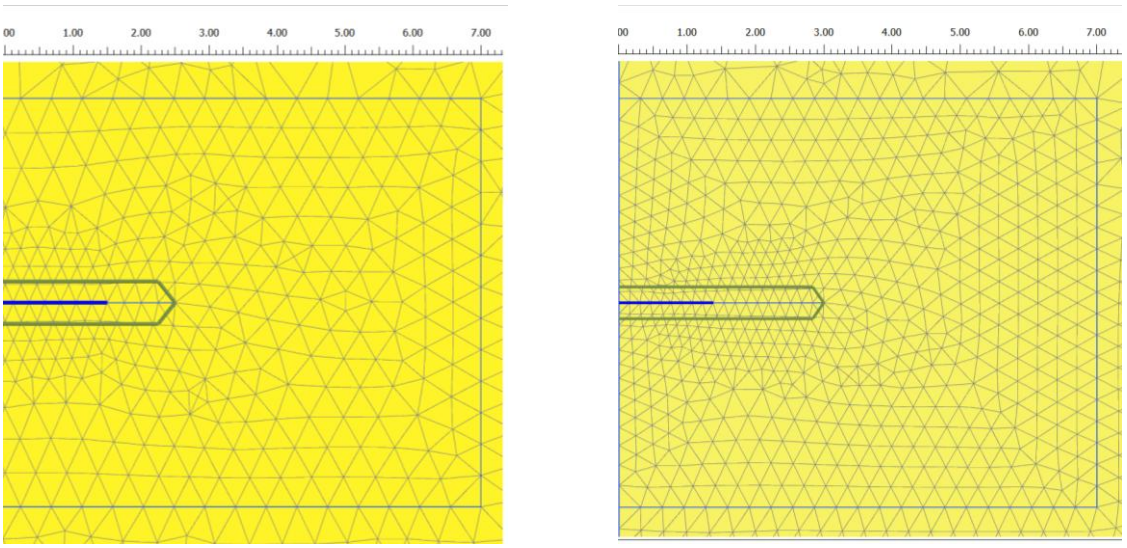

(a) (b)

Figure 2-2 Used mesh around the plate in (a) plane strain condition, (b) axisymmetric condition

Load per meter width versus displacement for plane strain condition and load versus displacement for axisymmetric condition at *H/B (H/D)*=2 and *H/B (H/D)*=7 are shown in Figure 2-3 respectively.

The load-displacement curves show the similar trends of increase in capacity with reaching an ultimate value. The dimensionless breakout factor is considered as:

$$N_q = \frac{F}{\gamma' AD} \qquad \text{Equation 2-11}$$

Where the F is pullout force (kN),

γ' (kN/m^3) is the effective unit weight of soil,

A (m^2) is the area of plate anchor,

D (m) is the embedment depth.

The results from analyses are summarized in terms of N_q factor and are plotted in Figure 2-4 for both plane strain and axisymmetric conditions.

The ultimate breakout factor for plane strain condition from using MC model is =3.84, from using SS =2.78 and from using MCC =2.17. These values for the axisymmetric condition are from using MC=4.54, from using SS=4.10 and from using MCC=4.01. For the depth range considered in this study, the MC model yields the highest N_q values. SS model and MCC model provide a relatively good agreement with each other. MCC model gives the lowest capacity in both axisymmetric and plane strain conditions.

For the axisymmetric condition, there is more similarity between the results based on the different constitutive models in comparison to those that modeled in plane strain condition. This may be due to the strain concentration at plate edges at plane strain condition. Figure 2-5 shows the strain around the plate at failure in a model with an embedment depth equal to 9 m and friction angle equal to 30 degrees; the soil is represented by MC model. The strain concentration around the plate at plane strain condition is higher than axisymmetric condition.

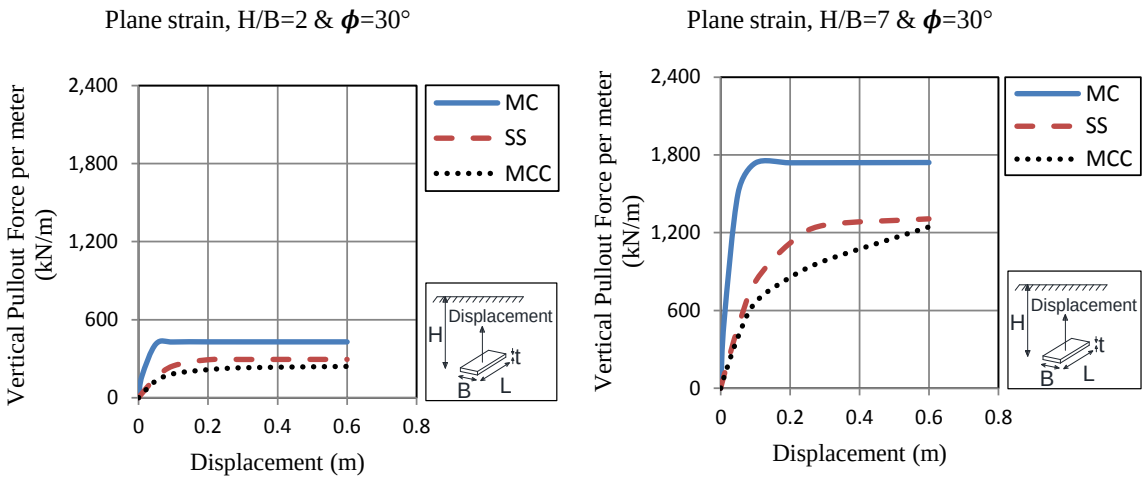

(a)

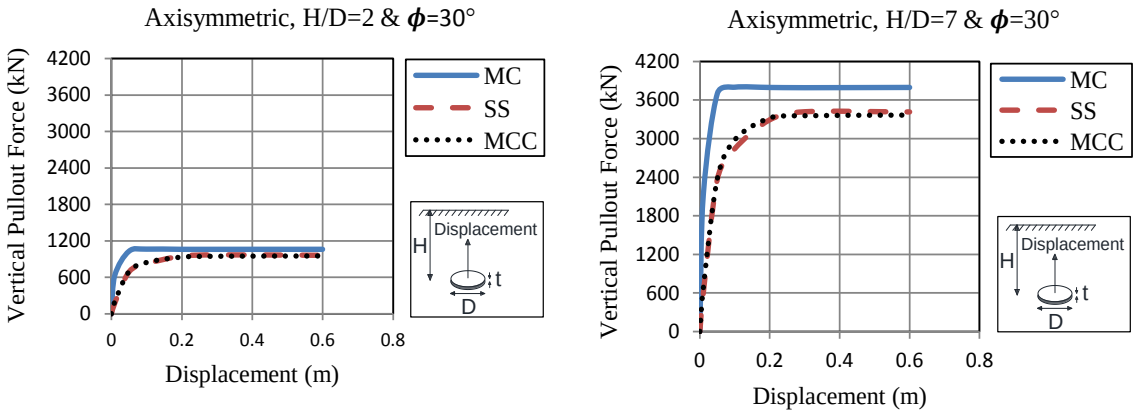

(b)

Figure 2-3 Load-displacement curve for (a) plane strain condition and (b) axisymmetric condition

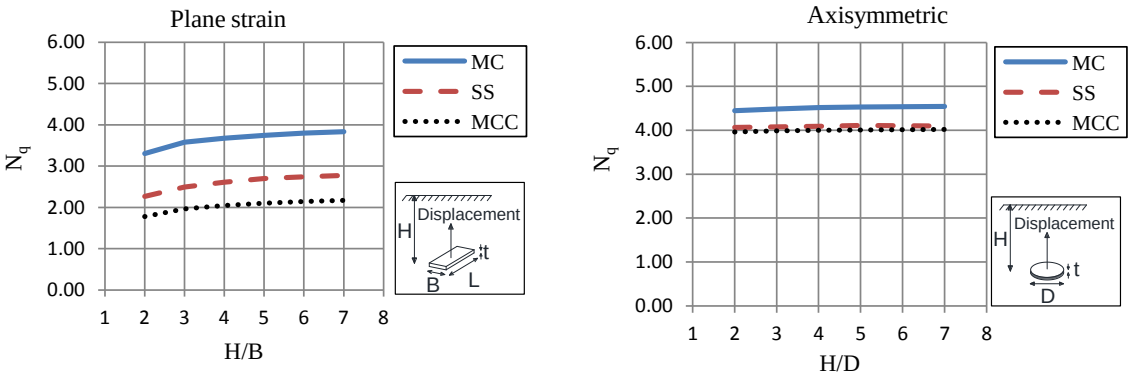

(a) (b)

Figure 2-4 Dimensionless vertical breakout factor in (a) plane strain condition, (b) axisymmetric condition

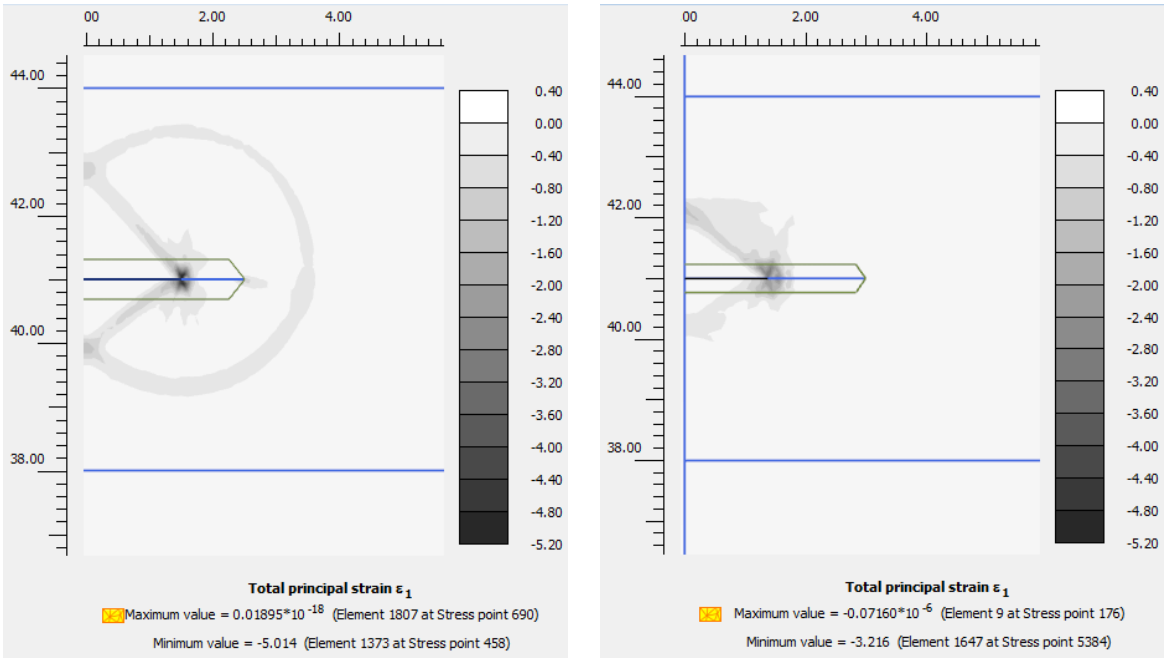

(a) (b)

Figure 2-5 Strain concentration around the plate at embedment depth equal to 9m with a friction angle equal to 30 degrees using MC model at (a) plane strain condition, (b) axisymmetric condition.

The effect of soil properties is also investigated by changing the effective friction angle while other parameters are maintained the same as Table 2-1 and Table 2-2. The ϕ' is varied from 15 to 30 degree (M from 0.56 to 1.2). Figure 2-6 shows the effect of ϕ' on N_q at the depth equal to 9 meters. In this case, the higher effective friction angle provides a higher pull out capacity and in all cases the use of the MC criterion yields a higher capacity in comparison with the MCC and SS models. The difference in results between those obtained using the MC versus the two other models increases with the increasing effective friction angle in plane strain model.

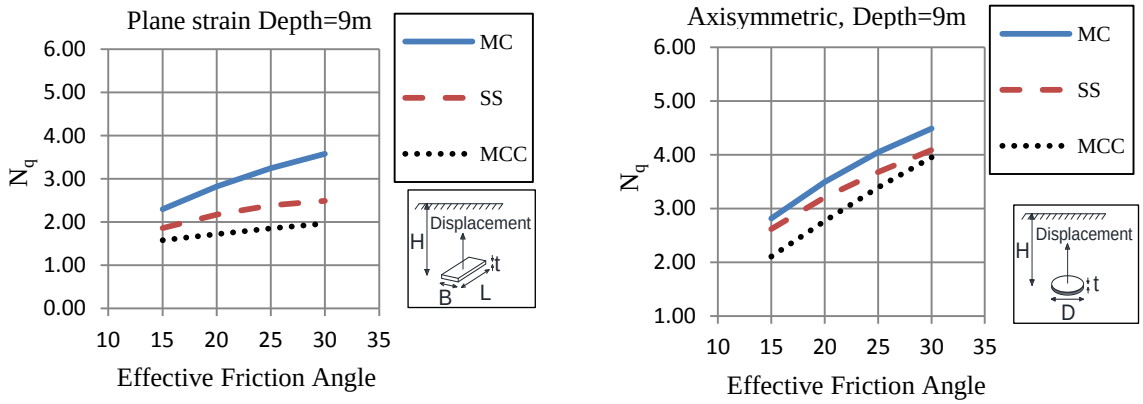

(a) (b)

Figure 2-6 Effect of friction angle on N_q in (a) plane strain condition, (b) axisymmetric condition

The effect of soil stiffness is also investigated; models for the same strip and circular plate anchors at the depth equal to 9 meters with ϕ' equal to 30 degrees are considered. These were analyzed with a different set of stiffness parameters shown in Table 2-3. In these cases, a reasonable number for λ is assumed, from Brinkgreve (2005) $\lambda = C_c / 2.3$, C_c is soil's compression index and for normally consolidated medium sensitive clays is in the range of 0.2 to 0.5 (Holts et al. 2011). Therefore λ is assumed equal to 0.1, 0.15 and 0.2 and κ is considered equal as $\lambda / 5$ (Brinkgreve 2005). The other corresponding parameters are calculated based on Equation 2-7, 2- 8 and 2-10.

Table 2-3 Different Stiffness Parameters for Investigating Stiffness Effects

Case	λ	κ	λ^*	κ^*	$E\,(\mathrm{kN/m^2})$
1	0.1	0.02	0.066	0.013	756*depth
2	0.15	0.03	0.1	0.02	504*depth
3	0.2	0.04	0.133	0.026	378*depth

The trends of load-displacement curves for these cases [Figure 2-7] show that the stiffness does not have any effect on the ultimate vertical pull out force at the range of chosen parameters. The stiffer soil (higher Young's modulus and lower swelling and compression indexes) however reaches the ultimate state at a smaller displacement.

Figure 2-8 shows the N_q values as a function of λ (compression index) according the capacity definition (as a load where the load-displacement curves becomes a plateau, or where the displacement is 10% of the plate width or diameter, whichever occurs first). Results from using the MC model show the highest N_q values for the chosen range of stiffness parameters. MC model is almost constant and is not affected by the stiffness except at the plane strain condition and at very small stiffness such that the N_q value is decreased slightly. SS model and MCC models show a reduction in N_q values in softer soils and these reductions are more significant at the plane strain condition where there is a significant strain concentration around the plate.

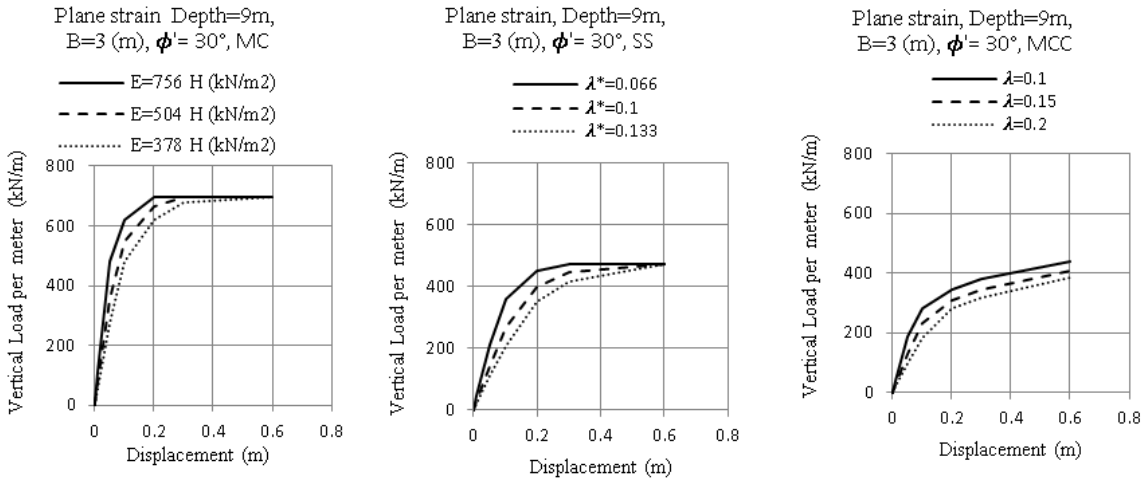

(a)

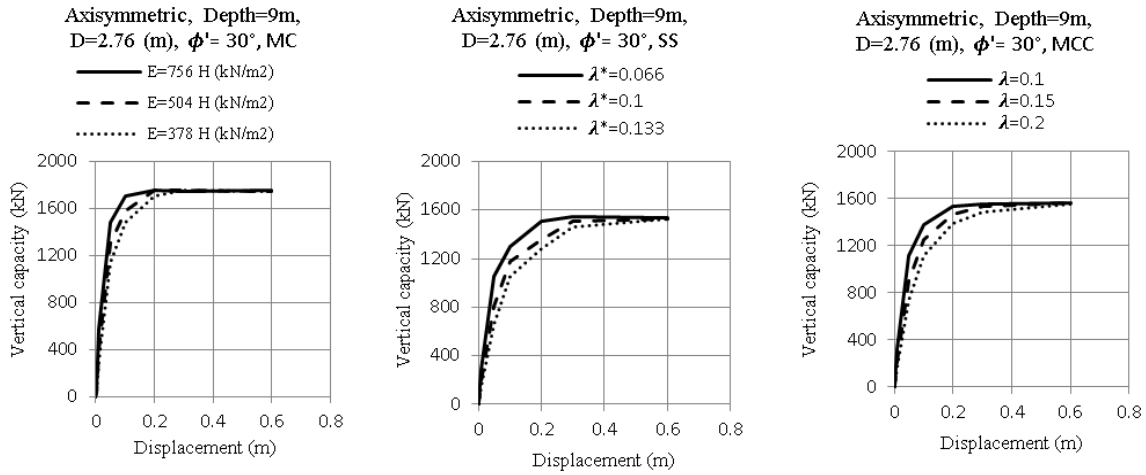

(b)

Figure 2-7 Load-displacement for different soil stiffness for MC, SS and MCC at (a) plane strain condition, (b) axisymmetric condition

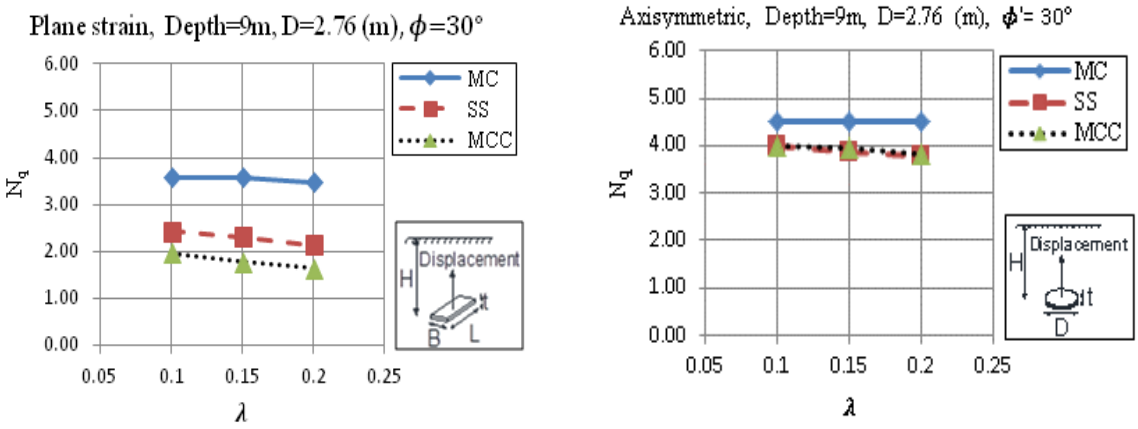

(a) (b)

Figure 2-8 Effect of soil stiffness on N_q in (a) plane strain condition, (b) axisymmetric condition

2.5 Comparative Analysis

Das et al. (1980) reported experimental results of plates' pullout capacities in the form of N_c factor:

$$N_c = \frac{F}{A.S_u} \qquad \text{Equation 2-12}$$

Where, S_u is the undrained shear strength at the face of plate anchor.

For comparing the results from this study with those from Das et al. (1980), an equivalent soil's undrained parameter is computed based on the effective stress parameter (ϕ') (Figure 2-9). The undrained shear strength parameter is calculated by using the following equation (Brinkgreve 2005):

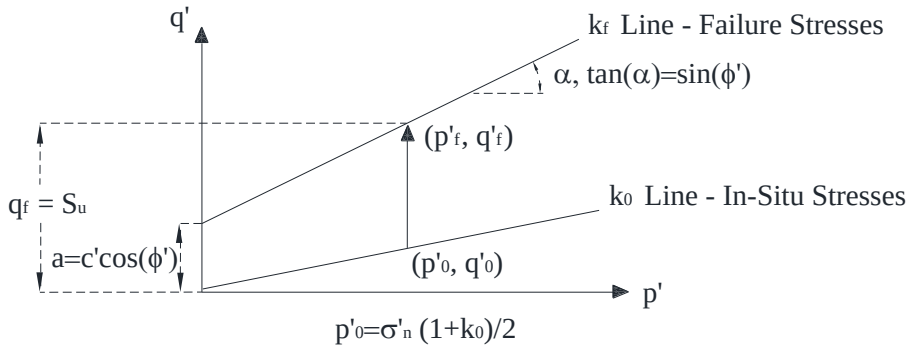

Figure 2-9 Correlation between friction angle and undrained strength

$$S_u = \sin\phi'[c'\cot\phi' + (\frac{1+K_0}{2})\sigma'_n]$$ Equation 2-13

Where, σ'_n is the vertical effective stress at the place of the plate. Accordingly, N_c is calculated by using Equation 2-12. It is noted that estimating an equivalent S_u value from Equation 2-13 necessitate that the mean effective stress remains constant during loading. This condition is satisfied when the MC model is used.

To compare the results from the three constitutive models, the same S_u value is used as an input into the SS and MCC models as well. The N_c value increases with embedment depth until an ultimate amount N_c^* at a depth termed as the critical depth (H_{cr}) is reached. For the case of shallow anchors ($H \le H_{cr}$), the failure plane reaches to the surface but in the deeply installed anchors ($H > H_{cr}$), failure plane is localized around the plate and is not affected fully by the overburden pressure anymore (Rowe 1978; Yu 2000; Merifield et al. 2003). Some of the researchers presented their results in the form of N_{c0} (weightless soil's breakout factor) without considering the overburden pressure. Therefore, for depths less than critical depth, $N_c = N_{c0} + \gamma H / S_u$ (in saturated conditions, $N_c = N_{c0} + \gamma' H / S_u$) and for depths beyond the critical depth $N_c = N_c^*$. Critical depth (H_{cr}) depends on the soil density

(higher soil density, higher capacity in the shallow depths and smaller critical depth) but N_c^* is independent of soil density. This issue was investigated by Merifield et al. (2003) and will not be further discussed herein. The ultimate value of the breakout factor N_c^* (which is independent of soil weight) is compared with results from existing numerical and experimental data. In the case of the shallow plates, the failure surface extends into the soil surface, which causes the movement of soil above the plate. The uplift resistance of the plate in this situation includes the soil's effective weight and the mobilized shear strength along the failure surface. The amount of soil moved by plate depends on the failure mechanism. Considering the failure mechanism as a cylinder, as was assumed for circular plates by Ali (1968) then this weight is almost equal to $\gamma' HA$. Therefore, it is reasonable that in shallow depths (less that critical depth) the estimates of the breakout factors N_c in this research, with $\gamma_{sat} = 17$ (kN/m^2), are higher than N_{c0} of the existing results and the differences is be equal or less than $\gamma' H / S_u$.

2.6 Comparison of N_c^* with Existing experimental data and other Approaches

Figure 2-10 shows the results of plane strain condition as compared with experimental and analytical results found in the literature.

The breakout factor for the three considered models are increasing with embedment depth until an ultimate value N_c^*=5.95 using MCC model, 7.65 using SS model, and 10.4 using MC model. The comparison shows that N_c^* from the SS and MCC models have a good agreement with the experimental data, but those obtained based on the MC model overestimate the ultimate capacity. Das (1980) data were for clay (LL=54% and PL=31%, B=38.1mm) and rectangular plate anchor $(L/B = 5)$. The value of N_c^*=7.65 based on the SS model matches well with Das (1980)'s experimental data. The ultimate breakout factor based on the MCC model covers well Rowe (1978)'s N_c^*, which corresponding to his raw laboratory data at ultimate load.

Some of the researchers [Figure 2-10(b)] proposed simplified relation for calculating the bearing capacity of plate anchors. As mentioned earlier, Yu (2000) applied the cavity expansion theory and proposed the following formula for calculating the weightless bearing capacity factor of plate anchors in clay:

$$N_{c0} = \frac{p - p_0}{S_u} = 2k * \ln(\frac{H}{B}) + \frac{2k}{1+k} \qquad \text{Equation 2-14}$$

$k = 1$ for strip plates, p is pressure on the plate and p_0 is pressure at the initial state $(= \gamma H)$. Yu (2000) assumed the pull out capacity is equal to the internal cavity pressure when the plastic region reaches to the surface. Because of such assumption, this solution cannot capture the localized failure mechanism of the deep anchors and does not reach to an ultimate amount.

The comparison shown in Figure 2-10 (b) indicates that N_c^* of SS model and MCC are relatively in good agreement with Yu (2000) at the range of embedment depth equal to $4 < H / B < 10$.

Merifield et al. (2003) proposed the following formula for the strip plate anchor ($L / B = \infty$) with an ultimate value of 11.16:

$$N_{c0} = 2.56 \ln(2\frac{H}{B}) \le 11.16 \qquad \text{Equation 2-15}$$

Figure 2-10(b) illustrates the comparison between results computed herein and those from Merifield et al. (2003)'s lower bound solution for $L / B = 5$ and $L / B = \infty$. For $L / B = \infty$, Merifield et al. (2003)'s solution increases until the limiting value of 11.16 (at $H / D > 10$, which is not shown in the figure). Merifield et al. (2003) formula provides a good estimation of the capacity at the shallow depths range but overestimates the ultimate capacity of a plane strain condition in comparison with experimental data.

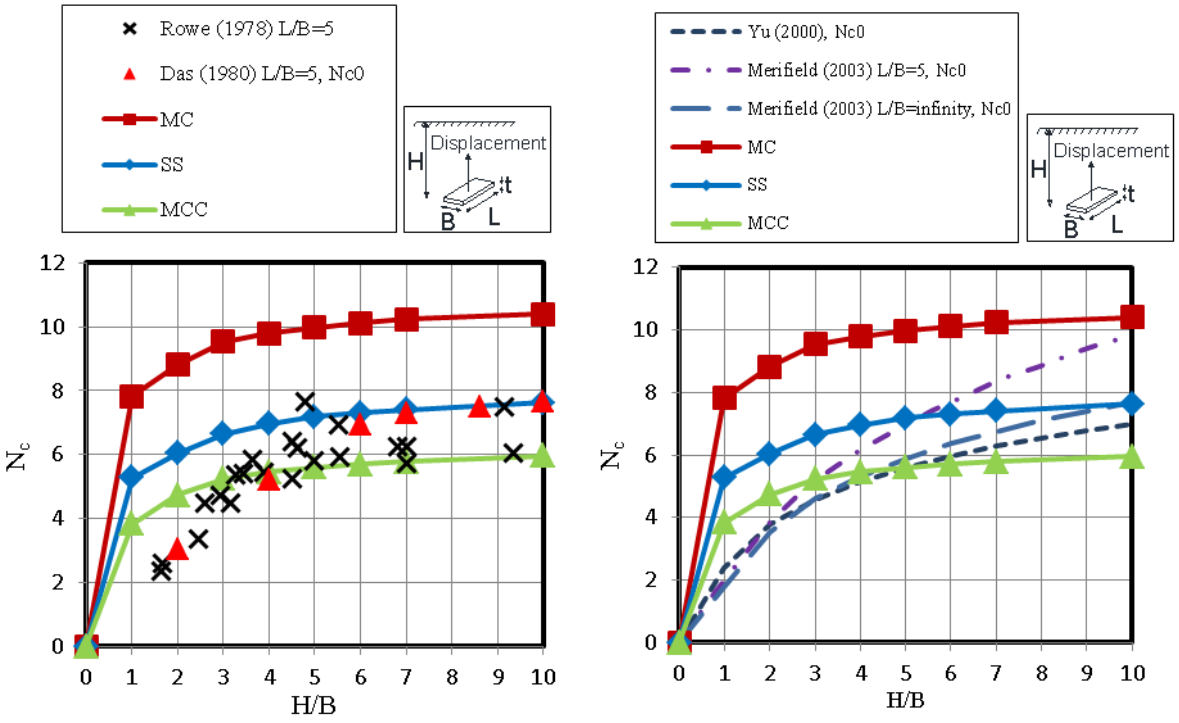

(a) (b)

Figure 2-10 Comparison of plane strain's results with (a) existing experimental data, (b) analytical solutions

Figure 2-11 illustrates a comparison of experimental and analytical results with those obtained herein from the numerical analyses for the circular plate.

The breakout factor N_c for the axisymmetric condition is found to increase at a relatively higher rate in comparison with that evaluated assuming weightless soil, with N_c^* of 10.8 when using both SS and MCC models and 12.2 when using the MC model. These values are compared with those from experimental data as shown in Figure 2-11(a).

Kupferman (1965) used Panther Creek Bentonite (LL=114.6% and PL=53.6%) and performed pullout tests on an anchor fluke with a circular horizontal projected area equal to 159.35 cm^2, and the testing was conducted vented without suction. The N_c^* based on SS and

MCC model was found to be 10.84 which is close to Kupferman (1965)'s value of 9.6, as compared to the 12.2 evaluated based on the MC model (see Figure 2-11).

Ali (1968) used soft Bentonite (LL=542%, PL=59% and w=300%) and performed tests on a smooth circular plate with 7.62 cm diameter. In his experiments, a suction force was allowed to develop between the soil and the plate. Yu (2000) and Merifield et al. (2003) used modified data of Ali (1968) to evaluate their model and introduced a correction factor for eliminating the suction effect on the estimated capacity. The ultimate breakout factor N_c^* of SS and MCC models are close to ultimate amounts of Ali (1968)'s modified data, as shown in Figure 2-11.

Das et al. (1994) used two types of clay, Kaolinite (LL=63%, PI=27%) and Montmorillonite (LL=406% and PI=372%), and an anchor with a diameter of 5.1 cm and performed a series of pullout testing. Results based on SS and MCC models yielded N_c^* equal to 10.64 and 10.84, respectively which are in good agreement with Das et al. (1994)'s value of 10.64. The result based on the MC model was 12.2, which is higher than the value evaluated by Das et al. (1994).

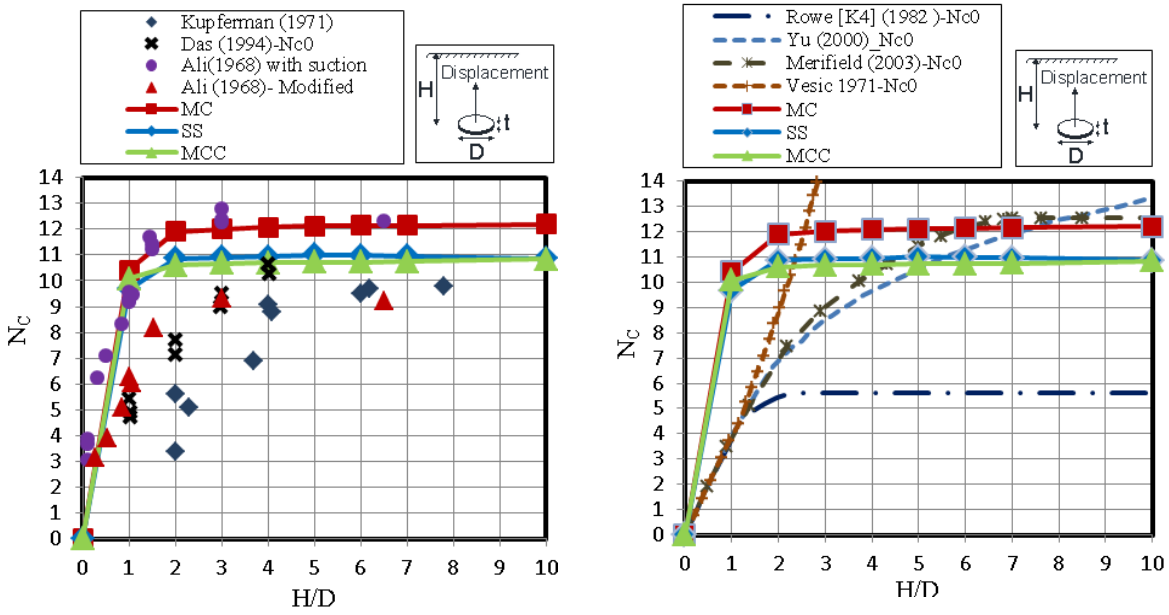

(a) (b)

Figure 2-11 Comparing axisymmetric's results with existing (a) experimental data, (b) analytical and numerical solutions

Figure 2-11(b) compares the N_c^* presented herein with those from existing analytical solutions. The cavity expansion solution by Vesic (1971) provides unconservative prediction for the deep anchors $(H/D > 2.5)$. The FEM solution with MC model (Rowe and Davis, 1982) yielded a critical depth of $H/D = 3$ and seems to be conservative for large H/D ratios. This is due to the definition of failure criterion where Rowe and Davis (1982) found that failure can occur because of the large deformation at a load less than collapse load. For these cases, Rowe and Davis (1982) defined the failure load equal to a load that corresponds to displacement equal to four times of that predicted by an elastic analysis. Consequently, they limited collapse load by this condition (named as k_4) for embedment ratio greater than about 3.

Yu (2000) proposed the same equation as strip anchor (Equation 2-15) but with $k=2$ for circular plate anchor.

$$N_{c0}=\frac{p-p_0}{S_u}=4*\ln(\frac{H}{D})+\frac{4}{3} \qquad \text{Equation 2-16}$$

As explained earlier, the results from Yu (2000) do not reach a defined constant ultimate amount. Merifield et al. (2003), using lower bound solution, provided the following equation for circular plate anchors and specified N_c^* of 12.56.

$$N_{c0}=S\,[2.56\ln\,(2\frac{H}{B})]\leq 12.56 \qquad \text{Equation 2-17}$$

In the above equation, S is the shape factor ($S=\ N_{c0\ circular}\ /\ N_{c0\ strip}$) and depends on (H/D). This shape factor is between 1.6 and 2 (Merifield et al. 2003). The N_c^* by using MC model yielded 12.2 which is similar to Merifield et al. (2003)'s value of 12.56. Both of these values are larger than the N_c^* from experimental data by Kupferman (1971) and Das et al. (1994).

In summary, comparisons with experimental data show that the SS and MCC models provide a better estimation of N_c^* values in comparison to those from MC model for both axisymmetric and plane strain conditions.

2.7 Stress Path and Development of Pore Water Pressure

To further explain differences in results using the three constitutive models, the stress path and mobilized shear strength obtained from the numerical analyses are examined. The axisymmetric condition with 9-meter depth and friction angle = 30 degrees with the same stiffness parameters at Table 2-1 and Table 2-2 is chosen for the comparative discussion. Figure 2-12(a) shows the vertical displacement and the corresponding vertical load and Figure 2-12(b) shows the stress paths obtained based on using each of the three models.

Figure 2-12(a) shows that the use of the MC model yields a higher pullout force in comparison with the SS and MCC models. The use of SS and MCC models provide results that are in good agreement with each other. Since the soil above the plate is normally

consolidated clay under compression, the computed stress path [Figure 2-12(b)] fall below the critical state line [$M = 6\,sin(\phi')/(3-sin(\phi'))$]. Figure 2-12(b) shows that in MC model, q increases with a constant p' (which is not a realistic undrained soft soil behavior) and it reaches the critical state line with a highest mobilized q in comparison with results from the two other models. SS and MCC models have more realistic effective stress trends as q increases while p' decreases until reaching the critical state line. SS model provides a q that crosses the critical state line with reaching a residual state, this is due to Plaxis limitation at the modeling the behavior of soil after the failure at this model (PLAXIS 2D Manuals 2012).

The development of pore water pressure and shear stress are presented in Figure 2-13. During the undrained effective stress analysis, the stiffness of water is added to the stiffness of soil automatically, and the final amount of the excess pore pressure is almost the same in these three models. MCC, however, yields a higher amount of deviatoric strain (note that the volumetric strain is equal to zero in all of them).

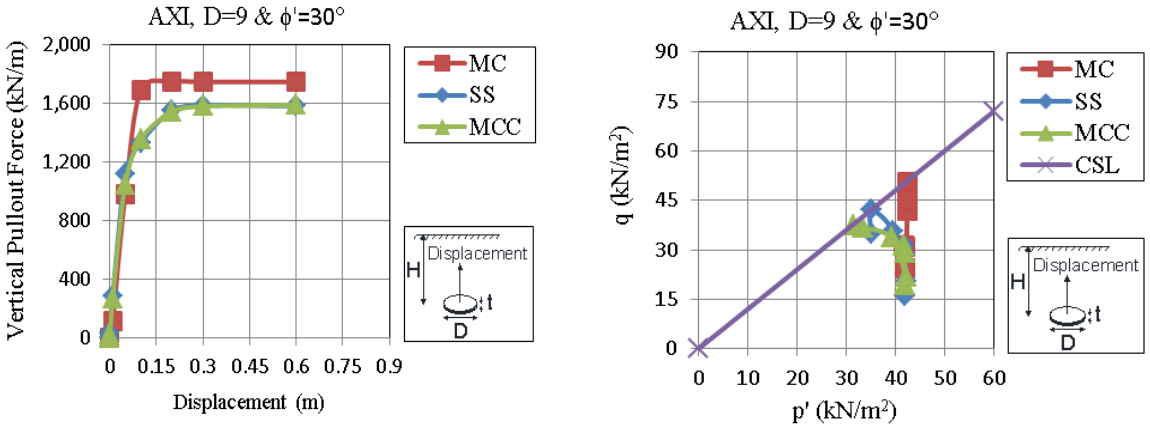

(a) (b)

Figure 2-12 (a) Load- displacement, (b) stress path and critical state line (CSL)

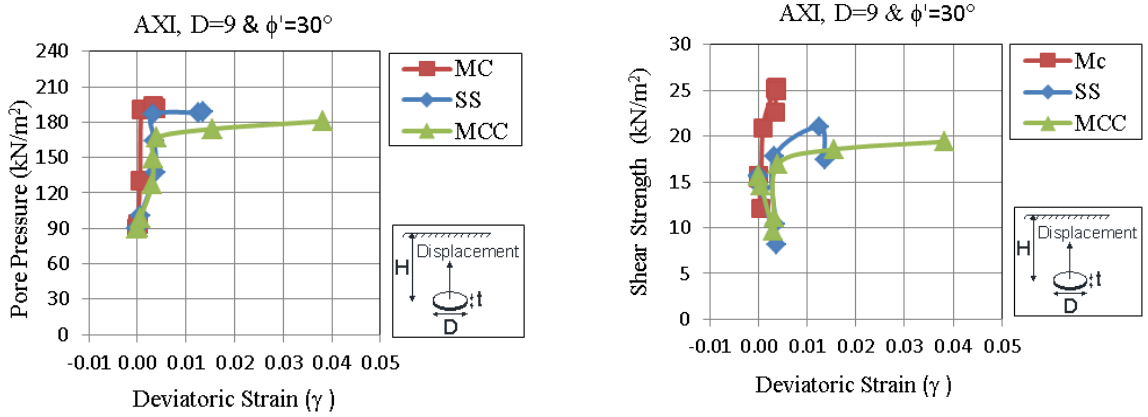

(a) (b)

Figure 2-13 (a) Developing of the pore water pressure, (b) developing of the shear strength

Data in Figure 2-13(b) show that shear resistance obtained by using MC model is the highest in comparison with SS and MCC models shear resistance. The ultimate shear strength is almost the same for SS and MCC (they have a very good agreement in the estimation of

the capacity). However, the results based on using MCC yield a higher deviatoric strain in the final state. The reason of such a higher deviatoric strain in MCC is related to the failure criteria in the MCC model. The failure in MCC occurs when the internal friction is fully mobilized, and the soil is in the state of the critical void ratio. At this state, no volume change occurs, and the deviatoric strain goes to infinity (Brinkgrave 2005). As shown in Figure 2-13(b) shear strength initially decreases and then increases. It happens due to numerical instability at the beginning of the mobilization. When the plate anchor is activated, the soil experiences a small downward deformation, by applying the upward displacement on the plate, this initial shear stress drop occurs, at a very small range of displacement, less than 0.005 (m).

Although the MC model's parameters are relatively easy to define, the model cannot capture softening aspects of soil behavior, such as variation of modulus at different stress states and the reduction of shear strength to a residual value. The use of SS and MCC models can help to overcome some of the issues of traditional MC model.

Merifield et al. (2003)'s formulas provide a very good estimation of the breakout factors in the shallow depths. For depth values beyond the critical depth ($H > H_{cr}$), Merifield et al. (2003) approach over predict the breakout factors. Therefore, it is proposed herein that N_c^* factor can be modified to the 7.65 for the strip plate (instead of 11.16) and 10.84 for a circular plate anchor (instead of 12.6). The N_c factor can then be calculated as $N_c = N_{co} + \gamma H / S_u \leq N_c^*$.

2.8 Summary and Conclusions

In this study, effective stress analyses for the uplift capacity of plate anchors are performed while utilizing MC, MCC and SS constitutive models, for both plane strain and axisymmetric conditions. The capacities of plate anchors are assessed through the application of a displacement control approach, and equivalent input parameters are used for the three different models. A series of finite element analyses are performed using the computer program PLAXIS. The results show that the use of MC model in the analysis generally yields a higher estimated pullout capacity in comparison with those from the SS and MCC models.

The SS and MCC models provide predictions that are good agreement with each other as well as experimental data, especially for the axisymmetric condition. The effective stress parameters are correlated with the undrained shear strength and the ultimate dimensionless breakout factors (N_c^*) from the three constitutive models are compared to each other and to the lower bound solution by Merifield et al. (2003). Based on the soil properties and plate dimensions assumed in this study, the following conclusions are advanced:

- SS and MCC models provide closer results to the experimental data in comparison with MC.
- Results based on the use of MC model over predict N_c. In this case, the stress paths (p' - q graphs) show that in the effective stress analysis for the undrained material, MC model considers a constant mean effective stress during shearing while soils experience a decrease in the mean effective stress in this state.
- Results based on using the MCC yield a higher deviatoric strain in the final state. The reason of higher deviatoric strain in MCC is related to its failure criterion. At MCC model failure occurs when the internal friction is fully mobilized, and the soil is in the state of the critical void ratio. At this state, no volume change occurs, and the deviatoric strain goes to infinity.
- In the case of the shallow plates, the failure surface extends into the soil surface, which causes the movement of soil above the plate. The uplift resistance of the plate in this situation includes the soil's effective weight and the mobilized shear strength along the failure surface. The amount of soil moved by plate depends on the failure mechanism. Therefore, it is reasonable that in shallow depths (less that critical depth) the estimates of the breakout factors in this study are higher than values for weightless soil reported in the literature and the differences is be equal or less than $\gamma' H / S_u$.
- It is proposed that the ultimate breakout factor in Merifield et al. (2003)'s equations are modified to 7.65 for strip plates and 10.84 for circular plate anchors. Such a modification will provide a better estimation of capacity, especially for large H/D ratios.

2.9 References

Ali, J. I. (1968). ‘‘Pullout resistance of anchor plates and anchor piles in soft bentonite clay.’’ *MSc thesis, Duke Univ., N.C.*

Brinkgreve, R. B. J. (2005). “Selection of soil models and parameters for geotechnical engineering application.” *In: Yamamuro, JA and Kaliakin, VN, editors. Geotechnical Special Publication No.128, ACSE, 69-98.*

Burland, J. B. (1965). “The yielding and dilation of clay.” *Geotechnique, Vol.15, 211-214.*

Budhu, M. (2007). Soil Mechanics and Foundations, *2nd Ed., John Wiley & Sons, Inc, Hoboken, NJ.*

Das, B. M (1980). “A procedure for estimation of ultimate capacity of foundations in clay.” *Soils and Foundations, 20 (1), 77–82.*

Das, B. M., Shin, E. C., Dass, R. N., and Omar, M. T. (1994). ‘‘Suction force below plate anchors in soft clay.’’ *Marine Georesources and Geotechnology, 12, 71–81.*

Equihua-Anguiano, L. N., Orozco-Calderon, M., and Foray, P. (2012). “Numerical finite element method and experimental study of uplift capacity anchors.” *Proc. SUT the 7th International Conference 12–14 September 2012 Royal Geographical Society, London, UK, 643-647.*

Holtz, R. D., Kovacs, W. D., and Sheahan, T. C. (2011). An Introduction to Geotechnical Engineering, *2nd Ed., Pearson Education, Inc., Upper Saddle River, NJ.*

Kupferman, M. (1965). ‘‘The vertical holding capacity of marine anchors in clay subjected to static and cyclic loading.’’ *MSc thesis, Univ. of Massachusetts, Amherst, Mass.*

Merifield, R. S., Lyamin, A. V., Sloan, S. W., and Yu, H. S. (2003). “Three-Dimensional lower bound solutions for stability of plate anchors in clay.” *Journal of Geotechnical and Geoenvironmental Engineering 129, 243–253.*

PLAXIS 2D Manuals (2012). Plaxis BV, Delft, the Netherlands.

Roscoe, K. H., and Schofield, A. N. (1963). "Mechanical behavior of an idealized wet clay." *Proc. European Conference. on Soil Mechanics and Foundation Engineering, Wiesbaden, Deutsche Gesellschaft fur Erd- und Grundbau e. V., Essen, Vol. 1, 47-54.*

Roscoe, K. H. and Burland, J. B. (1968). "On the generalized stress-strain behavior of wet clay." *Eng. plasticity, Cambridge Univ. Press, 535-609.*

Rowe, R. K (1978). ''Soil structure interaction analysis and its application to the prediction of anchor behavior.'' *Ph.D. thesis, Univ. of Sydney, Sydney, Australia.*

Rowe, R. K., and Davis, E. H. (1982). ''The behavior of anchor plates in clay.'' *Geotechnique, 32(1),* 9–23.

Schofield, A., and Wroth, P. (1968). "Critical state soil mechanics." *McGraw-Hill, p.310, London.*

Vesic, A. S. (1965). ''Engineering properties of nuclear craters.'' *Tech. Rep. No. 3-699, Rep. 2: U.S. Army Engineer Waterways Experiment Station, Vicksburg, Miss., 123.*

Vesic, A. S. (1971). ''Breakout resistance of objects embedded in ocean bottom.'' *J. Soil Mech. Found. Div., 97(9) 1183–1205.*

Yu, H. S. (2000). Cavity expansion methods in geomechanics, *Kluwer, Dordrecht.*

Chapter 3 Evaluation of Plate Anchors Capacity in Saturated Soils Using Different Constitutive Models

This chapter was published and presented at Proceedings of the 33rd International Conference on Ocean, Offshore and Arctic Engineering, OMAE 2014, June 8-13, 2014, San Francisco, CA, USA.

The authors are Zahra Aghazadeh Ardebili[1], Mohammed A. Gabr[2], and M.S. Rahman[3]

3.1 Abstract

Evaluation of the uplift capacity of plate anchors in saturated clay is an important aspect in offshore anchoring of various structures. In most of the literature reviewed, a constitutive model such as Tresca or Mohr-Coulomb has been used in analyses. There exists a need to study the anchors pull out capacity using other advanced soil models and discern differences in results. This study presents the results of finite element simulation of a rectangular or circular plate anchor in saturated clay. The capacity factors (N_c) of the plate are assessed through the application of displacement control approach and the results are compared to the lower bound solution as well as to data obtained from similar studies available in the literature. In addition to Mohr-Coulomb model, two other constitutive models are used to represent the soil deformation. These are Modified Cam-Clay, and Soft Soil models. Undrained effective stress analyses are conducted using the computer program PLAXIS. A series of analyses using different embedment depths are performed for all three constitutive models. Results as N_q value from the three constitutive models are presented and discussed.

[1] Graduate Research Assistant, North Carolina State Univ., Campus Box 7908, Raleigh, NC 27695 (corresponding author). E-mail: zaghaza@ncsu.edu
[2] Alumni Distinguished Undergraduate Professor, North Carolina State Univ., Campus Box 7908, Raleigh, NC 27695.E-mail: gabr@ncsu.edu
[3] Professor, North Carolina State Univ., Campus Box 7908, Raleigh, NC 27695.E-mail: rahman@ncsu.edu

3.2 Introduction

Plate Anchors are frequently used as a foundation system for the structures subjected to uplift pressures such as storage tanks subjected to flooding, offshore structures, and transmission towers. Precise estimation of the uplift capacity of these plate anchors is one of the important issues for the robust application of these types of foundation systems. Such estimation is based on several factors including embedment depth, plate's shape, soil properties and installation.

Merifield et al. (2003) used finite element limit analysis, and Equihua-Anguiano et al. (2012) used finite element analysis and reported N_c breakout capacity factors for plate anchors.

Merifield et al. (2003) proposed a three-dimensional lower bound solution for estimating N_c by using Tresca yield criterion for soil, while Equihua-Anguiano et al. (2012) did some laboratory tests and used Mohr-Coulomb instead of Tresca in their numerical model to do the plane strain and axisymmetric condition. Since their numerical results overestimated their experimental ones, they concluded that for better estimation of plate bearing capacity, using more complex constitutive models is necessary.

The dimensionless capacity factors (N_c or N_q) of the plate anchors herein are assessed through the application of displacement control approach in both, plane strain, and axisymmetric finite element conditions. Simulations are performed using PLAXIS with the soil considered undrained. An undrained total stress analysis by Mohr-Coulomb model is conducted and compared with the results from Equihua-Anguiano et al. (2012) and the lower bound solution from Merifield et al. (2003). In Addition, two more constitutive models, namely the Modified Cam-Clay model and the Soft Soil model are used to assess comparative solutions for plate anchors capacity by using effective stress analysis.

3.3 Theory and Formulation

During the past 60 years, researchers have tried to develop mathematical models to represent the rather complex behavior of the soils to be used in finite element analysis. The five basic aspects of "real" soil behavior were summarized by Brinkgreve (2005),

recommending that a comprehensive soil model should consider: 1- Influence of water, 2- Variable stiffness of soil (which is function of stress level, stress path, strain level, soil permeability, consolidation and anisotropy), 3- Plastic deformation, 4- Variable strength (which is function of loading speed, age, density, undrained behavior, consolidation and anisotropic shear strength) and 5- Other aspects such as dilatancy, compaction and stress history.

For the plate anchor problem addressed herein, the following three models are chosen: Mohr- Coulomb, Modified Cam-Clay and Soft Soil model. These are considered appropriate for modeling soft soils, and their parameters are relatively easy to estimate and correlate with other selected models.

3.3.1 Mohr-Coulomb Model

Mohr-Coulomb model is one of the most frequently used soil models because of simplicity in defining its parameters and good failure estimations. It consists of a completely reversible linear elastic stress- strain part and an irreversible perfectly plastic stress–strain part [Figure 3-1] with a fixed yield surface, which is independent of strain.

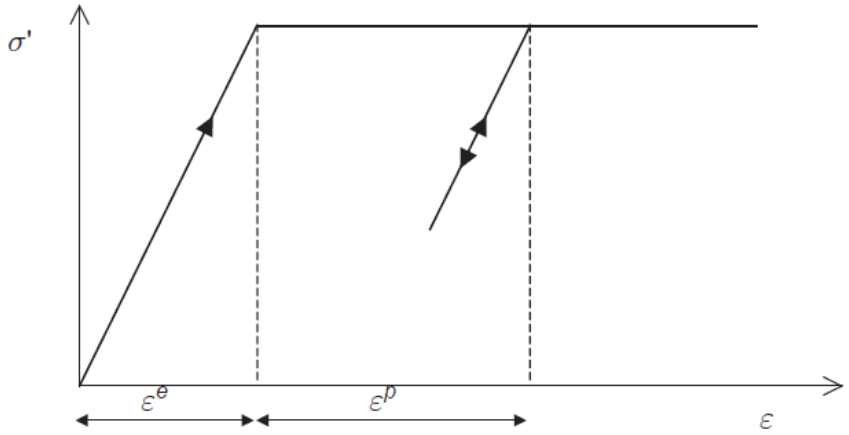

Figure 3-1 Elastic perfectly plastic model (PLAXIS 2012)

The yield functions in Mohr-Coulomb model in a three- dimensional state of stresses give a fixed hexagonal cone in principal stress space. Mohr- Coulomb model captures failure behavior well but the stiffness behavior is poorly modeled especially before reaching the local shear strength. Below the failure contour, the stiffness is linear elastic. The model considers constant elastic parameters and it cannot explain the deformation accurately before failure where the stress level is changing significantly or in the case that multiple different stress paths are followed, which may produce unrealistic results.

3.3.2 Modified Cam-Clay Model

Modified Cam-Clay model, in contrast, is based on critical state theory and was developed to model the behavior of normally consolidated clays. The volumetric deformation is represented through a logarithmic relation between the void ratio and the mean effective stress. It has linear stress-dependent stiffness, which is seen in nearly consolidated clay behavior. In this model, the hardening plasticity is used to develop the non-linear stress-strain behavior of the soft soil. Loading on normally consolidated clay results a plastic strain, which increases the pre-consolidation stress and develops the plastic volumetric straining. The failure occurs when the internal friction is fully mobilized, and the soil is in the critical state, which means no volume change will occur and the deviatoric strain increases to infinity. Figure 3-2 shows yield surface of Modified Cam-Clay model in p'-q plane.

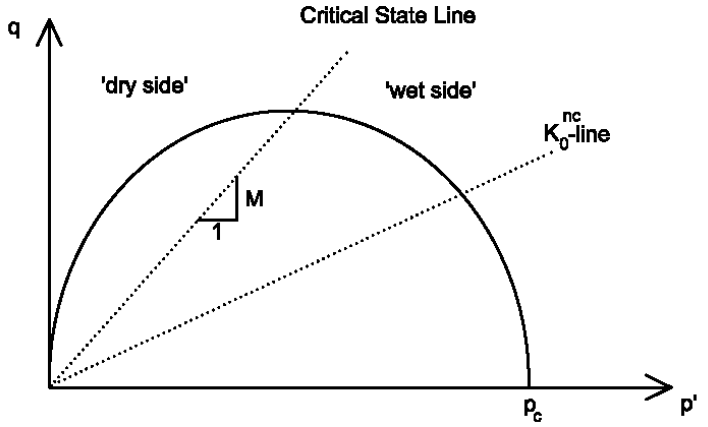

Figure 3-2 Yield surface of Modified Cam-Clay model in p'-q plane (PLAXIS 2012)

3.3.3 Soft Soil Model

Soft Soil model is applicable for material with a high degree of compressibility. The stiffness in this model is stress dependent (logarithmic compression behavior) and considers primary loading, pre-consolidation, unloading and reloading situation PLAXIS (2012). The failure criterion is the same as Mohr-Coulomb [Figure 3-3]. Soft-Soil model is based on Modified Cam-Clay model, and it improves upon issues such as over-prediction of the shear strength for over consolidated states; also Mohr-Coulomb's ability in failure is added to this model, therefore it is good in capturing failure behavior. Instead of void ratio, it has a logarithmic relation between mean effective stress and volumetric strain by modified parameters. It is a good choice for primary loading problems and it is better than Mohr-Coulomb in unloading problems. But still it can't capture the anisotropy in strength and stiffness (Brinkgreve 2005).

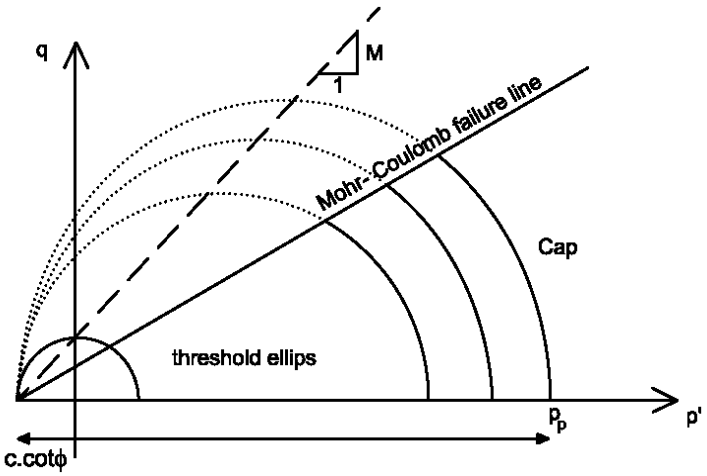

Figure 3-3 Yield surface of Soft Soil model in p'-q plane (PLAXIS 2012)

3.4 Model Parameters and Their Correlation

The needed parameters for developing the Mohr-Coulomb model in PLAXIS are Young's modulus (E), Poisson's ratio (ν), and parameters from Coulomb failure criterion:

cohesion (c), friction angle (ϕ) and a non-associate flow rule parameter, which is dilatancy angle (ψ).

The parameters needed for developing the Modified Cam-Clay model are Poisson's ratio in unloading/ reloading (ν_{ur}), Cam-Clay swelling index (κ) and Cam-Clay compression index (λ), tangent of the critical state line (M) and initial void ratio (e_0).

The Soft Soil model is defined in PLAXIS by modified compression and swelling indexs (λ^* , κ^*), cohesion (c), friction and dilatancy angles (ϕ and ψ) and Poisson's ratio in unloading/ reloading (ν_{ur}).

For estimating the equivalent parameters, the following equations are used, and the parameters for each model are chosen such that they are correlated with other models parameters:

$$E' = \frac{3p'(1+e_0)(1-\upsilon')}{\kappa} \qquad \text{Equation 3-1}$$

$$M = \frac{6sin\phi'}{3-sin\phi'} \qquad \text{Equation 3-2}$$

$$\lambda^* = \frac{\lambda}{1+e_0} \qquad \text{Equation 3-3}$$

$$\kappa^* = \frac{\kappa}{1+e_0} \qquad \text{Equation 3-4}$$

Where p' is the mean effective stress.

3.5 Finite Element Model of Plate Anchor

For analyzing a rectangular plate anchor (especially with L/B<10), a 3-D model should be used. In this study, however, we have replaced the rectangular shape by an equivalent circular one and used axisymmetric modeling for simplicity. Additionally, we have used the plane strain condition only to compare the results with those reported in an earlier study by Equihua-Anguiano et al. (2012), who has also used plane strain condition. The authors will be using 3-D modelling in their subsequent study.

The analysis conducted herein is displacement controlled with a series of prescribed displacements applied to the plate, and the corresponding force is computed. The yield or ultimate load is defined as where the load-displacement graph becomes a plateau or where the displacement is 10% of the plate width (diameter).

Figure 3-4 and Figure 3-5 present the model domains for the two conditions (plane strain and axisymmetric) used in the analyses.

For minimizing the boundary effects, large domains are used in the FEM model (60m*50m) for plane strain and (30m*50m) for asymmetric. The mesh is chosen as cluster fine elements. Dimensions of plates are chosen to be the same as in Equihua-Anguiano et al. (2012) and are summarized in

Table 3-1. For the axisymmetric condition, an equivalent circular plate anchors with the equivalent area are used.

Several depth values (H) are considered such that embedment ratio H/L (H/D_{equi} in the axisymmetric condition) is in the range of 2-10. The plate anchor is considered as a rigid steel with a high stiffness (Young's modulus equal to 200 Gpa).

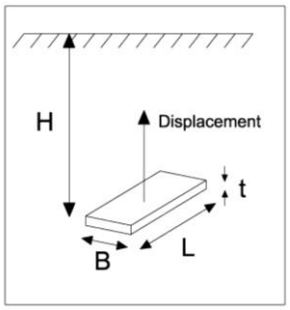

Figure 3-4 Plane strain condition

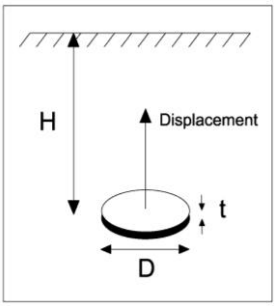

Figure 3-5 Axisymmetric condition

Table 3-1 Plate Anchors Dimensions

Anchor	2D Strip anchor		Axisymmetric	Thickness
	L(m)	B(m)	D_{equi}(m)	t (m)
1	2	4	3.20	0.3
2	2	3	2.76	0.3

3.6 Analysis with Traditional Models; Total Stress Analysis

Merifield et al. (2003) presented a method for calculating the ultimate capacity of plate anchors in saturated clay, which considered Tresca yield criterion for soil. Equihua-Anguiano et al. (2012) used Mohr- Coulomb as the soil model and compared their results to those obtained from Merifield et al.'s (2003). On the other hand, Merifield et al. (2003) suggested an equation for computing plate anchors capacity based on geometry and soil properties. In Merifield et al.'s (2003) procedure, N_{c0} depends on the embedment ratio H/L and B/L, which are provided in design charts. The effect of overburden pressure is considered as $N_{c\gamma}=N_{c0}+\gamma H/s_u$, which has a limiting value of $N_{c*}=11.2$ for a strip anchor and $N_{c*}= 12.6$ for the circular anchor.

Equihua-Anguiano et al. (2012) used load control method in total stress analysis and computed relatively higher capacities. The soil parameters for the undrained clay used by Equihua-Anguiano et al. (2012) are shown in Table 3-2 (where γ_{sat} is saturated unit weight (kN/m^3), ϕ_u undrained friction angle (°), s_u undrained shear strength (kN/m^2), E_u undrained Young's modulus (kN/m^2) and ν_u is undrained Poisson´s ratio.

Table 3-2 Soil Parameters Used by Equihua-Anguiano et al.(2012)

Soil	γ_{sat}(kN/m^3)	ϕ_u (°)	S_u (kN/m^2)	E_u (kN/m^2)	υ	Interface rigidity factor
Clay	17	0	1.6z	$500S_u$	0.49	1

Mohr-Coulomb model is used as a soil yielding criterion, and the same configuration is solved by displacement control and total stress analysis herein. Interface elements are used in all around of the plate with a rigidity factor of 1, as used in Equihua-Anguiano (2012). The pull out factor is calculated as ($N_c = \frac{F}{As_u}$). N_c increases with embedment depth until an ultimate depth which is termed as critical depth. N_c factor for different depths are presented in Figure 3-6 and Figure 3-7. The ultimate N_c values are presented in Table 3-3.

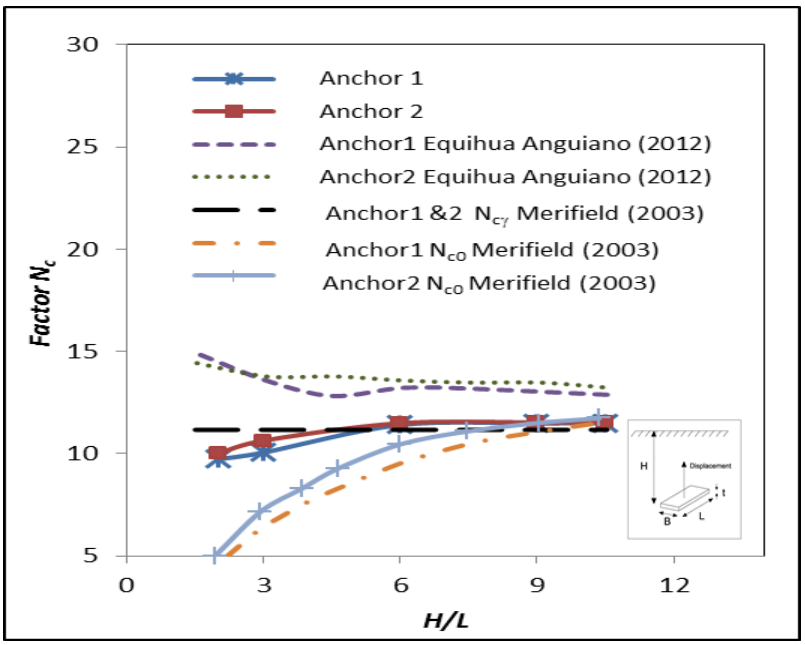

Figure 3-6 N_c obtained from current Plane Strain condition

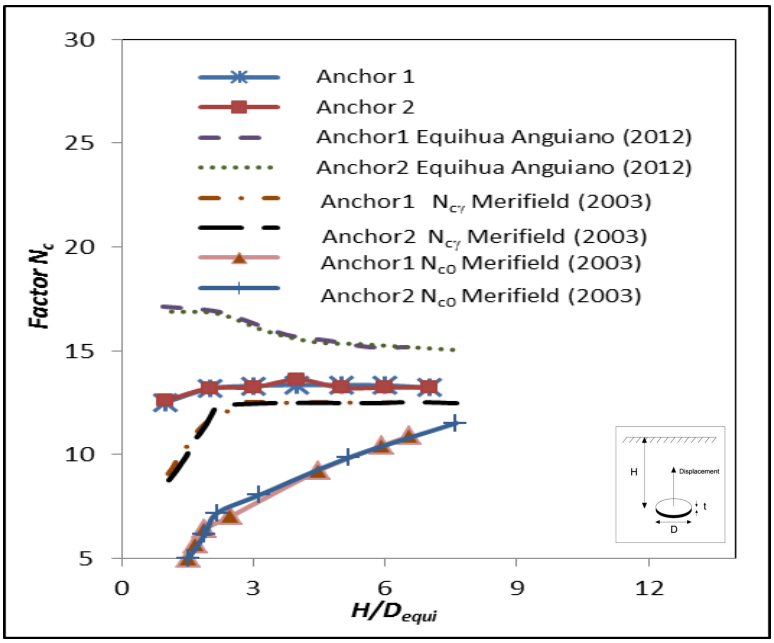

Figure 3-7 N_c obtained from current Axisymmetric condition

Comparing the results shows that N_c obtained for strip and circular anchors are in a very good agreement with Merifield (2003) estimated capacity factors and also in the shallow depth this research shows more reasonable results in compare with Equihua-Anguiano's (2012) results who used load control instead of displacement control. Since the plate anchor in both Equihua-Anguiano's (2012) analysis and this research are considered as a rigid one, we expect the same results in both displacement control and load control method but the results show big differences. All other assumptions are the same and this researcher's results show more reasonable trend increasing capacity by increasing the depth and final capacity in compare with a lower bound.

Equihua-Anguiano (2012) used a circular steel plate scaled down in a lab modeling and obtained N_c=13.9 for D=310mm and N_c=14.7 for H=187mm for D=187mm, Which are lower than his numerical break out factors. He proposed to use complex models to have a better approximation in the numerical analysis.

Table 3-3 Results Comparison

N_c values						
	2D Plane Strain			Axisymmetric		
Plate	This Study	Equihua-Anguiano (2012)	Merifield (2003)	This Study	Equihua-Anguiano (2012)	Merifield (2003)
1	11.5	13.0	11.2	13.2	15.1	12.6
2	11.5	12.9	11.2	13.2	15.1	12.6

3.7 Analysis with Complex Models; Effective Stress Analysis

As explained earlier, Soft Soil model and Modified Cam-Clay model are chosen to compare with Mohr-Coulomb model. The only common type of analysis between the mentioned models in PLAXIS menu is the undrained effective stress analysis using effective stress parameters. In this analysis, the effective strength parameters are defined, and PLAXIS adds the stiffness of water to the stiffness matrix of soil. (PLAXIS 2012). The dimensions of plate anchor 2 are used in the following axisymmetric models. The effective strength properties used in the analyses are summarized in Table 3-4.

Table 3-4 Effective Stress Parameters of Soil

γ_{sat} (kN/m^3)	Φ'	c' (kN/m^2)	ν_{ur}	λ	κ	ψ	e_0
17	30°	0	0.3	0.1	0.02	0	0.5

Table 3-5 shows correlated parameters of three models, which are calculated based on assumptions of Table 3-4 and Equation 3-1 to 3-4.

Table 3-5 Correlated Parameters

MC	SS	MCC
E=720*depth (kN/m^2)	λ^* =0.066 κ^*=0.013	M= 1.2

Different depths are considered such that embedment ratio, which considered as H/D_{equi} is varying in the range of 1-10. The interface elements are used in all around of the plate by rigidity factor of 0.7. This value is recommended in PLAXIS (It does not affect the results too much just for minimizing the errors).

Load displacement curves for H/D_{equi}=2 and H/D_{equi}=7 are shown in Figure 3-8 and Figure 3-9. Load-Displacement curves show similar trends, which increases until a constant amount.

The dimensionless break out factor for this analysis is considered as:

$$N_q = \frac{F}{\gamma A H} \qquad \text{Equation 3-5}$$

Where F is the ultimate pull out force (kN),

γ (kN/m^3) is the saturated unit weight of soil,

A (m^2) is the area of plate anchor

H (m) is the embedment depth.

By using the above equation, all of the data are summarized in the dimensionless N_q factor and plotted in the graph of Figure 3-10. A comparison of the results shows that in all depths, Mohr-Coulomb model gives higher values. Soft Soil model and Modified Cam-Clay model provide a relatively good agreement. Modified Cam-Clay model gives the lowest capacity.

The ultimate breakout factors for axisymmetric analysis are Mohr-Coulomb = 1.92, Soft Soil =1.74 and Modified Cam-Clay =1.70.

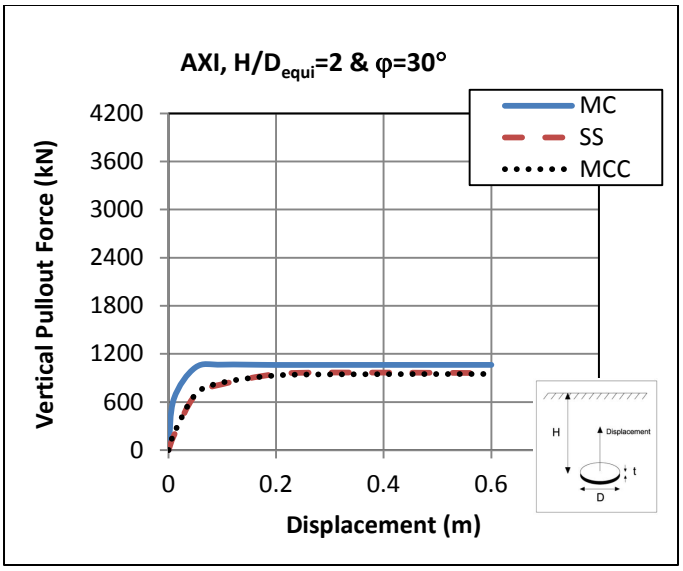

Figure 3-8 Load-Displacement curves H/D$_{equi}$=2

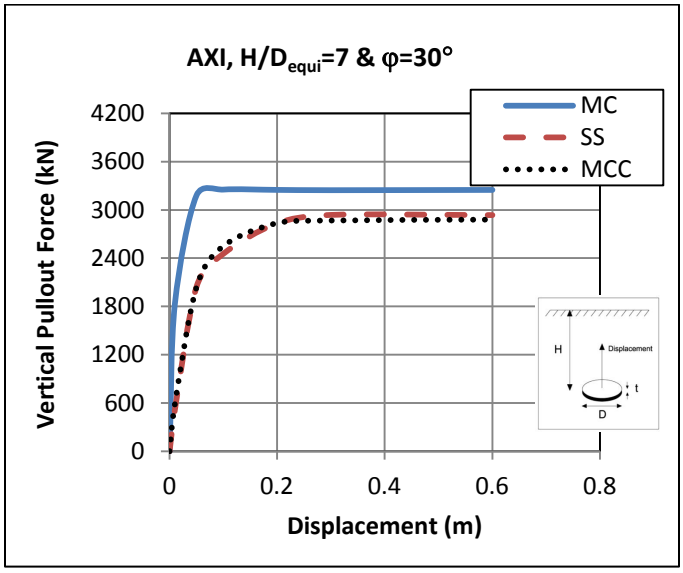

Figure 3-9 Load-Displacement curves H/D$_{equi}$=7

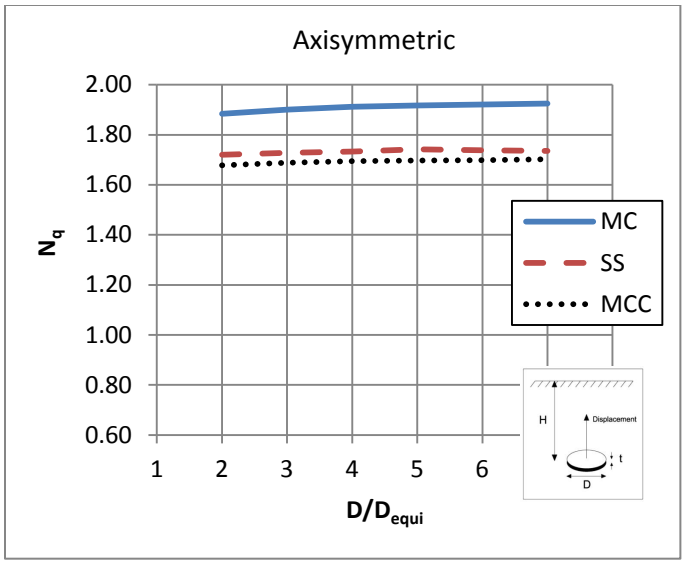

Figure 3-10 Dimensionless vertical break out factor in axisymmetric condition

3.8 Comparison with Experimental Data

Previous experimental data by Das (1980) were reported as N_c= F/(A.su) factor. For comparing the results from this study with theirs, the soil's undrained parameter is computed based on the effective stress parameter (ϕ') [Figure 3-11] and s_u undrained shear strength is calculated by using Equation 3-6.

$$s_u = sin\emptyset'[c'cot\emptyset' + \left(\frac{1+K_0}{2}\right)\sigma'_v] \qquad \text{Equation 3-6}$$

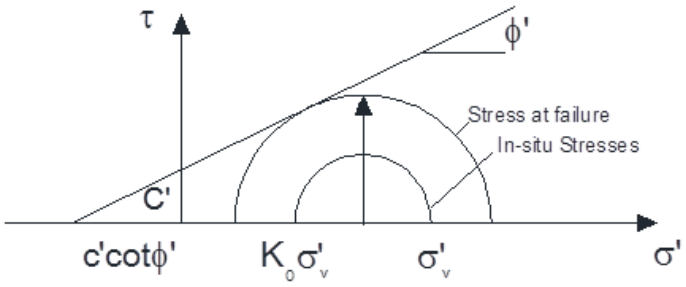

Figure 3-11 Parameters correlation

Figure 3-12 compares experimental data from Das (1994), Kupferman (1971) and Ali (1968)) for the weightless condition with the results here from axisymmetric analyses (γ_{sat}=17 kN/m^3). The comparison shows that Modified Cam-Clay and Soft Soil are in reasonable agreements with experimental data for H/D>4. For the depth less than critical one, the breakout factor is dependent on soil weight.

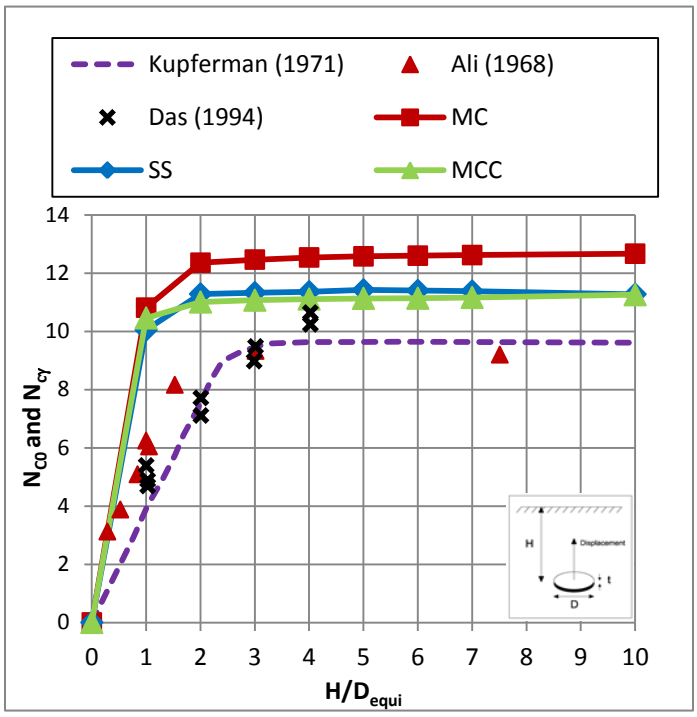

Figure 3-12 Comparing of the results with experimental data

3.9 Summary and Conclusions

In this study, the Mohr-Coulomb model was used in total stress analysis to estimate pullout capacity factor N_c assuming undrained parameters. In addition, the Modified Cam-Clay and Soft Soil models, with non-linear strain-dependent stiffness and yielding criteria, were used for comparative analyses. Effective stress analyses were also performed using PLAXIS, and the results were used to calculate and compare the pullout factor N_q. Based on the results from these analyses, the following conclusions are advanced:

- Based on the total stress analysis, results using Mohr-Coulomb model provided a good agreement with Tresca, which was used by Merifield, et al. (2003). As expected Mohr-Coulomb and Tresca are the same when dilation angle is zero.
- The calculated pull out factors by total stress analysis N_c are 11.5 for plane strain and 13.2 for axisymmetric which are in a good agreement with the values the 11.2 and 12.6 values, respectively, reported in Merifield (2003) but lower compared to Equihua-Anguiano, et al. (2012)'s results (12.9 & 15.1).
- Using the effective stress analyses with the axisymmetric model, the Mohr-Coulomb model provided a higher N_q in comparison with the Soft Soil and Modified Cam-Clay models.
- The results from Soft Soil and Modified Cam-Clay models are in a very good agreement.
- The N_q for Mohr-Coulomb, Soft Soil and Modified Cam-Clay are (1.92 1.74, 1.70).
- In the effective stress analysis for the undrained material (clays), Mohr-Coulomb model considers a constant mean effective stress during shearing while soils experience a decrease in the mean effective stress in this state. Therefore, Mohr-Coulomb model over-predicts N_q.
- The predictions from the analyses presented in this study (with Modified Cam-Clay and Soft Soil models) are in a reasonably good agreement with the experimental results for H/D>4.

3.10 References

Ali, J. I. (1968). ‘‘Pull-out resistance of anchor plates and anchored piles in soft bentonite clay.’’ *MSc thesis, Duke Univ., N.C.*

Brinkgreve, RBJ. (2005) . "Selection of soil models and parameters for geotechnical engineering application". *In: Yamamuro, JA and Kaliakin, VN, editors. Geotechnical Special Publication No.128, ACSE, pg 69-98.*

Das, B. M., Shin, E. C., Dass, R. N., and Omar, M. T. (1994). ‘‘Suction force below plate anchors in soft clay.’’ Marine Georesources andGeotechnology, 12, 71–81.

[Equihua Anguiano LN, M Orozco-Calderon and P Foray. (2012). “Numerical finite element method and experimental study of uplift capacity anchors” *SUT the 7th International Conference12–14 September 2012 Royal Geographical Society, London, UK 643-647.*

Kupferman, M. (1965). ‘‘The vertical holding capacity of marine anchors in clay subjected to static and cyclic loading.’’ MSc thesis, Univ. of Massachusetts, Amherst, Mass.

Merifield R.S, Lyamin A.V, Sloan S.W and Yu H.S (2003). “Three-Dimensional lower bound solutions for stability of plate anchors in clay” *Journal of Geotechnical and Geoenvironmental Engineering 129: 243–253*

Lee Jae Young and Ahn Sung Youll (2010). “Interactive visualization of elasto-plastic behavior through stress paths and yield surfaces in finite element analysis” *Elsevier, Finite Elements in Analysis and Design 47 (2011) 496.*

Chapter 4 Application of Different Constitutive Models to Estimate Capacity of Circular Plate Anchors Including Size Effects in Sands

This chapter will be submitted to the International Journal of Geomechanics. The authors are Zahra Aghazadeh Ardebili, S.M.ASCE[1]; M.A. Gabr, F.ASCE[2]; M.S. Rahman[3]

4.1 Abstract

Evaluation of the uplift capacity of plate anchors in saturated sands is required for safe anchoring of various offshore structures in the shallow water depths. The mean effective stress has a significant effect on the behavior of sands, and some of the advanced soil models can consider this nonlinear stress dependent behavior. Also, in most of the literature reviewed, dry sand was considered. There exists a need to study the pullout capacity of these anchors in saturated sands using different constitutive models and compare the results. In addition, there is no comprehensive finite element study on circular plate anchors in saturated sands to specify the effect of plate's diameter (size) and the dilatancy angle at different embedment depths which have significant effects on the capacity as reported before. This study presents the results of a finite element simulation of a circular plate anchor in saturated sands investigating the effect of constitutive models, the size and the dilatancy angle on the estimation of the pull out capacity at different embedment depths. Two different constitutive models are used to represent the soil. These are Mohr-Coulomb (MC) and Hardening Soil (HS) Models. Analyses are conducted using the computer program PLAXIS. A series of analyses are performed for the chosen constitutive models using different relative densities (RD=30%, 55% and 80% - representing loose, medium and dense sands and their corresponding dilatancy angles), different plate sizes (diameters equal to 1m and 5m), and

[1] Graduate Research Assistant, North Carolina State Univ., Campus Box 7908, Raleigh, NC 27695 (corresponding author). E-mail: zaghaza@ncsu.edu
[2] Alumni Distinguished Undergraduate Professor, North Carolina State Univ., Campus Box 7908, Raleigh, NC 27695.E-mail: gabr@ncsu.edu
[3] Professor, North Carolina State Univ., Campus Box 7908, Raleigh, NC 27695.E-mail: rahman@ncsu.edu

different embedment depths ($1 \leq H/D \leq 7$). The effective capacity factors (N'_q) of the plate are assessed through the application of displacement control approach. Differences resulting from the characteristics of these two constitutive models are examined and discussed. Size and dilatancy effects are presented for the range of the chosen parameters.

Key Words: Constitutive models; Anchors; Capacity; Finite element method; saturated sands.

4.2 Introduction

Plate Anchors are frequently used as an economical and efficient foundation system for anchoring offshore structures in deep waters. Their behavior and capacity in undrained clays have been reported in the literature [Kupferman 1965; Das, et al. 1994; Merifield, et al. 2003]. Recently they are considered as an anchorage system for renewable energy power generation devices (such as wave energy converters) in shallow water depths, where the sandy soil is dominant. In most of the literature reviewed, dry sand is used and inconsistent results showing the measured capacity is under or overpredicted by finite element analysis [Niroumand et.al 2013; and Dickin and Laman 2007].

Niroumand et.al (2013) performed the model test on circular plates and did finite element analysis with HS model at dry loose and dense sands. Dickin and Laman (2007) performed centrifuge test and Finite element analysis on strip plate with HS model at dry loose and dense sands. In both of them, the results from numerical analysis slightly overestimated the capacity of the plate anchors in loose sand and underestimated the capacity of dense sand in comparison with their experimental data.

The anchor's uplift capacity is a function the effective weight of the soil mass above the plate, and the shear resistance developed along the failure wedge created during pull out. The capacity depends on several factors including embedment depth, plate's shape and size, and soil densities. The uplift capacity of a plate anchor in sands is generally reported in the literature in terms of dimensionless breakout factor (N_q). Past experimental studies on the

horizontal circular plate anchor include those by, among others, Ovesen (1981), Murry and Geddes (1987), Tagaya et al (1988), Sakai and Tanaka (1998), Ilamparuthi et al. (2002) and Niroumand et al (2013). In parallel, analytical studies on the horizontal circular anchor have been reported in literature including those by Meyerhof and Adams (1968), Murray and Geddes (1987), Koutsabeloulis and Griffiths (1989) and Niroumand et.al (2013). Review these studies provide the following general observations:

-Elasto plastic finite element analysis cannot fully explain the behavior of cohesionless soils during the failure (progressive failure) as was reported by Sakai and Tanaka (1998). The mean effective stress has a significant effect in the behavior of sands, and it is important to consider the nonlinear stress dependency of the stiffness during the numerical analysis.

- Some of the researchers reported that anchors geometry (diameter of anchors) has a significant effect on the breakout factor. Ovesen (1981), Dickin (1988), Sakai and Tanaka (1998), and Niroumand et al. (2013) have reported an influence of size effect on the breakout factor in sands based on their theoretical and experimental works. It has been reported that N_q value decreases by increasing the plate's diameter at a constant H / D value. This has been attributed to a decrease of the mobilized friction angle due to increase in confining pressure (Khatri and Kumar 2011) and progressive failure and larger shear banding around the larger plate (Sakai and Tanaka 1998). On the other hand, Ilamparuthi et al. (2002) studied the uplift behavior of relatively large-scale model circular plates in loose, medium dense and dense dry sand. They used circular plate anchors with diameters equal to 100, 150, 200, 300, 400(mm). They concluded that for a given density of soil, break out factor depends only on H/D and is not affected by plates size (D). There is a need to investigate the size effect numerically, especially along with the consideration of embedment and dilation effects.

-It is proven that dilatancy angle has a significant effect on the capacity [Rowe and Davis 1982]; the more investigation and parametric studies by considering relatively an appropriate amount of dilatancy angle are recommended at literature [Rowe and Davis 1982].

The objective of this paper is to investigate the development of the vertical uplift capacity of circular plate anchors in saturated sands with the use of two different constitutive models (MC and HS models). In addition, and within the context of the two constitutive

models utilized in the study, the effect of dilatancy angle and plate's size on the pullout capacity is investigated. Analyses are conducted using soil parameters that are equivalent for each constitutive model. The study is conducted using a computer program (PLAXIS 2012). An axisymmetric condition is utilized to model the plate using various embedment depths such that embedment ratio (*H/D)* is in the range of 1-7, three different relative densities (RD=30, 55 and 80 presenting loose, medium and dense sands, respectively) and their corresponding dilatancy angles. Also, different plate sizes (diameter equals to 1m and 5m) are assumed in the analyses. Results are presented in dimensionless graphs and discussed.

4.3 The Constitutive Models

Several researchers have presented models depicting the constitutive behavior of soils. According Brinkgreve (2005) a comprehensive soil model should be capable of incorporating the different aspects of soils; such as variable stiffness of soil (which is function of stress level, stress path, strain level, drainage conditions, and anisotropy), plastic deformation, influence of water, strength (which is a function of loading rate, age, density, undrained behavior, consolidation and anisotropic shear strength), dilatancy and compaction. For the plate anchor analyses addressed herein, Mohr- Coulomb (MC) and Hardening Soil (HS) models are chosen. HS model allows for the use of stress-dependent moduli. Brinkgreve (2005) presents a detailed description of these two models.

MC model provides a good estimation of failure for most of the problems. The model parameters are defined simply by soils' friction angle, an elastic modulus and poisons' ratio. A completely reversible linear elastic stress-strain part and an irreversible perfectly plastic stress–strain part represent the load-displacement behavior in MC model. In the principal stress space, the yielding functions of MC model represent a fixed hexagonal cone. On the other hand, the HS model (Brinkgreve & Vermeer 1997; Schanz et al. 1999) is a nonlinear (quadratic), stress dependent stiffness mode with the same yield criteria as in MC model. It is capable of capturing two types of hardening: friction hardening and cap hardening. Friction hardening models the plastic shear strain in deviatoric loading and cap hardening can model the plastic volumetric strain in primary compression. HS model has the potential to consider the stress dependent stiffness and can capture the hardening effects before the failure.

Therefore, it may be able to represent the deformation behavior of sand more realistically in comparison models like Mohr- Coulomb.

4.3.1 Model Parameters and Their Correlations

The parameters needed for defining the MC model in PLAXIS are: Young's modulus (E), Poisson's ratio (ν), parameters from Coulomb failure criterion which are cohesion (c), friction angle (φ) and a non-associate flow rule parameter which is dilatancy angle (ψ). The parameters needed for developing HS model are: stiffness parameters of triaxial compression (E_{50}^{ref}), triaxial unloading (E_{ur}^{ref}) and oedometer loading (E_{oed}^{ref}) at a reference stress level (p^{ref} which PLAXIS considers as equal to 100 stress units), power (m) for calculating stress dependent stiffness, unloading and reloading Poisson's ratio (ν_{ur}), cohesion (c), friction angle (φ) and a non-associate flow rule parameter which is dilatancy angle (ψ) and failure ratio parameter (R_f) which most of the time is assumed equal to 0.9 and refers to the deviatoric stress level at failure.

Brinkgrever (2010) proposed empirical formulas based on the relative density (*RD*) for sands to estimate the model parameters of HS model. Most of these parameters are also used in MC model. The following formulas (Brinkgreve, 2010) are used herein:

$$\gamma_{unsat} = 15 + 4.0RD/100 \ [kN/m^3] \qquad \text{Equation 4-1}$$

$$\gamma_{sat} = 19 + 1.6RD/100 \ [kN/m^3] \qquad \text{Equation 4-2}$$

$$E_{50}^{ref} = 60000RD/100 \ [kN/m^3] \qquad \text{Equation 4-3}$$

$$E_{ur}^{ref} = 60000RD/100 \ [kN/m^3] \qquad \text{Equation 4-4}$$

$$E_{oed}^{ref} = 180000RD/100 \ [kN/m^3] \qquad \text{Equation 4-5}$$

$$m = 0.7 - RD/320 \qquad \text{Equation 4-6}$$

$$\varphi' = 28 + 12.5RD/100\ [°]$$ Equation 4-7

$$\psi = -2 + 12.5RD/100\ [°]$$ Equation 4-8

$$R_f = 1 - RD/800$$ Equation 4-9

PLAXIS (2012) uses Equation 4-10 to calculate the confining stress dependent stiffness modulus (E_{50}) for primary loading. Therefore, for defining the corresponding stiffness modulus for MC model, the soil domain is divided into sub-layers and for each sub-layer the modulus is estimated and assigned to the MC model (σ_3' is negative for compression).

$$E_{50} = E_{50}^{ref}\left(\frac{c\cos\varphi - \sigma_3'\sin\varphi}{c\cos\varphi + p^{ref}\sin\varphi}\right)^m$$ Equation 4-10

4.4 Numerical Model Validation

Niroumand et al. (2013) conducted a series of experimental data using different plate sizes (D=50, 75 and 100 cm) and used HS model for their numerical analysis. A series of analysis using Niroumand et al. (2013)'s soil parameters for as loose and dry packing sand (

Table 4-1) and geometries are performed and results are compared to the experimental results for validation.

Table 4-1 Soil Parameters Used by Niroumand et al.(2013)

Parameter	γ (kN/m^3)	E_{50}^{ref} (kN/m^3)	E_{oed}^{ref} (kN/m^3)	E_{ur}^{ref} (kN/m^3)	m	$\varphi(°)$	$\psi(°)$	c (kN/m^3)	R_f	K_0	ν_{ur}
Loose Packing	15	20000	20000	60000	0.5	38	8	0.5	0.9	0.38	0.2
Dense Packing	17	30000	30000	90000	0.5	44	14	0.5	0.9	0.32	0.2

The axisymmetric condition is used to simulate a 75 cm diameter circular plate used in the experimental program. Figure 4-1 presents the model domain. The analyses are

developed using the displacement controlled method, in which a series of prescribed displacements is applied on the plate and the corresponding forces are computed. The displacement is increased until the load-displacement graph becomes a plateau. The large deformation analysis is utilized in PLAXIS and updates the mesh and stiffness matrix of the soil at each step. The dimensionless breakout factor is considered as:

$$N_q = \frac{F}{\gamma AH} \qquad \text{Equation 4-11}$$

Where the F is the pull out force (kN), γ (kN/m^3) is the unit weight of soil, A (m^2) is the area of plate anchor and H (m) is the embedment depth.

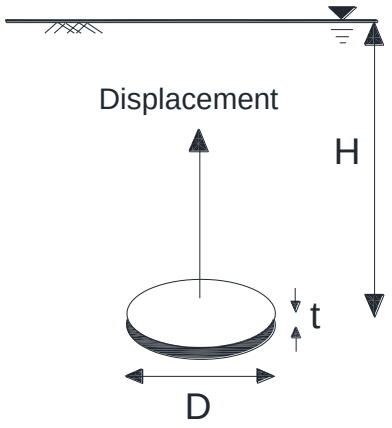

Figure 4-1 Model domain

In Figure 4-2 (a), N_q value for dry loose packing is compared with the results from the experimental data. Balla (1961) also reported on the pullout capacity of a circular plate anchors with diameters equal to 60 and 120 mm in dry sand with friction angle equal to 38 degrees. Andereadis and Harvey (1981) used a circular plate anchor (the diameter size is not available) in the dry sand with friction angle equal to 38 degrees. The comparison in Figure 4-2 (a) shows a good agreement between measured and computed data. In the deeper depths, the numerical model yielded a relatively higher breakout factor in comparison with

experimental data; this is related to the assumed amount of dilatancy angle. As will be shown later, dilatancy angle has a significant effect on the pullout capacity at the large embedment depths.

In Figure 4-2 (b), the results of the dense packing dry sands are compared with Niroumand, et al. (2013), Ilamparuthi, et. al (2002), and Murry and Geddes (1987). Ilamparuthi, et. al (2002) used different plate size at the different soil densities. They conclude that in their experimental data the breakout factor is just depend on H/D and soil properties, (the size effect is not observed). The results in this graph related to their 100mm circular plate (which is more consistent size with the rest of chosen experimental data herein) at the dense sand with friction angle equal to 43 degrees. Murry and Geddes (1987) used circular plate anchors with diameters equal to 51 and 89 mm in a dense sand with friction angle equal to 44 degree and relative density equal to 86%. The results in the dense packing match well with the experimental data.

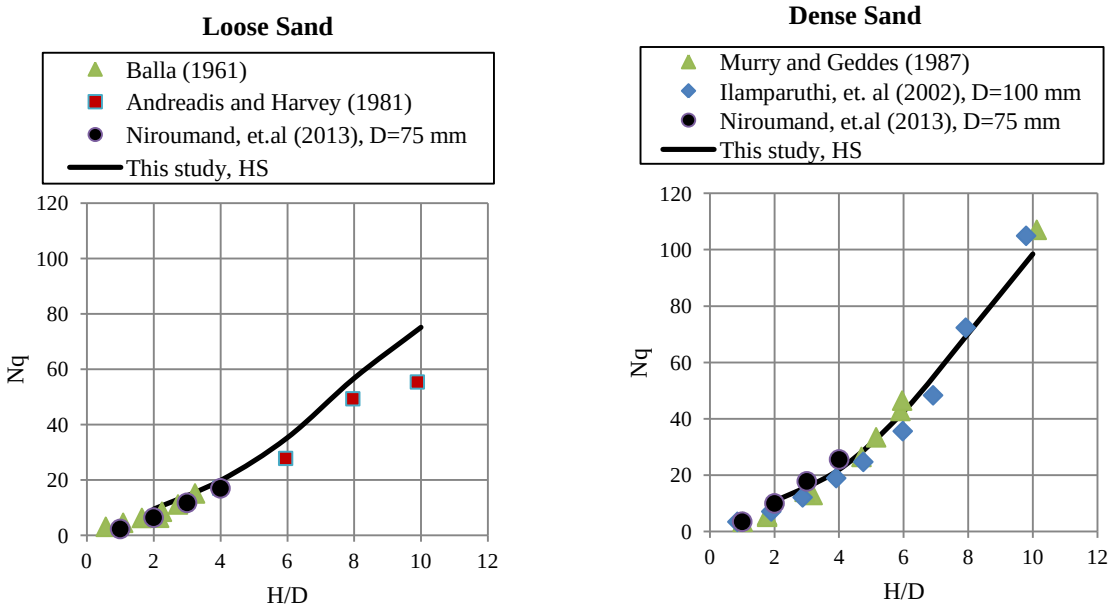

(a) (b)

Figure 4-2 Comparison of this study's results with existing experimental data for (a) loose sands, (b) dense sands

4.5 Drained Analyses of Saturated Sands Using Different Constitutive Models

One of the main objectives of this study is investigating the effect of the chosen constitutive models (HS model versus MC model) on the pullout capacity in saturated sands. Equations 4-1 to 4-10 are used to estimate soil parameters that are equivalent in both models, Brinkgreve (2010).

A finite element model is developed for analyzing the plate anchors in saturated sands. For minimizing the boundary effects, a large domain (30m*50m) is modeled. For the base analyses case, the diameter of the circular plate anchor is assumed equal to 2.76 meters (9 feet), and the thickness of the plate is considered 0.3 meters. The plate anchor is assumed as rigid steel with a Young's modulus equal to 200 Gpa. Several depth values (*H*) are considered such that embedment ratio *H/D* is in the range of 1-7. The analyses are performed for *RD*=30%, 55% and 80%, which are representative of loose, medium and dense sands, respectively. The soil properties used in the analyses are summarized in Table 4-2. These are calculated using Equations 4-1 to 4-9.

Table 4-2 Soil Parameters (Based on Brinkgreve 2010)

RD	γ_{unsat} (kN/m^3)	γ_{sat} (kN/m^3)	E_{50}^{ref} (kN/m^2)	E_{oed}^{ref} (kN/m^2)	E_{ur}^{ref} (kN/m^2)	m	$\varphi(°)$	$\psi(°)$	R_f	e_0	K_0	ν_{ur}
30	16.2	19.48	18000	18000	54000	0.606	31.8	1.8	0.963	0.72	0.474	0.32
55	17.2	19.88	33000	33000	99000	0.528	34.9	4.9	0.931	0.60	0.428	0.30
80	18.2	20.28	48000	48000	144000	0.450	38.0	8.0	0.900	0.49	0.385	0.28

In Table 4-3, the modulus of the soil at different depths for MC model is calculated for the three relative densities considered herein using Equation 4-10

Interface elements are used at the upper part of the plate with a rigidity factor of R_i= 1. R_i is the ratio between the shear strength of the soil structural interface and shear strength of the soil. The mesh is chosen as a cluster that has finer elements around the plate.

Figure 4-3 shows the mesh and interface elements around the plate anchor (units are in meter).

The computed load displacement curves using the two constitutive models used in this study are shown in Figure 4-4, for different embedment depths. The load-displacement curves show the similar trends of increase in pullout capacity reaching ultimate values, which are nearly the same for HS model and MC model. As expected, the higher relative densities and larger embedment provide higher resistance.

Table 4-3 Stiffness of the Soil at Mohr- Coulomb Model

RD	30%		55%		80%	
Soil Depth (m)	E_{50} *(kN/m²)*	E_{50} (avg) *(kN/m²)*	E_{50} *(kN/m²)*	E_{50} (avg) *(kN/m²)*	E_{50} *(kN/m²)*	E_{50} (avg) *(kN/m²)*
5	7376	3688	14691	7345	23345	11673
10	11227	9301	21183	17937	31890	27618
15	14354	12790	26240	23712	38274	35082
20	17087	15720	30545	28393	43564	40919
30	21847	19467	37837	34191	52283	47924
40	26007	23927	44043	40940	59510	55897
50	29773	27890	49551	46797	65796	62653

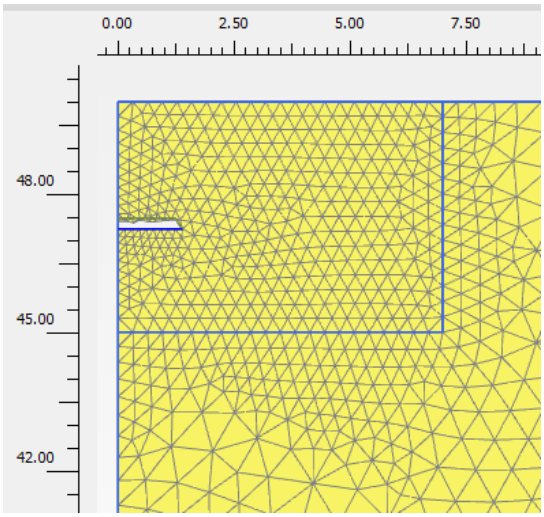

Figure 4-3 Used mesh around the plate

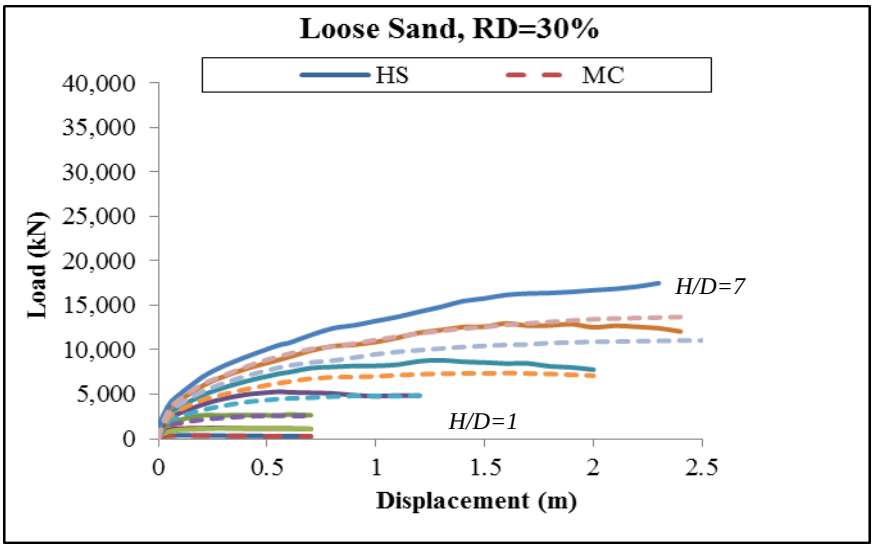

(a)

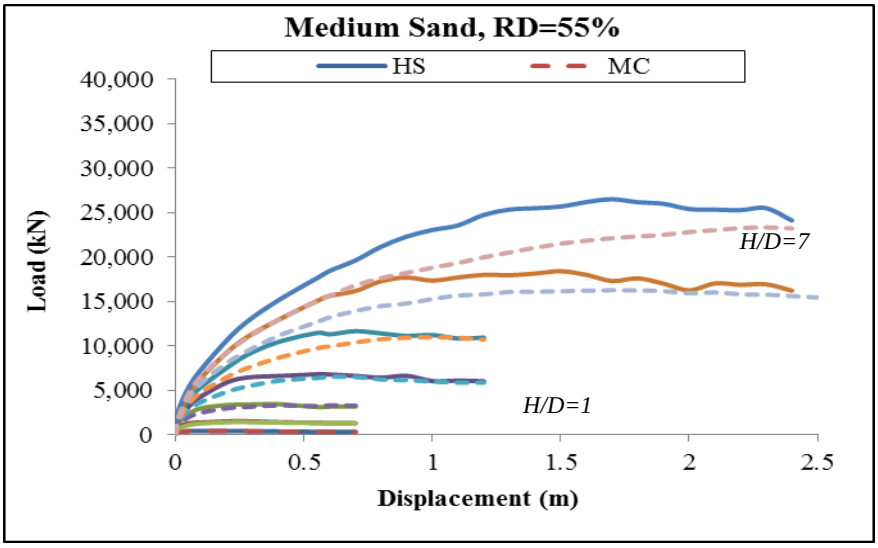

(b)

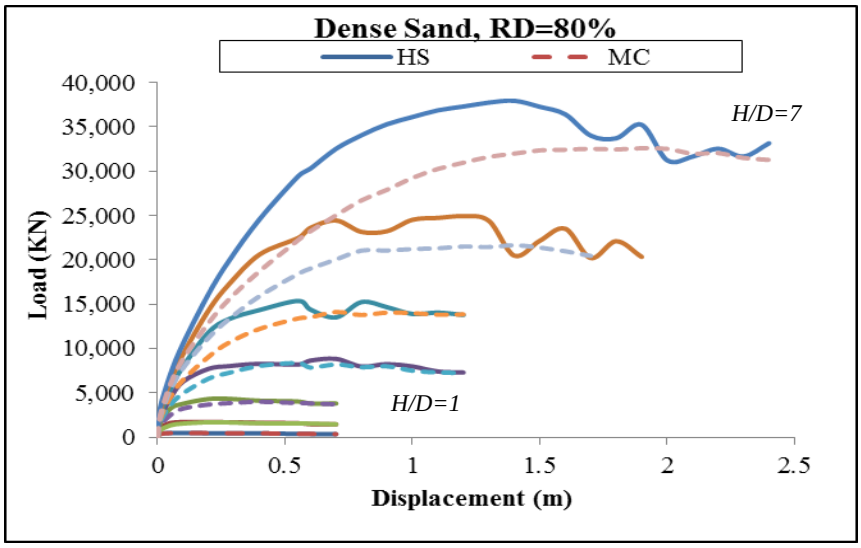

(c)

Figure 4-4 Load-Displacement curves for H/D=1 - 7 (by increasing H/D, curves move upward) at (a) Loose, (b) Medium and (c) Dense Sands

The load-displacement curves from HS model for the dense sand and deeper embedment show an oscillation behavior (Figure 4-4 b and c). This oscillation seems to be from an error associated with the numerical analysis of large displacement rather than from progressive failure phenomenon reported in the literature. The progressive failure reported for deep anchors and large displacements, is oscillatory behavior between load and displacement in dense sands (Rowe and Davis 1982; Dickin, 1988; IIamparuthi et al. 2002). These oscillations are related to the collapse and flow of the sand from the above of the plate anchor towards a gap created below it (Fityus et al. 2000) with the pullout movement. Since the soil medium is considered continues in the numerical analysis, the finite element analysis cannot reproduce the discrete deformation and movement of soil particles (soil particles below the plate). In Figure 4-5, the plastic points around the plate for a case with embedment ratio of H/D=6 and RD=80%, are shown for both constitutive models. HS model mobilizes a larger soil mass, which experiences hardening before reaching the failure. The transition between hardening state and failure state behavior and re-meshing procedure at the large deformation analysis can cause the observed oscillation behavior.

The dimensionless effective breakout factor N_q' for this saturated drained analysis is considered as:

$$N_q' = \frac{F}{\gamma' AH} \qquad \text{Equation 4-12}$$

Where γ' (kN/m^3) is effective unit weight of soil. Anchor's collapse in sands corresponds to extensive inelastic deformation (Rowe and Davis 1982), especially at the deep embedment depths. Definition of failure or capacity depends on how much deformation can be tolerated by the supported structure at its foundation (serviceability limitations). Some of the researchers defined the capacity equal to the load corresponding to the displacement equal to 20% of the plate width (Dickin and Laman 2007). Rowe and Davis (1982) defined failure load as the value corresponding to an apparent stiffness of one-quarter of the elastic stiffness and named it k_4 failure. Most of the experimental data are based on the ultimate load where the load-displacement graph becomes a plateau. In this research, the breakout factors (N_q) are presented corresponding to both the displacement equal to 20% of the plate's diameter and the ultimate load [Figure 4-6].

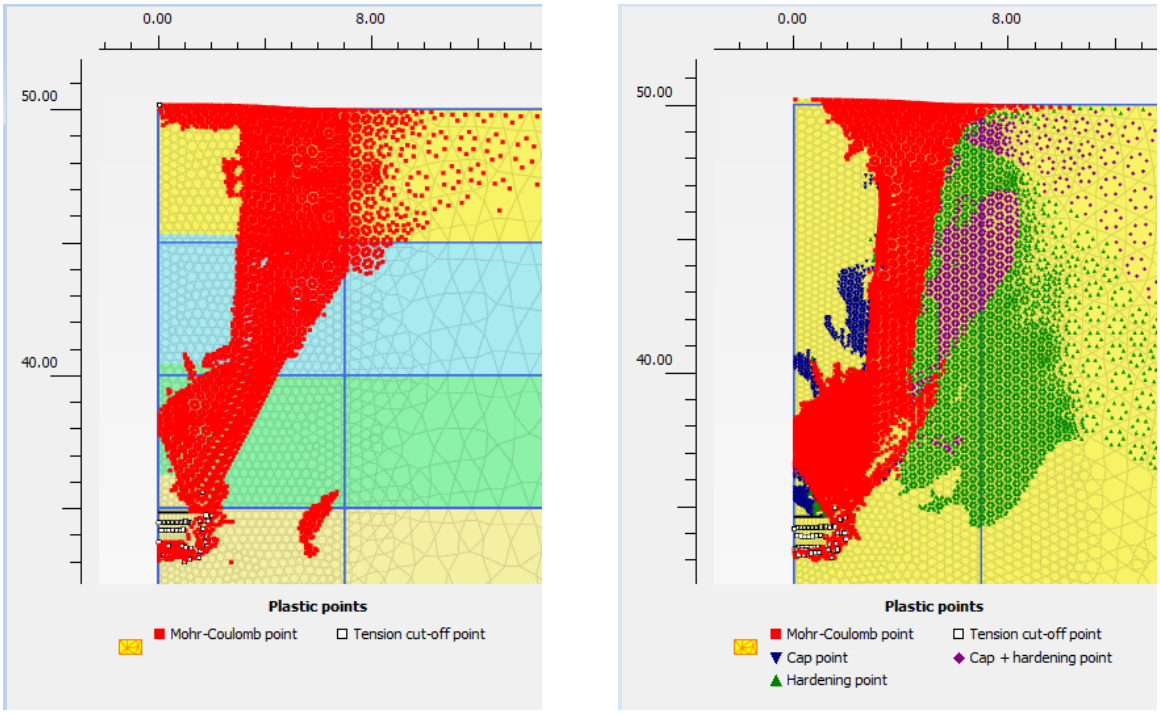

(a) (b)

Figure 4-5 Plastic Points at the maximum mobilized load (a) MC model (b) HS model

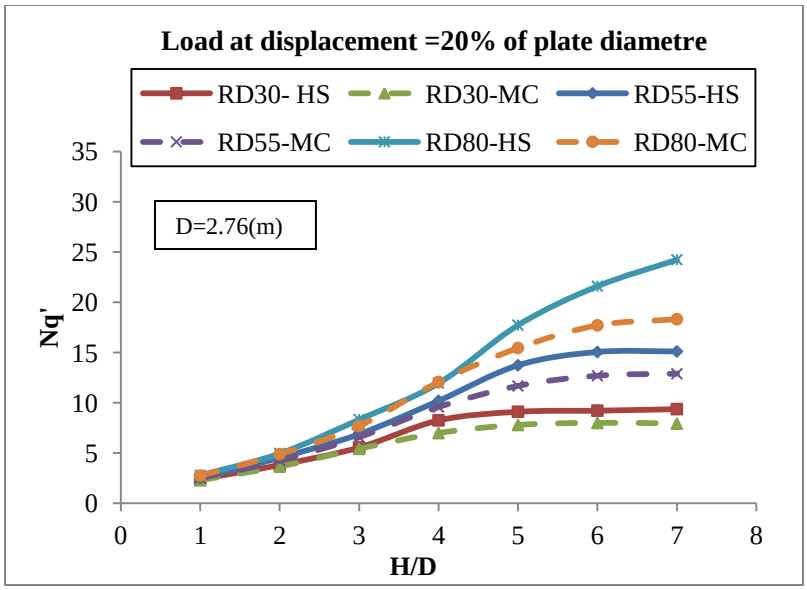

(a)

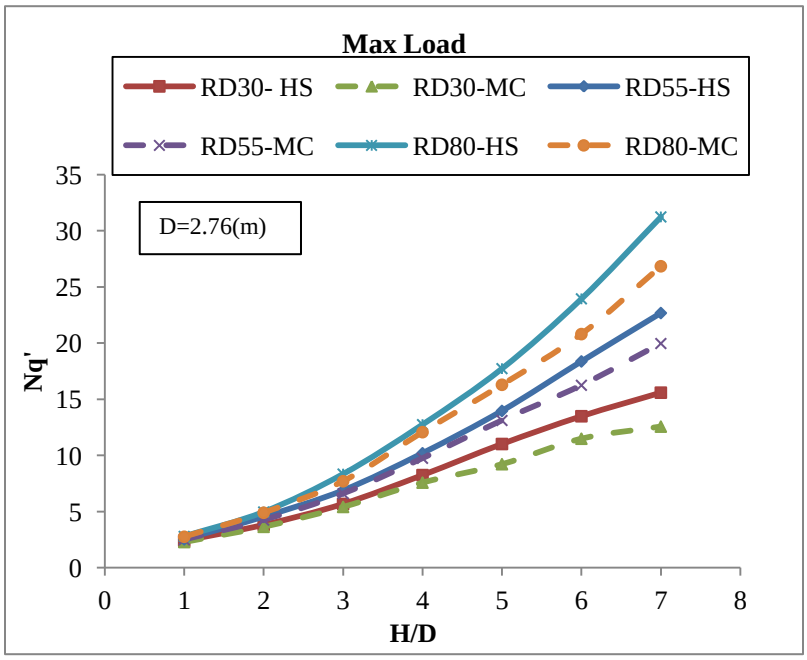

(b)

Figure 4-6 Dimensionless effective vertical breakout factor corresponding to (a) the displacement equal to 20% of plate's diameter, (b) the ultimate load

The failure criteria of MC model and HS model are the same, but HS model has a stress dependent modulus. At shallow depths (H/D<4) the use of MC and Hardening Soil models yield almost the same capacities. At larger depths, HS model yields slightly higher capacities, for example in the H/D=7, N_q' value form HS model and MC model are 31.2 vs 26.8 in the dense sand, 22.7 va 20 in medium sand and 15.6 va 12.6 in the loose sand (see Figure 4-6). With the use of HS model, stresses and consequently modulus are increased with loading, locally around the plate by applying a prescribed displacement while in MC model the modulus is constant. Figure 4-7 shows the unloading/reloading modulus of the soil around the plate with the use of HS model at the dense sand (RD=80%) and H/D=6 at the maximum load. Having expanding failure surface and stress dependent modulus in HS model can be a reason for yielding a higher capacity than MC. This difference is pronounced at the larger depths, which have higher mean effective stresses.

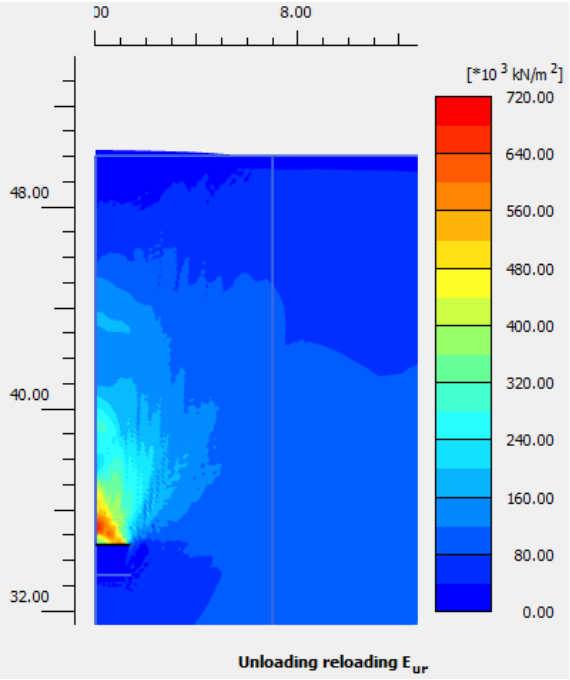

Figure 4-7 Moduli of soil around the plate at HS model at dense sand, H/D=6 in the failure

Figure 4-8 shows the vertical displacement contours around the plate, at the maximum uplift resistance for the two constitutive models, for $RD = 80\%$ and $H / D = 7$. The failure mechanisms are almost the same when using both models, but the soil modeled by MC is mobilized at higher displacement (1.9 meters versus 1.4 meters). As explained, the modulus around the plate at HS model is higher than that at MC model. Therefore, in HS model by smaller uplift displacement soil reaches to the failure state in comparison with MC model (also see Figure 4-7).

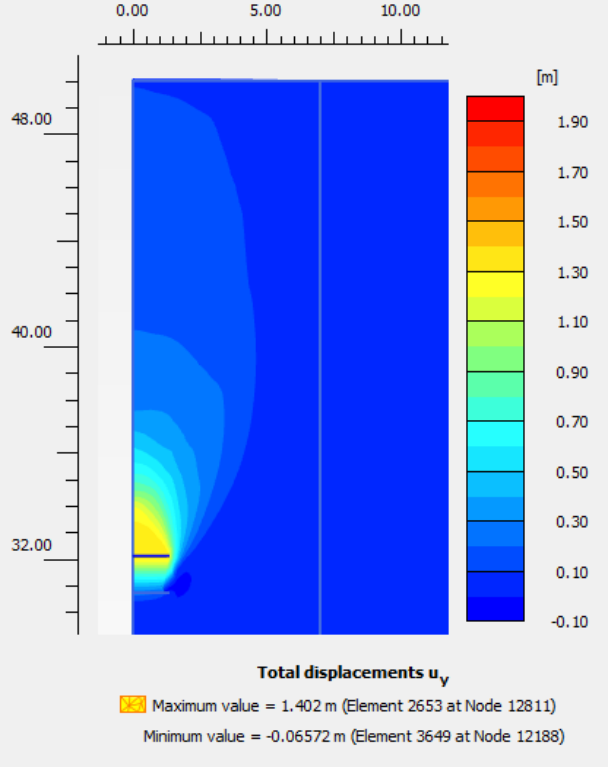
0.00
5.00
10.00
48.00
40.00
32.00
[m]
1.90
1.70
1.50
1.30
1.10
0.90
0.70
0.50
0.30
0.10
-0.10
Total displacements u_y
Maximum value = 1.402 m (Element 2653 at Node 12811)
Minimum value = -0.06572 m (Element 3649 at Node 12188)

(a)

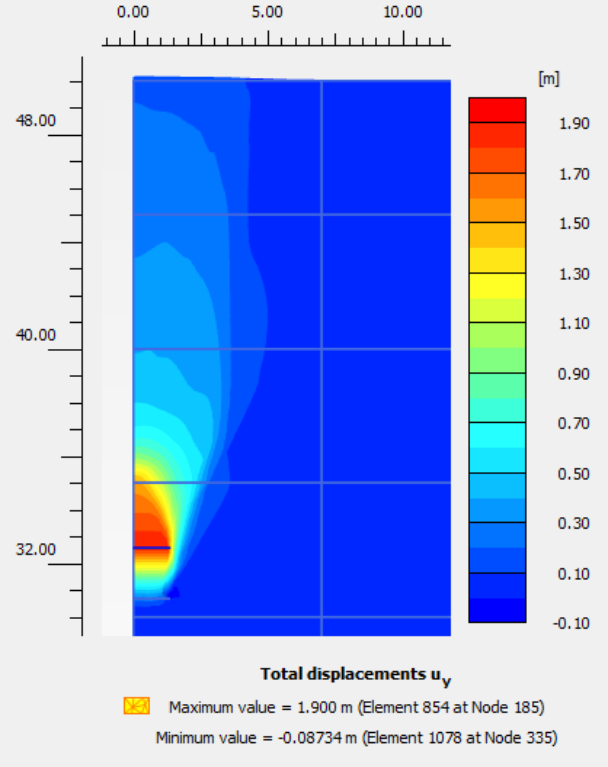

(b)

Figure 4-8 Vertical displacement contours for (a) HS and (b) MC

4.6 Dilatancy Effect

Dense sands show dilation behavior during the plastic deformation, which causes the soil in front of the anchors to lock up and develop an extensive plastic region before the collapse (Rowe and Davis 1982). By mobilizing more soils in an enlarged failure zone, dilatancy tends to increase the capacity of plates. In Figure 4-9 vertical displacement fields corresponding to the maximum uplift resistance with and without dilatancy angle are shown (for the case of H/D=7 and HS model). Results indicate enlargement of failure zone by dilation. The comparison also shows that soils without dilatancy is mobilized and collapsed at a higher displacement level (1.7 m versus 1.4 m, see Figure 4-9). With dilation, more energy is expended during deformation with tend to mobilize larger soil mass while reaching failure at lower displacement level.

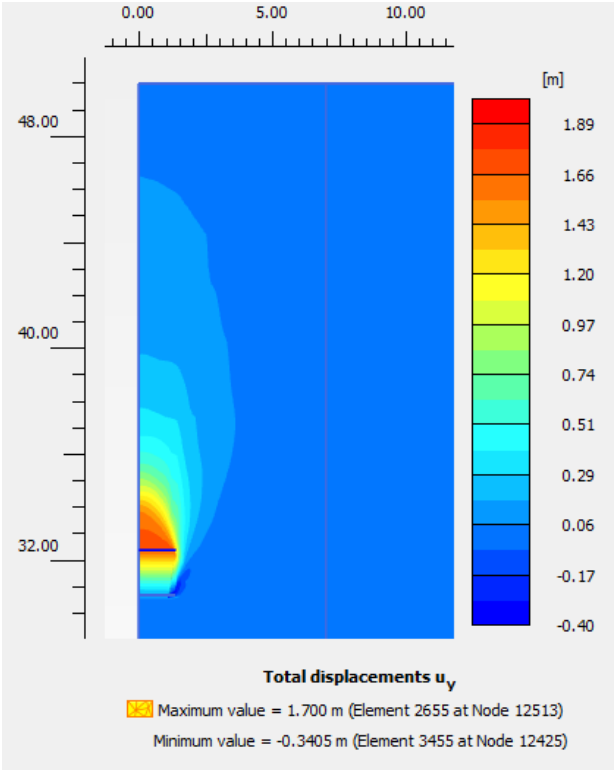
0.00
5.00
10.00
48.00
40.00
32.00
[m]
1.89
1.66
1.43
1.20
0.97
0.74
0.51
0.29
0.06
-0.17
-0.40
Total displacements u_y
Maximum value = 1.700 m (Element 2655 at Node 12513)
Minimum value = -0.3405 m (Element 3455 at Node 12425)

(a)

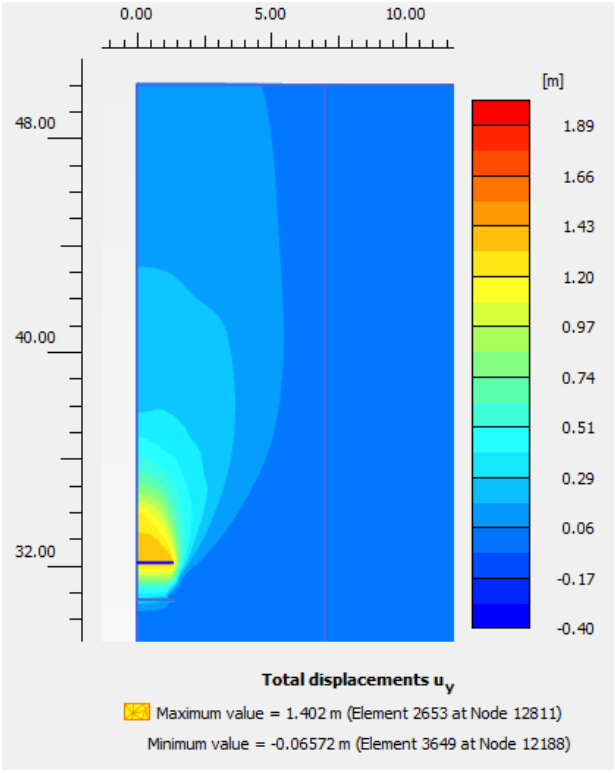

(b)

Figure 4-9 Failure mechanism (a) without dilatancy, (b) with dilatancy angle

The effect of dilatancy angle is shown by presenting a factor ($R_\psi = N'_{q(with\ Dilatancy)} / N'_{q(without\ Dilatancy)}$) providing the ratio of the breakout factor with and without dilatancy. As shown in Figure 4-10, the dilatancy effect almost linearly increases with the embedment depth. In Table.3, the $R_\psi = N'_{q(with\ Dilatancy)} / N'_{q(without\ Dilatancy)}$ values are summarized for different embedment depths. The effect of dilatancy captured by using MC and HS models is almost the same. For dense sands ($\psi = 8°$) and by increasing the embedment depth, the dilatancy angle shows a significant effect on the breakout factor. In the case H/D=7, the capacity increases 50% based on the use of MC and 40% based on HS (Table.4) in dense sand.

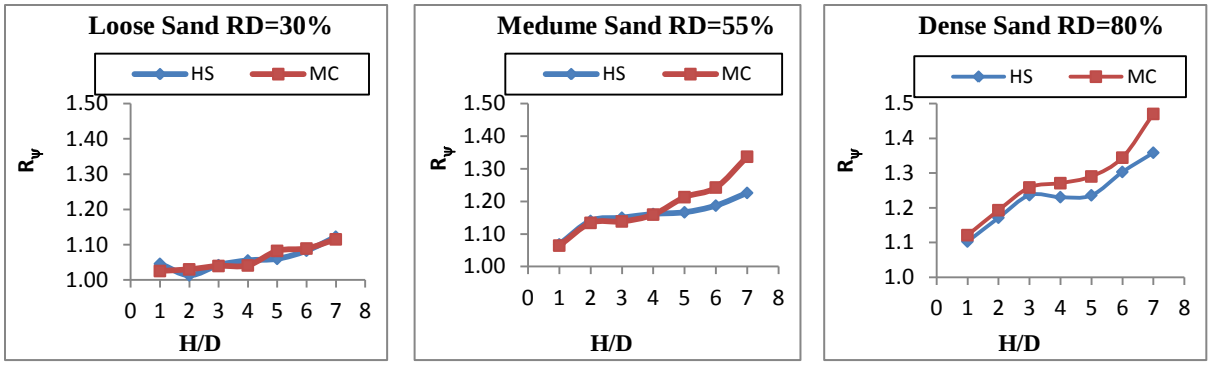

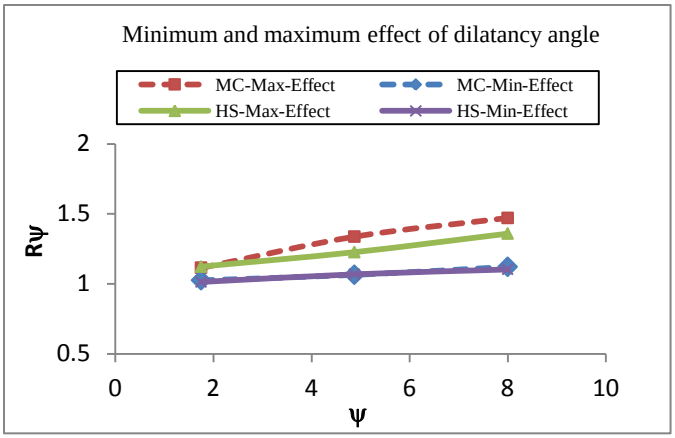

Figure 4-10 The effect of dilatancy

Table 4-4 Dilatancy Effect at Different Embedment Depths

$R_\psi = N_{q(with\ Dilatancy)} / N_{q(without\ Dilatancy)}$								
RD	H/D	1	2	3	4	5	6	7
30%	HS	1.0	1.0	1.0	1.1	1.1	1.1	1.1
	MC	1.0	1.0	1.0	1.0	1.1	1.1	1.1
55%	HS	1.1	1.1	1.1	1.2	1.2	1.2	1.2
	MC	1.1	1.1	1.1	1.2	1.2	1.2	1.3
80%	HS	1.1	1.2	1.2	1.2	1.2	1.3	1.4
	MC	1.1	1.2	1.3	1.3	1.3	1.3	1.5

4.7 Size Effect

HS model is used to model a dense saturated sand with RD=80% and dilatancy angle of 8 degrees. Two sizes of the plate are considered with diameters equal to 1 meter and 5 meters, respectively, and embedment ratios of 3 and 4. The domain size and elements coarseness are considered such that the convergence is satisfied. The 15 node element is used. The clustered medium mesh with the local coarseness factor of 0.1 around the plate is applied. The meshing information is shown for the case of H/D=4 in Figure 4-11. In Figure 4-12 N'_q values are presented at different embedment depths for the two plate diameters considered herein. The results are summarized at

Table 4-5, N'_{q1} and N'_{q5} refer to the plate anchor with diameters equal to 1 m and 5 m, respectively. The results show that the N'_q value decreases only slightly by increasing plates diameter. Given the analyses parameters used herein, it seems that the size effect on N'_q is insignificant.

According to Khatri and Kumar (2011) and Sakai and Tanaka (1998), as a result of size effect, N_q value decreases by increasing the plate's diameter at a constant H/D value, due to the following:

i) Decreasing of the mobilized friction angle by increasing confining pressure (Khatri and Kumar 2011) .

ii) Progressive failure and larger shear banding around the larger diameter plate (Sakai and Tanaka 1998).

Since the friction angle dependency on the mean effective stress was not considered in the modeling presented herein, the results do not show such size dependency. On the other hand, no differences between the shear banding around these two size of the plate are found in these numerical analyses. The soil domain is continuous in the finite element analysis and can not have the discrete deformation to represent the progressive failure. The size dependency explained by Khatri and Kumar (2011), and Sakai and Tanaka (1998) is not observed at this numerical analysis. The results of this part have more agreement with the observation of Ilamparuthi et al. (2002). In his experimental data, N_q value only depends on the H/D and soil's properties.

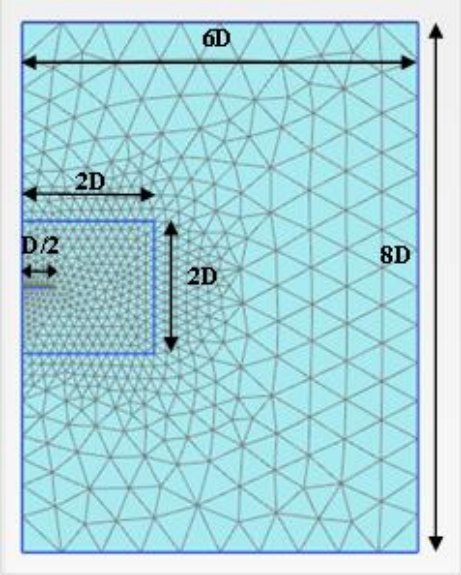

Figure 4-11 Meshing Information

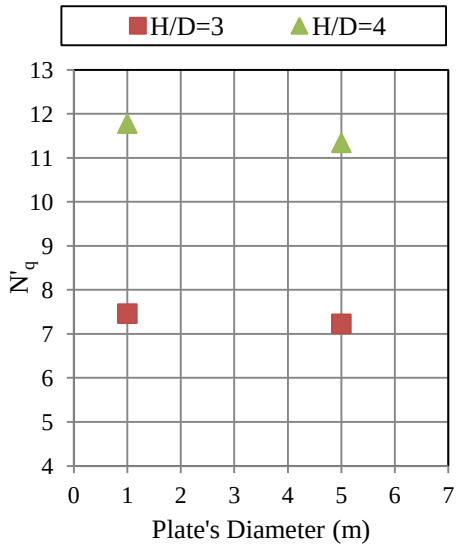

Figure 4-12 Effective breakout factor for different plate's sizes

Table 4-5 Results of Size Effect's Analyses

H/D	N'_{q1}	N'_{q5}	$(N'_{q1} - N'_{q5}) / N'_{q1} * 100$
3.0	7.5	7.2	3%
4.0	11.8	11.3	4%

The size effect analyses are repeated for a soil that its friction angle is reduced by increasing the mean effective stress. Duncan and Wong (1999) conducted hyperbolic stress–strain parameters for drained soil, based on laboratory test data. Equation 4-13 is borrowed from Duncan and Wong (1999) to estimate the friction angle at the different level of the soil. At this equation φ_0 is related to the case where σ_3 is equal to the atmospheric pressure (p_a = 101.3 kPa), φ_0 and $\Delta\varphi$ are assumed equal to 38 and 7 degrees.

$$\varphi = \varphi_0 + (\Delta\varphi) * [\log_{10}(\sigma_3 / p_a)] \qquad \text{Equation 4-13}$$

The soil domain is divided to several sublayers with a thickness equal to 2 m and the friction angle for each sublayer using try and error method is calculated based on Equation 4-13 and assigned. The rest of soil parameters are assumed the same as the properties of sand with RD=80% at Table 4-2, without dilatancy angle ($\psi = 0$). The results as breakout factors are presented in Figure 4-13. The results show that by increasing the plate size break out factor decreases. This reduction is almost equal to 12.3% for H/D=3 and 12.7% for H/D=4 [Table 4-6].

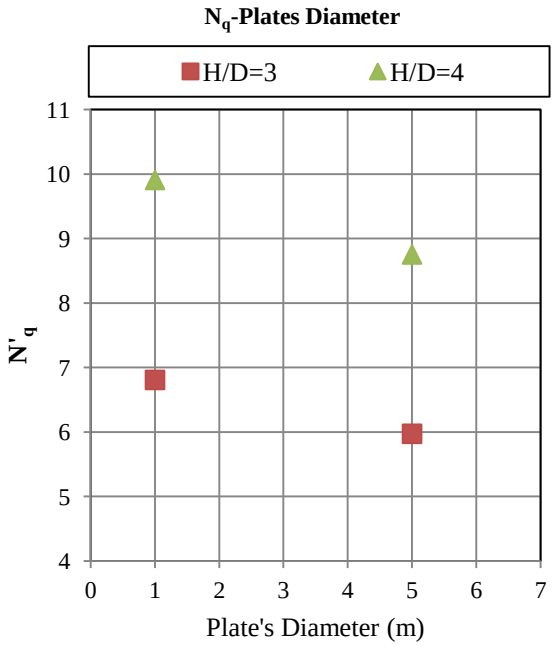

Figure 4-13 Effective break out factor for different plate's sizes by considering stress dependent friction for the sand

Table 4-6 Results of Size Effect's Analyses for Sands with Stress Dependent Friction Angle

H/D	N'_{q1}	N'_{q5}	$(N'_{q1} - N'_{q5}) / N'_{q1} * 100$
3.0	6.8	6.0	12.3%
4.0	9.9	8.8	12.7%

In Figure 4-14 deviatoric shear strain around the plates with diameters equal to 1 m and 2 m are presented (unit is meter) at H/D=4 at the highest resistance. The shear band around the bigger plate (D=5m) is more intense and vast in comparison with the shear band around the plate anchor with a diameter equal to 1m.

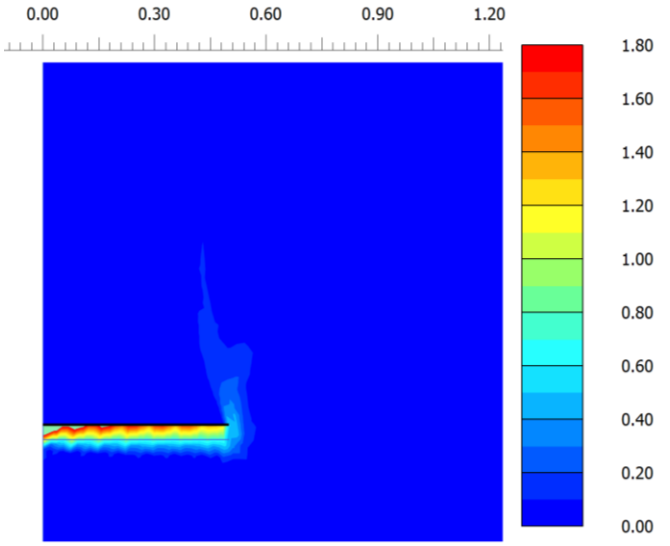

(a)

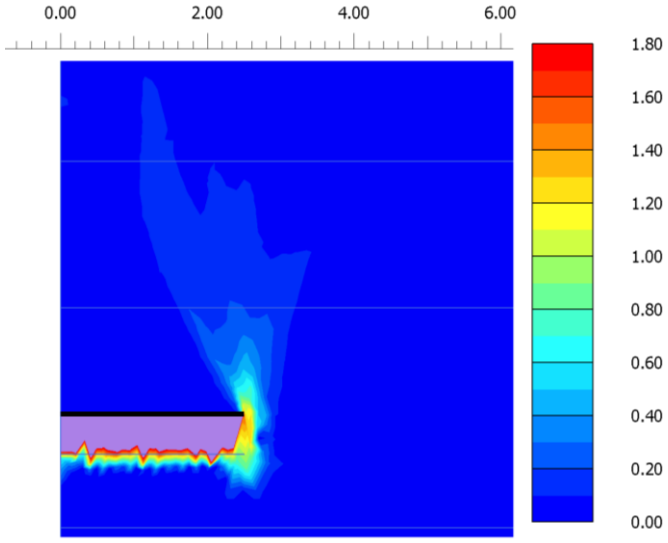

(b)

Figure 4-14 Deviatoric shear strain around the plate anchor with diameter equal to (a) 1m and (b) 5 m

The size effect is observed just for the sands that have stress dependent friction angle. As a result of size effect, bigger plate gives the smaller breakout factor. At this case, soil's

partial shape can change the capacity. According Duncan and Wong (1999), the stress dependency of the friction angle in the sand with rounded grain is less than the same soil with angular grain.

4.8 Summary and Conclusions

In this study, the pullout capacity of a horizontal circular plate anchor in sand is investigated using numerical analyses to study the influence of stress-dependent modulus, friction angle dilation, and the size of the plate on the pullout capacity of plate anchors. The capacities of plate anchors are assessed through the application of displacement control approach. A series of large deformation analyses are performed using HS model in dry sands, and the results are compared with available experimental data. The drained large deformation analyses are conducted in the saturated sands using two different constitutive models (MC and HS models) and the results are presented and discussed. The effects of dilatancy angle and size of the plate in saturated sands at different embedment depths are investigated. The main conclusions from this study are summarized in the following:

- The results of the large deformation analyses using HS Model are in good agreement with existing experimental data for the dry loosely packed sands at shallow embedment depths (H/D<6). For higher embedment depths (H/D>6), this analysis overpredicts the experimental data. It can be related to the assumed dilatancy angle. Assuming the higher amount of the dilatancy angle results a higher capacity especially at the deep embedment depths.
- The results of the large deformation analyses using HS Model are in an encouraging agreement with existing experimental data for the dry densely packed sands at embedment ratio, between1 to 10.
- In saturated sands, the results show that although MC cannot explain the hardening behavior of the sands. However, a very good agreement is found with a nonlinear soil model such as HS model at the shallow depths ($H/D \leq 4$). The advantage of using MC model over HS model is obviously fewer model parameters. MC model requires just five parameters while HS model needs ten. At larger depths, MC model provides lower capacities.

- MC has a failure surface fixed in stress space and a stress independent stiffness. HS model has a confining stress dependent modulus. Stresses and consequently modulus intensely increase, locally around the plate by applying a prescribed displacement at HS model. HS model by having expanding failure surface and stress dependent stiffness provides higher capacity than MC model at saturated sands. This difference becomes significant at larger depths with higher initial stresses.
- The ultimate residual capacity in the saturated sands is the same for MC and HS models.
- The increase in dilatancy angle increases the capacity in the saturated sands by extending the failure zone. The effect of dilatancy angle in the shallow embedment depths and loose sands is negligible. However, this effect becomes significant at larger embedment depths and dense sands. For a dense saturated sand with relative density of 80% and a dilatancy angle equal to 8 degrees, capacity increases by more than 40% at a $H/D=7$ while this increase is just 10% at a $H/D=1$.
- The size effect in different embedment depths is investigated in the dense saturated sands. Analyses are conducted by using plate anchors with diameters equal to 1 and 5 m at embedment depths ($H/D=3,4$). The results show that the size effect is negligible in this range of assumed data when the friction angle is independent of stress level. When friction angle is changing (decreasing) by increasing the stress level, the bigger plate provides smaller breakout factor.

4.9 References

Andreadis, A., and Harvey, R.C. (1981). "A design procedure for embedded anchors". *Applied Ocean Research, 3(4): 171–182.*

Balla, A. (1961). "The resistance to breaking out of mushroom foundations for pylons". *In Proceedings of the 5th International Conference on Soil Mechanics and Foundation Engineering, Paris, France, Vol. 1, pp. 569–576.*

Brinkgreve, R. B. J. and Vermeer, P. A. (1997). Plaxis finite element code for soil and rock analysis- Version 7. Balkema, Rotterdam.

Brinkgreve, R. B. J. (2005). "Selection of soil models and parameters for geotechnical engineering application." *In: Yamamuro, JA and Kaliakin, VN, editors. Geotechnical Special Publication No.128, ACSE, pg 69-98.*

Brinkgreve, RBJ. Engin, E. Engin, H.K. (2010). "Validation of empirical formulas to derive model parameters for sands" *Numerical Methods in Geotechnical Engineering – Benz & Nordal (eds)*

© 2010 Taylor & Francis Group, London, ISBN 978-0-415-59239-0.

Das, B. M., Shin, E. C., Dass, R. N., and Omar, M. T. (1994). ''Suction force below plate anchors in soft clay.'' *Marine Georesources and Geotechnology, 12, 71–81.*

Dickin, E, A (1988). "Uplift behavior of horizontal anchor plate in sand". *Journal of Geotechnical Engineering, Vol.114, No.11.*

Dickin, E.A. and Laman, M. (2007). "Uplift response of strip anchors in cohesionless soil." Advances in Engineering Software, 1(38), 618-625 (2007).

Dickin. Edward A. (1989). "Uplift behavior of horizontal anchor plates in sand." Journal of Geotechnical Engineering, Vol.114, No.11.

Duncan, J. M., and Wong, K. S. (1999). "User's Manual for SAGE: Volume II – Soil Properties Manual." *Center for Geotechnical Practice and Research, Dept. of Civil Engineering, Virginia Polytechnic Institute and State University, Blacksburg.*

Fityus, S. G. Yu, S. and Pearce, A.G. (2000). "Failure mechanisms of vertically loaded plate anchors in sand" *ISRM International Symposium, International Society for Rock Mechanics, 19-24 November, Melbourne, Australia.*

Kupferman, M. (1965). ''The vertical holding capacity of marine anchors in clay subjected to static and cyclic loading.'' *MSc thesis, Univ. of Massachusetts, Amherst, Mass.*

Ilamparuthi, K. Dickin, E.A. and Muthukrisnaiah, K. (2002). " Experimental investigation of the uplift behavior of circular plate anchors embedded in sand". *Can. Geotech. J. 39: 648-664.*

Merifield R.S, Lyamin A.V, Sloan S.W and Yu H.S (2003). "Three-Dimensional lower bound solutions for stability of plate anchors in clay." *Journal of Geotechnical and Geoenvironmental Engineering 129: 243–253.*

Khatri, V. N and Kumar, J. (2011) "Effect of anchor width on pullout capacity of strip anchors in sands"*, Can. Geotech. J. 48: 511-517.*

Koutsabeloulis, N. C., and Griffiths, D.V. (1989). "Numerical modeling of the trap door problem." *Geotechnique, 39(1): 77-89.*

Merifield, R.S and Sloan, S.W. (2006) "The ultimate pullout capacity of anchors in frictional soils." *Can. Geotech. J. 43: 852-88.*

Meyerhof, G. G., and Adams, J.I. (1968) "The ultimate uplift capacity of foundations." *Canadian Geotechnical Journal, 5(4): 225-244.*

Murray, E.J and Geddes, J.D. (1987) "Uplift of anchor plate in sand" *Journal of Geotechnical Engineering, Vol.113, No.3.*

Niroumand, H. Kassim, k.A. and Nazir, R. (2013) "The influence of soil reinforcement on the uplift response of symmetrical anchor plate embedded in sand" *Measurement: Journal of the International Measurement Confederation, 46: 2608-2629.*

PLAXIS 2D Manuals (2012), PLAXIS BV, Delft, The Netherlands

Rowe, R. K and Davis, E. H. (1982) ''The behavior of anchor plates in sand" *Geotechnique, Vol.32, pp. 25-41.*

Ovesen, N.K. (1981) "Centrifuge tests of the uplift capacity of anchors." *In Proceedings of the 10th International Conference on Soil Mechanics and Foundation, Rotterdam, The Netherlands. Vol. 1, pp. 717-722.*

Sakai, T. and Tanaka, T (1994): “Finite element analysis of progressive failure and scale effect of anchor problems in dense sand,” *Int. Conf. on Computational Methods in Structural and Geotech. Engrg., Vol.4, pp.1283-1288.*

Sakai, T. and Tanaka, T (1998): “Scale effect of shallow circular anchor in dense sand.” Soils and Foundations, Japanese Society of Soil Mechanics and Foundation Engineering.” Vol. 38, No 2, 93-99, June 1998.

Schanz, T., Vermeer, P. A. and Bonnier, P. G. (1999): “The hardening soil model: formulation and verification” Beyond 2000 in Computational Geotechnics, 281-296.

Tagaya, K. Tanaka, A. and Aboshi, H. (1983): “Application of finite element method to pullout resistance of buried anchor.” Soils and Foundations, Japanese Society of Soil Mechanics and Foundation Engineering.” Vol. 23, No 3, Sept. 1983.

Tagaya, K. Scott, R.F. and Aboshi, H (1988): “Pullout resistance of buried anchor in sand” Soils and Foundations, Japanese Society of Soil Mechanics and Foundation Engineering.” Vol. 238, No 3, 114-130, Sept. 1988.

Tanaka,T. and Sakai, T. (1993). “Progressive failure and scale effect of trap-door problems with granular materials” *Soil and Foundations Vol. 33, No 1, 11-22, Mar. 1993 Japanese Society of Soil Mechanics and Foundation Engineering.*

Chapter 5 Shape Effects on the Failure Mechanism of the Vertically Loaded Plate Anchors in Sands: 3D Analyses

This chapter will be submitted to the International Journal of Geomechanics. The authors are Zahra Aghazadeh Ardebili, S.M.ASCE[1]; M.A. Gabr, F.ASCE[2]; M.S. Rahman[3]

5.1 Abstract

A comprehensive 3D numerical study is performed to investigate the behavior and capacity of the plate anchors in sands subjected to the pull out loading. The aims of this study are verifying the ability of 3D numerical modeling by experimental data in capturing the failure mechanism, investigating the shape effect on the plate's behavior and identifying the accuracy of 2D modeling in comparison with 3D modeling. All of these investigations are performed considering other dominant effective parameters such as density and embedment depths. The failure mechanism of a circular plate anchor is calibrated by an existing experimental data in the literature and then the failure mechanisms of the square and strip plates are investigated. The shape effect on the breakout factor in the dense and loose sands in the shallow and deep plates is investigated. The differences between the results from 2D and 3D numerical analyses are investigated. The efficiency of using of axisymmetric and plane strain conditions for modeling the circular and strip plates at different embedment depths are presented.

Key Words: Plate Anchors in Sands; 3D Finite element analysis; Sands, Failure mechanism; Shape factor.

[1] Graduate Research Assistant, North Carolina State Univ., Campus Box 7908, Raleigh, NC 27695 (corresponding author). E-mail: zaghaza@ncsu.edu
[2] Alumni Distinguished Undergraduate Professor, North Carolina State Univ., Campus Box 7908, Raleigh, NC 27695.E-mail: gabr@ncsu.edu
[3] Professor, North Carolina State Univ., Campus Box 7908, Raleigh, NC 27695.E-mail: rahman@ncsu.edu

5.2 Introduction

The development of anchoring systems for offshore renewable energy devices and other energy-related infrastructures is a challenging task. These devices are in most cases free floating and flexibly anchored to buoys or directly to the seabed using one or more mooring lines. Using these foundation systems at shallow water depths needs to investigate the behavior of them in sandy soils.

The capacity of the plate anchors in sands is presented in the literature in the form of dimensionless breakout factor (N_q) which is a function of the soil properties and the geometry. Many studies have been performed on the plate anchors in sands. Some of the related finite element studies were conducted by Row and Davis (1982), Dickin and Laman (2007), Kumar and Kouzer (2007) and Vishwas, et al. (2011).

Most of the initial studies of plate anchors in sand were empirical, More (1955), Morse (1959), Bella (1961) and Downs and Chieurzzi (1966). They considered a failure mechanism and calculated the uplift resistance by using equilibrium equations. Saeedy (1987), Sarac (1989), Koutsabeloulis& Griffiths (1989), Basudhar & Singh (1994), kanakapura et al (1994), Ghaly & Hanna (1994), Smith (1998), Merifield and Sloan (2006), and White et al (2008) used limit equilibrium for estimating capacity of plate anchors by assuming a failure mechanism.

Meyerhof and Adams (1968) proposed an approximate semi-empirical theory for calculating the uplift capacity of circular, rectangular and strip anchors based on laboratory tests. Vesic (1971) used the cavity expansion method for the strip and circular plate anchors. Murry and Geddes (1987) studied plate anchors both theoretically and experimentally. They performed several laboratory tests in the medium sand to investigate the effect of size and shape of plates, plate roughness, depth of embedment and sand density. They used a limit analysis method (upper bound and lower bound solution) and found that all the methods overestimated the ultimate pull out capacity in medium to loose sand.

Researchers proposed several failure mechanisms within these seven decades [Majer 1955]. Liu et al. (2012) summarize the three distinctive failure mechanisms proposed by

several researchers in Figure 5-1. Majer (1955) proposed a cylindrical failure mechanism with frictional edges [Figure 5-1.a]. The uplift capacity at this failure mechanism comes from the weight of soil cylinder and the mobilized shear resistance along the failure edges. In the reality in many cases, the failure zone is larger than the cylinder above the anchor and this failure mechanism, underestimates the capacity for them [Ilamparuthy et al. 2002; Liu et al. 2012]. The truncated conical failure mechanism [Figure 5-1 b] is introduced and proposed by Mors (1959), which had an apex angle equal to $90+\varphi$, where φ is the soil's friction angle. He neglected the shear resistance at the edges and the capacity at this case is equal to the weight of the truncated cone. This failure mechanism overestimates the capacity at the deep embedment depths. At the real cases, the failure mass is not extended to the surface and localized around the plate. On the other hand, It underestimates the shallow anchors' capacity because of neglecting the sides shear resistance [Liu et al. 2012]. Balla (1961) and Baker and Kondner (1966) observed a circular failure surface that intersects the ground surface with an angle equal to $45-\varphi/2$, presented at Figure 5-1 (c). Meyerhof & Adams (1968) performed some full-scale and model tests of transmission towers' footings. They found that the failure surface in sand depends on relative density and rigidity of soil and depth to width ratio of the foundation. Fityus et al. (2000) and Liu et al. (2012) considered the effect of soil densities and embedment in their experimental works. Fityus et al. (2000) used a circular plate with a diameter equal to 7.5 (cm) with deep and shallow embedment ratios (H/D=2 and H/D=6) in loose and dense sands. They monitored the deformation of the soil during the uplift loading and captured the failure mechanisms. They also explained the reason for oscillations in the pullout resistance by capturing the discrete free flow of sand grains under the gravity into the created gap bellow the plate. Liu et al. (2012) presented an experimental investigation on soil deformation around uplift plate anchors by using digital image correlation (DIC). They investigated the influence of particle size, soil density and anchor embedment depth on soil deformation.

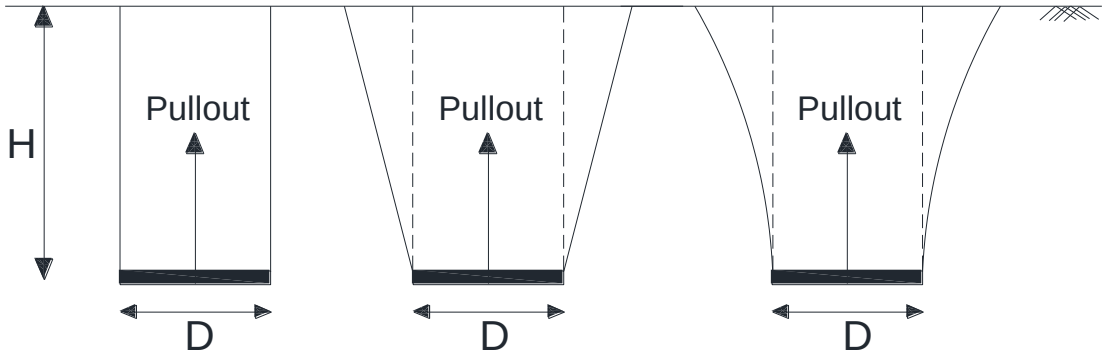

(a) (b) (c)

Figure 5-1 Different failure modes of a soil anchor (a) frictional cylinder, (b) truncated cone; (c) circular failure surface (summorized by Liu, et al. 2012)

5.3 Aims of This Study

The accuracy of the analytical methods in predicting the pullout capacity under axial pullout loading, and its expression in terms of a breakout factor, is dependent on the assumed failure mechanism. Therefore capturing the failure mechanism of plate anchors in sands, considering different embedment depths and densities, is an important aspect of the estimation of the pullout capacity. Also, understanding the shape effect on the development of the failure surface and the breakout factor can assist in the design of these foundation systems.

Although many studies experimentally, numerically and analytically are conducted on the plate anchors at sands over the past seven decades, comparing the failure mechanism of different plate's shape at different embedment depths and soil densities is still an interesting aspect to be investigated.

In this paper, the 3D numerical analysis is used to study the failure mechanism of a circular plate anchor in sand. The numerical model is calibrated using experimental data reported in the literature. After calibration of the model, analyses are conducted using square

and strip plates to investigate the effect of the plate's shape on the emergence of the failure plane and breakout factor. The results are compared at the different embedment depths for loose and dense sands and are discussed in the context of the pullout breakout factor.

In continue, since axisymmetric and plane strain conditions are frequently used to model the circular and strip plate anchors in 2D numerical analysis a comparison between 2D and 3D modeling is studied. The results conducted from these two methods are compared, and the accuracy of 2D models is investigated.

5.4 Numerical Model

A circular plate anchor with the diameter of 7.5 cm [Fityus et al. 2000] is numerically modeled in PLAXIS 3D with a thickness of 1.5 cm and steel stiffness= 200 Gpa. The embedment ratio assumed equal to 2 and 6 to simulate shallow and deep plates, [Fityus et al. 2000] respectively. Hardening Soil model is considered and drained large deformation analysis is conducted. For simulating Fityus et al. (2000) experimental condition, the sand is considered as dry. Exact soil properties of the dense and loose sand, which were used by Fityus et al. (2000) in their experimental program, were not reported. The following equations (Brinkgrave 2005) are used to estimate relatively proper soil properties for relative densities equal to 30% (loose sand) and 80% (dense sand). The parameters needed for developing the Hardening Soil model are saturated and unsaturated densities (γ_{unsat} , γ_{sat}), stiffness parameters of triaxial compression (E_{50}^{ref}), triaxial unloading (E_{ur}^{ref}) and oedometer loading (E_{oed}^{ref}) at a reference stress level (p^{ref} which PLAXIS considers as equal to 100 stress units), power (m) for calculating stress dependent stiffness, unloading and reloading Poisson's ratio (ν_{ur}), cohesion (c), friction angle (φ) and a non-associate flow rule parameter which is dilatancy angle (ψ) and failure ratio parameter (R_f) which most of the time is assumed equal to 0.9 and refers to the deviatoric stress level at failure.

$$\gamma_{unsat} = 15 + 4.0RD/100 \ [kN/m^3] \qquad \text{Equation 5-1}$$

$$\gamma_{sat} = 19 + 1.6RD/100 \ [kN/m^3] \qquad \text{Equation 5-2}$$

$$E_{50}^{ref} = 60000RD/100\ [kN/m^3]$$ Equation 5-3

$$E_{ur}^{ref} = 60000RD/100\ [kN/m^3]$$ Equation 5-4

$$E_{oed}^{ref} = 180000RD/100\ [kN/m^3]$$ Equation 5-5

$$m = 0.7 - RD/320$$ Equation 5-6

$$\varphi' = 28 + 12.5RD/100\ [°]$$ Equation 5-7

$$\psi = -2 + 12.5RD/100\ [°]$$ Equation 5-8

$$R_f = 1 - RD/800$$ Equation 5-9

The soil properties are summarized in Table 5-1.

Table 5-1 Assumed Soil Properties

RD	γ_{unsat} (kN/m^3)	γ_{sat} (kN/m^3)	E_{50}^{ref} (kN/m^2)	E_{oed}^{ref} (kN/m^2)	E_{ur}^{ref} (kN/m^2)	m	$\varphi(°)$	$\psi(°)$	R_f
30	16.2	*19.48*	18000	18000	54000	0.606	31.8	1.8	0.963
80	18.2	*20.28*	48000	48000	144000	0.450	38.0	8.0	0.900

Because of symmetry, only ¼ of the plate is modeled to reduce the running time. The convergence analyses are conducted. A medium mesh with a finer mesh around the plate with a coarseness ratio of 0.125 is sufficient. The analysis is performed as displacement control type in which a series of prescribed displacements is applied uniformly to the plate, and corresponding resistance on the plate is monitored. The load-displacement curve is developed, and the capacity is taken as equal to the ultimate load where the load displacements curve becomes plateau. The model domains and the developed mesh for deep plates are shown in Figure 5-2.

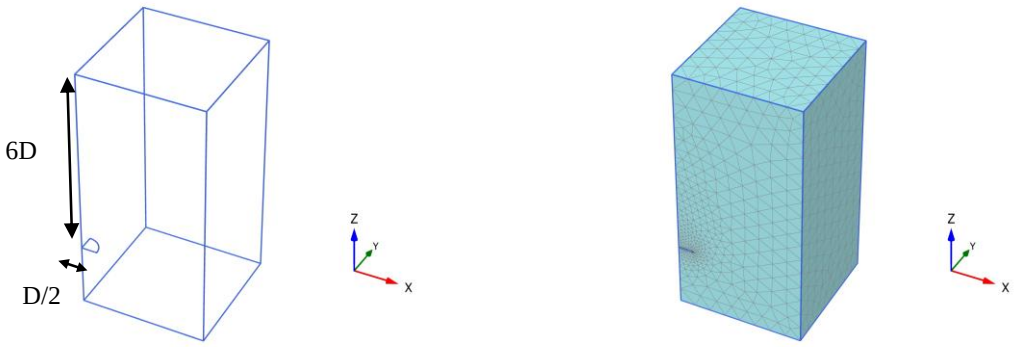

Figure 5-2 Model domain and mesh for a circular deep embedded plate

5.5 Model Calibration

The computed load displacement results are compared with the experimental data from Fityus et al. (2000) in Figure 5-3. The comparison shows a good agreement between the computed and measured responses except in the case of the deep plate at the loose sand. Since the exact properties of the sand in this experimental work are unknown, this difference in results for the case of the deep anchor at the loose sand might be due to the assumed properties. For example, the dilatancy angle has a significant effect at the deep embedment. The differences in results might be attributed to a small dilatancy angle (1.8) according to the Equation 5-8, while a higher value was the case for Fityus et al. (2000)'s loose sand.

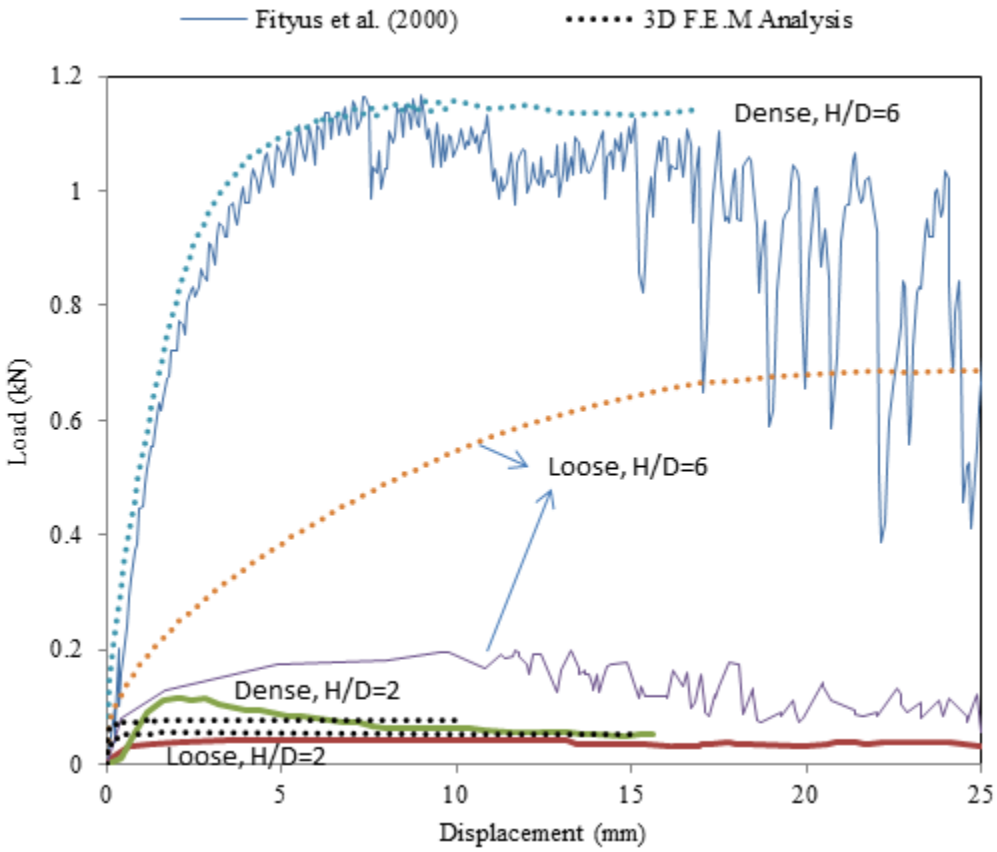

Figure 5-3 Load displacement curves for different embedment depths and soil types

Niroumand et al. (2013) studied the plate anchors numerically and experimentally. Since he used Hardening soil model, a series of analysis based on his assumed soil properties (Table 5-2) for loose and dense sands are also performed for validation of the analyses. The dimensionless breakout factor for dry analysis is considered as:

$$N_q = \frac{F}{\gamma AH} \qquad \text{Equation 5-10}$$

Where the F is the pull out force (kN), γ (kN/m^3) is the unit weight of soil, A (m^2) is the area of plate anchor and H (m) is the embedment depth.

As shown in Figure 5-4 the results from the numerical analysis performed herein (3D) are compared with the experimental analysis. In the loose sands, the results are compared with the experimental data reported by Niroumand et al. (2013), Andreadis and Harvey (1981)

and Balla (1961) all of them used a loose sand with friction angle equal to 38 degree. The diameter of the circular plate used by Andreadis and Harvey (1981) is not reported, but Balla (1961) used circular plates with diameters equal to 60 mm and 120 mm. The results have an encouraging agreement with the experimental ones, except at the larger depths (H/D>6) where, they deviate slightly from experimental data and overestimate the breakout factor. The comparison is between this study and the experimental data with a common friction angle. Assuming a higher dilatancy angle in the analyses rather than its real amount (unreported) at the tests, can be the reason of this overprediction. The results show very good agreement with experimental data for dense sand [Figure 5-4 b]. Ilamparuthi, et. al (2002) used different plate size at the different soil densities the results in this graph related to his 100 mm circular plate at the dense sand with friction angle equal to 43 degree (He did not obsereved size effect on the break out factor). Murry and Geddes (1987) used circular plate anchors with diameters equal to 51 and 89 mm in the sand with friction angle equal to 44 degrees. The comparison shows a good agreement between the 3D analysis and experimental data from Murry and Geddes (1987), Ilamparuthi, et al. (2012) and Niroumand, et al. (2013). Also, a series of 2D analyses were performed (for properties at Table 5-2) using 2D axisymmetric model. These comparisons show that using 3D numerical analysis provides the same capacity as a 2D axisymmetric model.

Table 5-2 Soil Parameters Used by Niroumand et al.(2013)

Parameter	γ (kN/m^3)	E_{50}^{ref} (kN/m^3)	E_{oed}^{ref} (kN/m^3)	E_{ur}^{ref} (kN/m^3)	m	$\varphi(^\circ)$	$\psi(^\circ)$	c (kN/m^3)	R_f	K_0	ν_{ur}
Loose Packing	15	20000	20000	60000	0.5	38	8	0.5	0.9	0.38	0.2
Dense Packing	17	30000	30000	90000	0.5	44	14	0.5	0.9	0.32	0.2

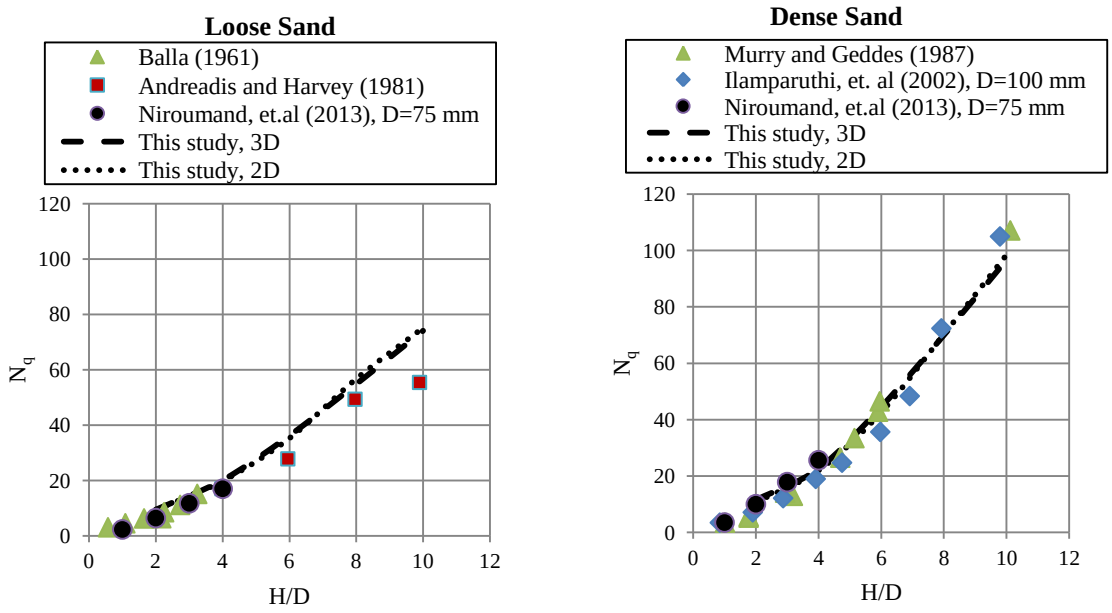

(a) (b)

Figure 5-4 Comparison of this study's results with experimental data (a) loose packing, (b) dense packing

5.6 Emerging Failure Surface

The failure mechanism depends on the density of the soil and the embedment ratio. In Figure 5-5 and Figure 5-6 the deformation of the soil and plastic points around the plate anchor at the ultimate resistance are compared with the experimental ones monitored by Fityus, et al. (2000). At the shallow embedment depth (H/D=2), the failure wedge has a shape of a cylinder in the loose sand while It has a truncated conical shape in the dense sand. These shapes present a very good agreement with Fityus et al. (2000)'s monitored failure mechanisms. For the larger depth (H/D=6), failure mechanism at the loose sand is a bulb shaped one (spherical shape) and does not reach the surface but in the dense sand the failure mechanism is a combination of a truncated cone and a U- shaped. Liu, et al. (2012) reported similar observations about the sand deformation around the uploaded plate. The confining pressure at the soil surface is too low and soil at this zone starts to failure by small amount of

the deformation. By increasing the displacement, the plastic points are developed around the plate but they do not extend to the surface at the loose sand and deep embedment ratio. At this case, the soil mass around the plate reaches to the failure before connecting with the surface's failed points. In the dense sand, these two failed mass are connected before the maximum resistance is mobilized.

Loose H/D=2 Dense H/D=2

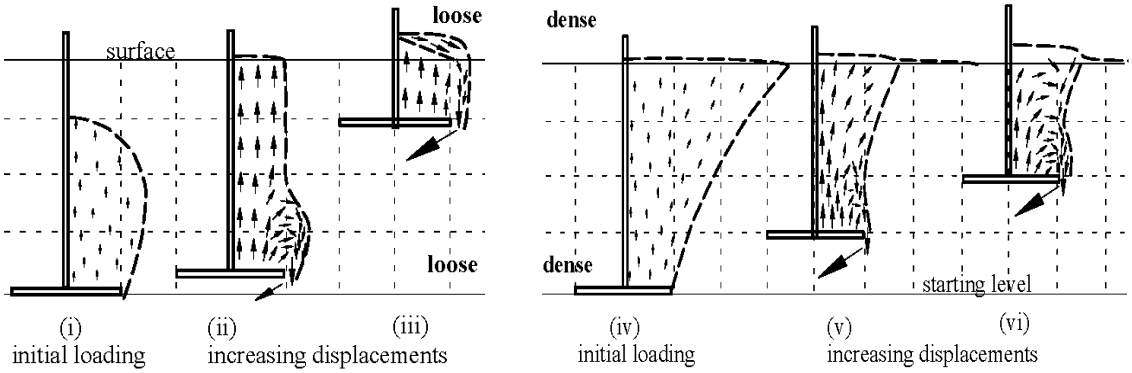

(a)

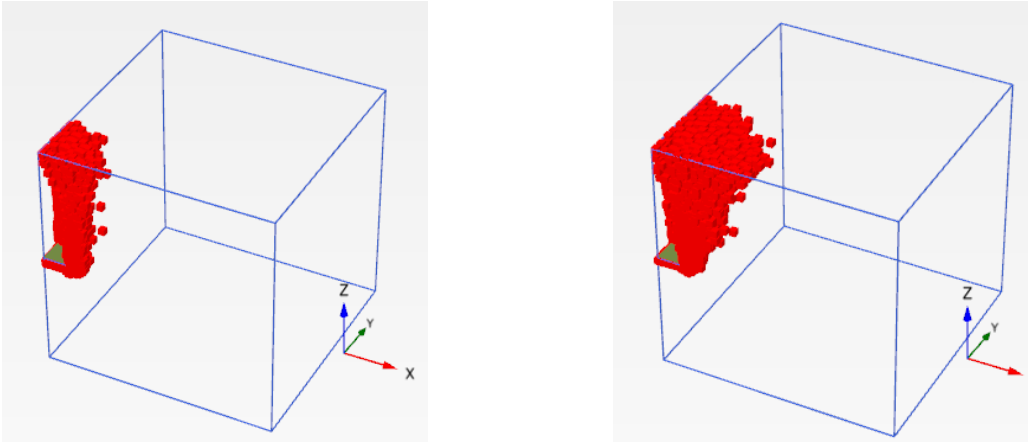

(b)

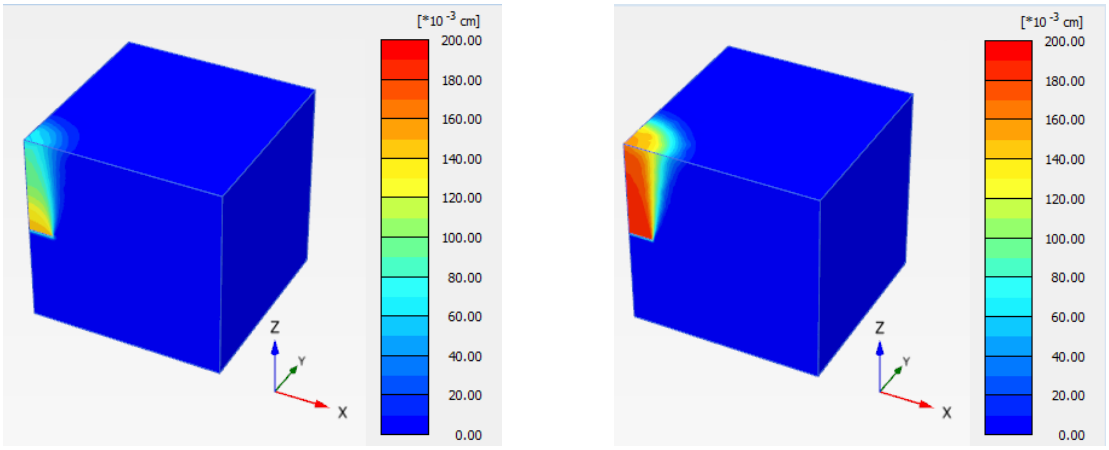

(c)

Figure 5-5 Comparison of failure mechanism at shallow embedment depths (a) Fityus et al. (2000) (b) plastic points around the plate at this study, (c) total displacement around the plate at this study

Loose H/D=6

Dense H/D=6

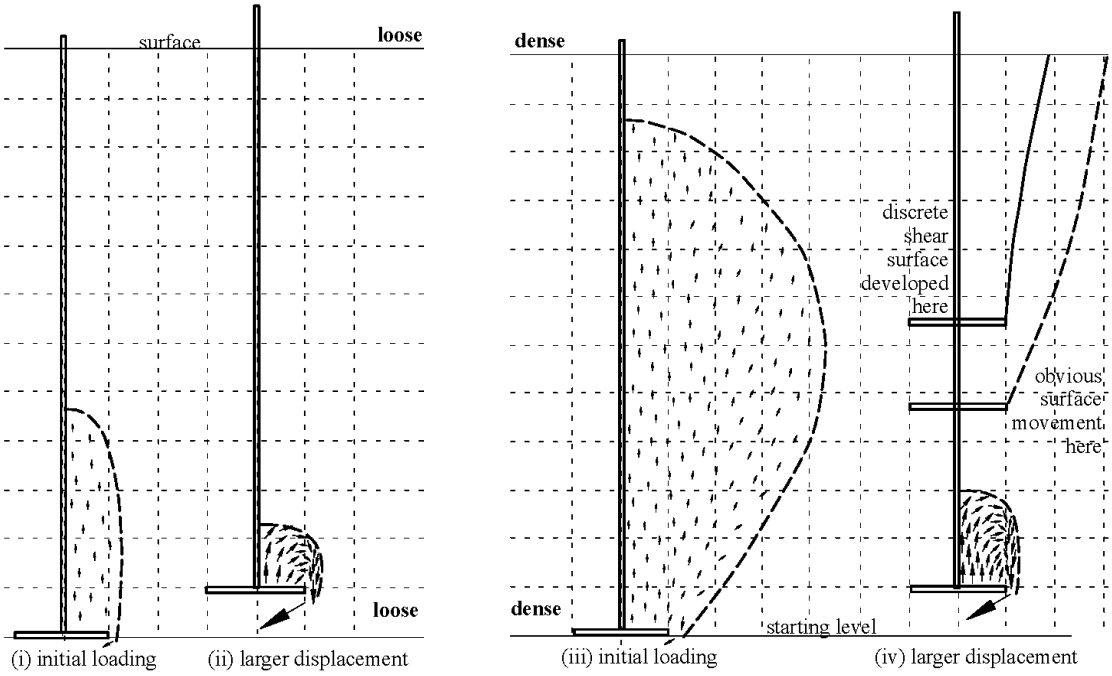

(a)

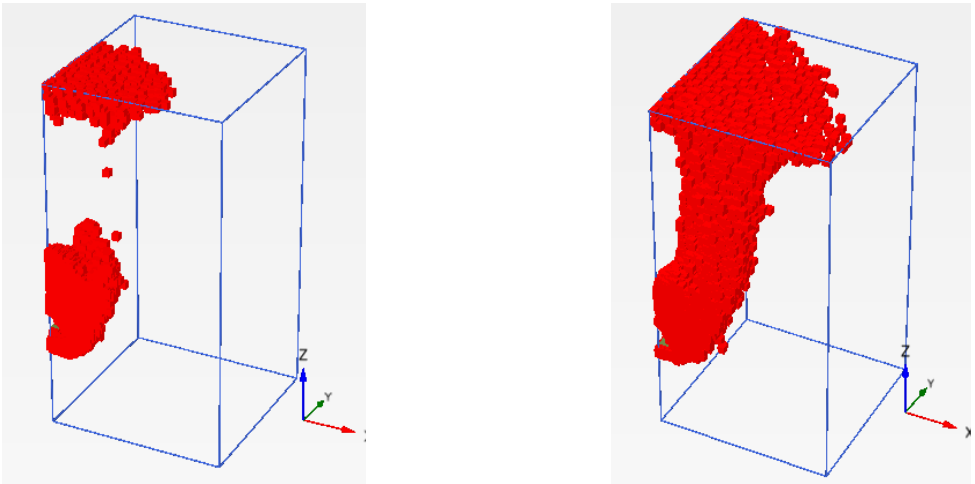

(b)

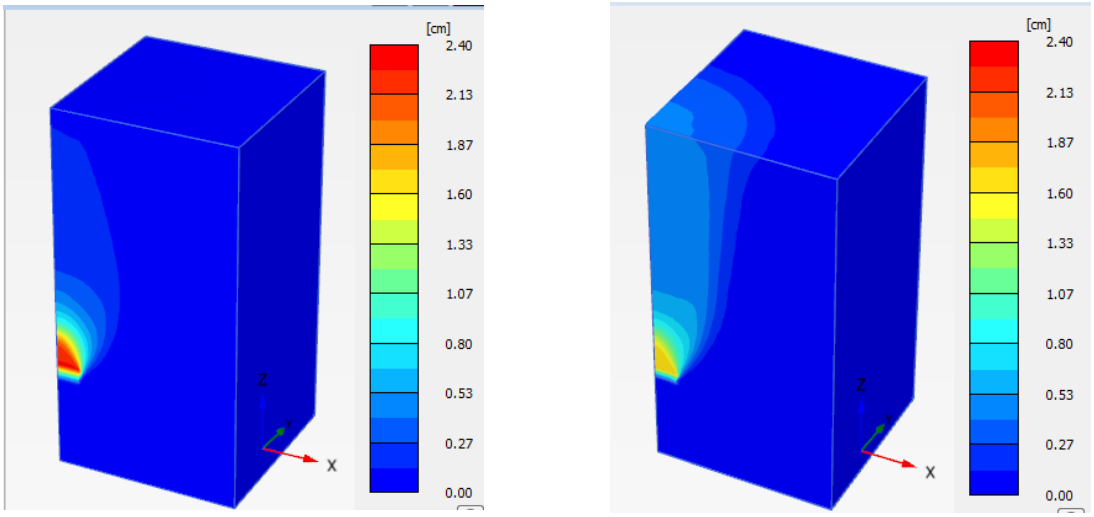

(c)

Figure 5-6 Comparison of failure mechanism at deep embedment depths (H/D=6) (a) Fityus et al. (2000) (b) plastic points around the plate, (c) total displacement around the plate

5.7 Square and Strip Plates

The shape effect on the breakout factor and failure mechanism is investigated by analyzing a square and a strip plates with a width equal to the diameter of the studied circular plate [Figure 5-7]. Analyses are performed on the loose and dense sand (Table 5-1). In Figure 5-8 N_q for different plates shape at the different embedment, depths are shown for both loose and dense sand. N_q values increase with embedment depths in all of the cases. The density has a significant effect on the N_q value such that N_q in the dense sands is significantly higher than that in loose sands at the same embedment depth. The circular plate anchor provides higher N_q value in comparison with a square and strip plates. Strip plates provide the least break out factors.

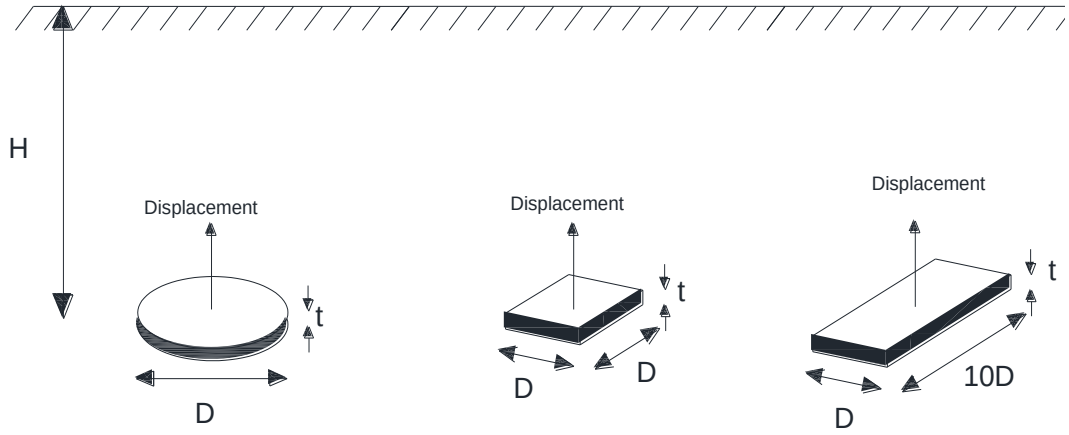

Figure 5-7 different shapes of applied plate anchors

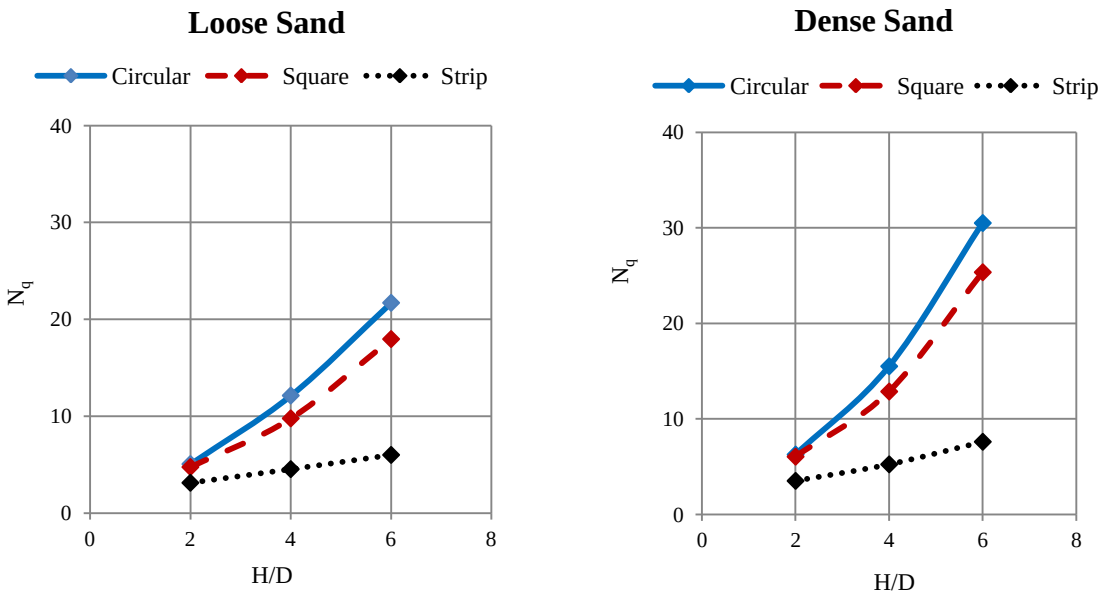

(a) (b)

Figure 5-8 Dimensionless breakout factor for different plate's shapes at (a) loose sand, (b) dense sand

Figure 5-9 shows the mobilized shear strength around the circular, square and strip plates at H/D=6 and dense sand. If the mobilized shear zone divided by the area of the plate is considered as a factor of effectiveness, the higher factor gives higher N_q. According the mobilized shear strength zone in Figure 5-9, the circular, square and strip plates provide consequently the highest to lowest breakout factor. Figure 5-10 presents the load displacement curves for these three shape of plate anchors for dense sand and H/D=6.

Circular Square Strip

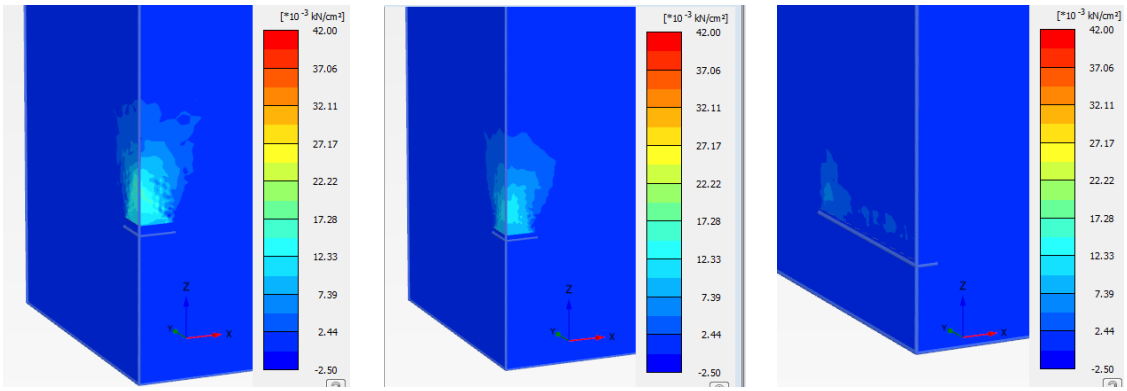

Figure 5-9 The mobilized shear strength at the highest resistance around the plate

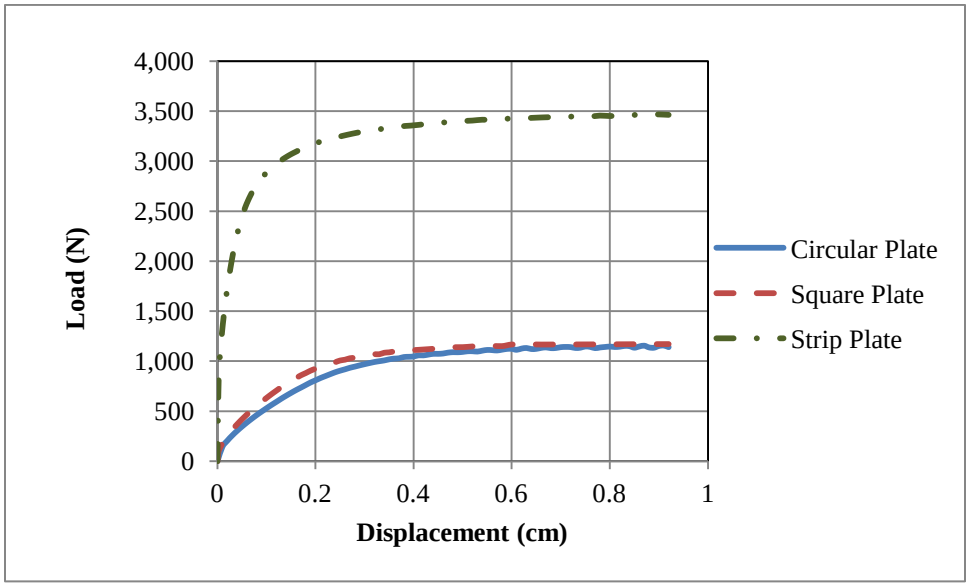

Figure 5-10 The load displacement curve for dense sand and H/D=6

In Figure 5-11, the shape factors of these plates are presented as a ratio of breakout factors ($N_{q\ circular}$/ $N_{q\ strip\ or\ square}$). The square plate provides almost the same amount of the

breakout factor came from the circular plate at H/D=2. The results are deviated slightly by increasing the depth such that at H/D=6 circular plate provides 20% higher N_q value. About the strip plate, circular plate provides higher breakout factor than strip plate, the ration of $N_{q\ circular}/\ N_{q\ strip}$ increases by embedment depth such that it is 1.8 at H/D=2 and almost 4 at H/D=6.

In Figure 5-12 the failure mechanism of square plate anchor are presented at H/D=2 and H/D=6 for loose and dense sands. The failure zones show similarity with those from the circular plate. In the case of square plate and shallow embedment depth (H/D=2), the failure mechanism is a truncated convex polyhedron. It has significantly steeper sides at the dense sand in comparison with that in loose sand. In the larger embedment depth (H/D=6), the failure mechanisms are also the same as a circular plate while a convex polyhedron is replaced instead of conical shape.

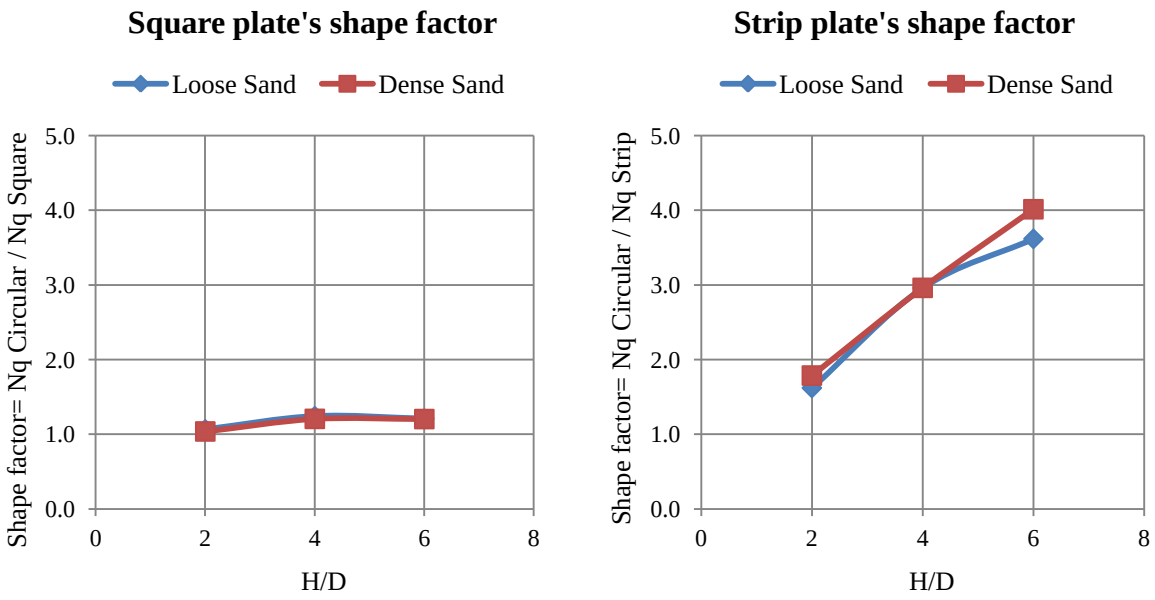

(a) (b)

Figure 5-11 Shape effect at different embedment depths for (a) square and (b) rectangular plates

Loose H/D=2

Dense, H/D=2

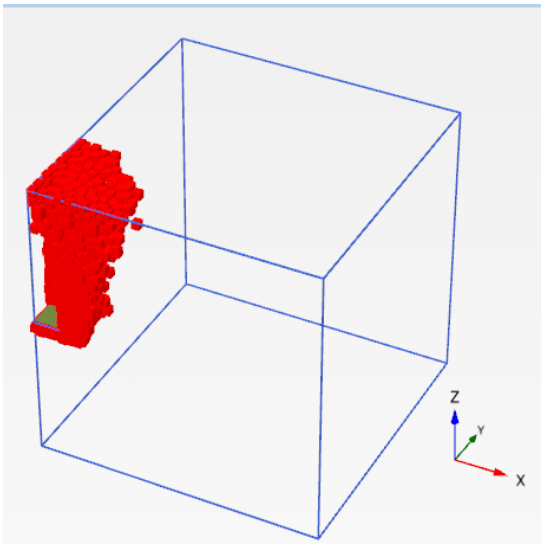

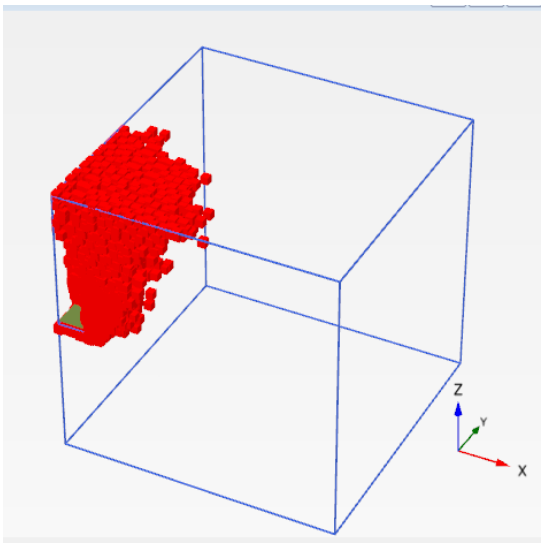

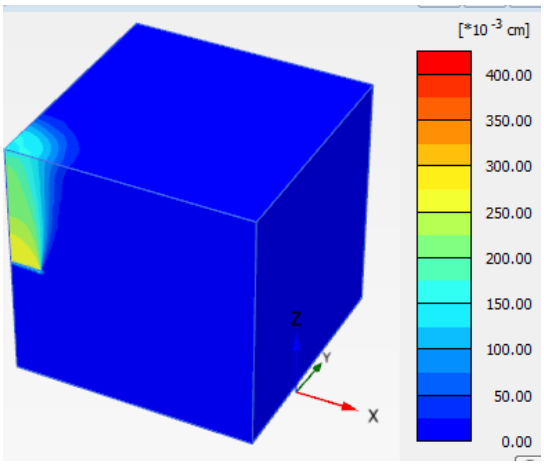

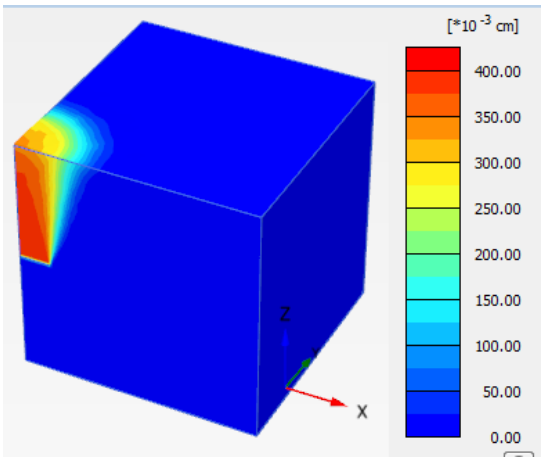

(a)

Loose H/D=6

Dense, H/D=6

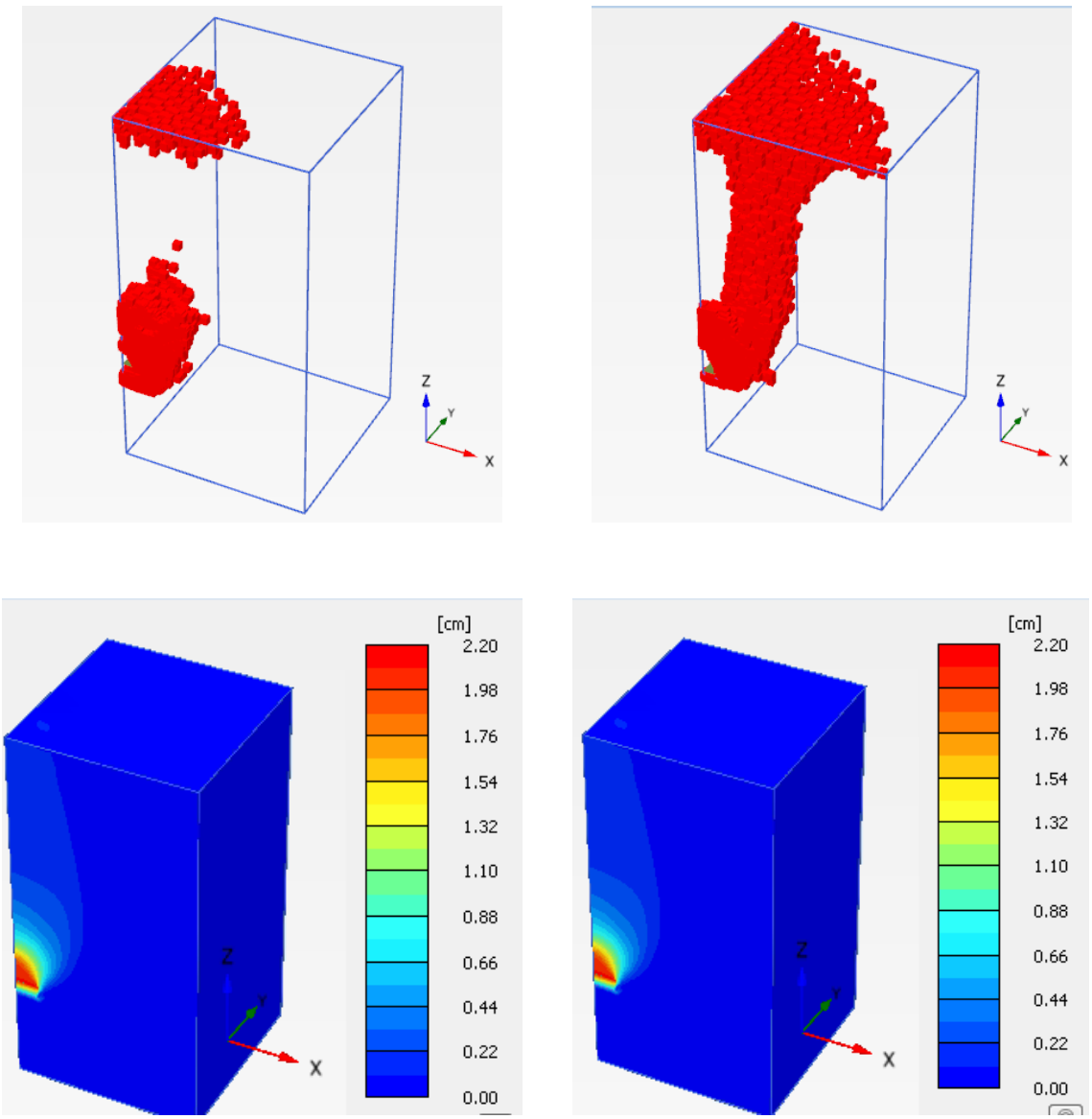

(b)

Figure 5-12 Plastic points and displacement around the square plate anchor at (a) H/D=2, (b) H/D=6

In Figure 5-13 and Figure 5-14 the failure mechanism of strip plate anchor are presented at H/D=2 and H/D=6, consequently. In the shallow embedment depth (H/B=2) the failure mechanisms look like those from the square plate with a stretched shape at a bigger base [Figure 5-13]. The failure zone at H/B=6 and loose sand [Figure 5-14] is not similar to that from the square plate and is still developed to the surface. The reason of that is related to the bigger dimension of the strip plate, at H/B=6 the embedment depth is not large enough for this case to be accounted as a deep plate. In this depth for both loose and dense sands [Figure 5-14], the failure mechanism looks like a combined of a convex polyhedron and U-shaped, which is stretched.

Loose, H/D=2

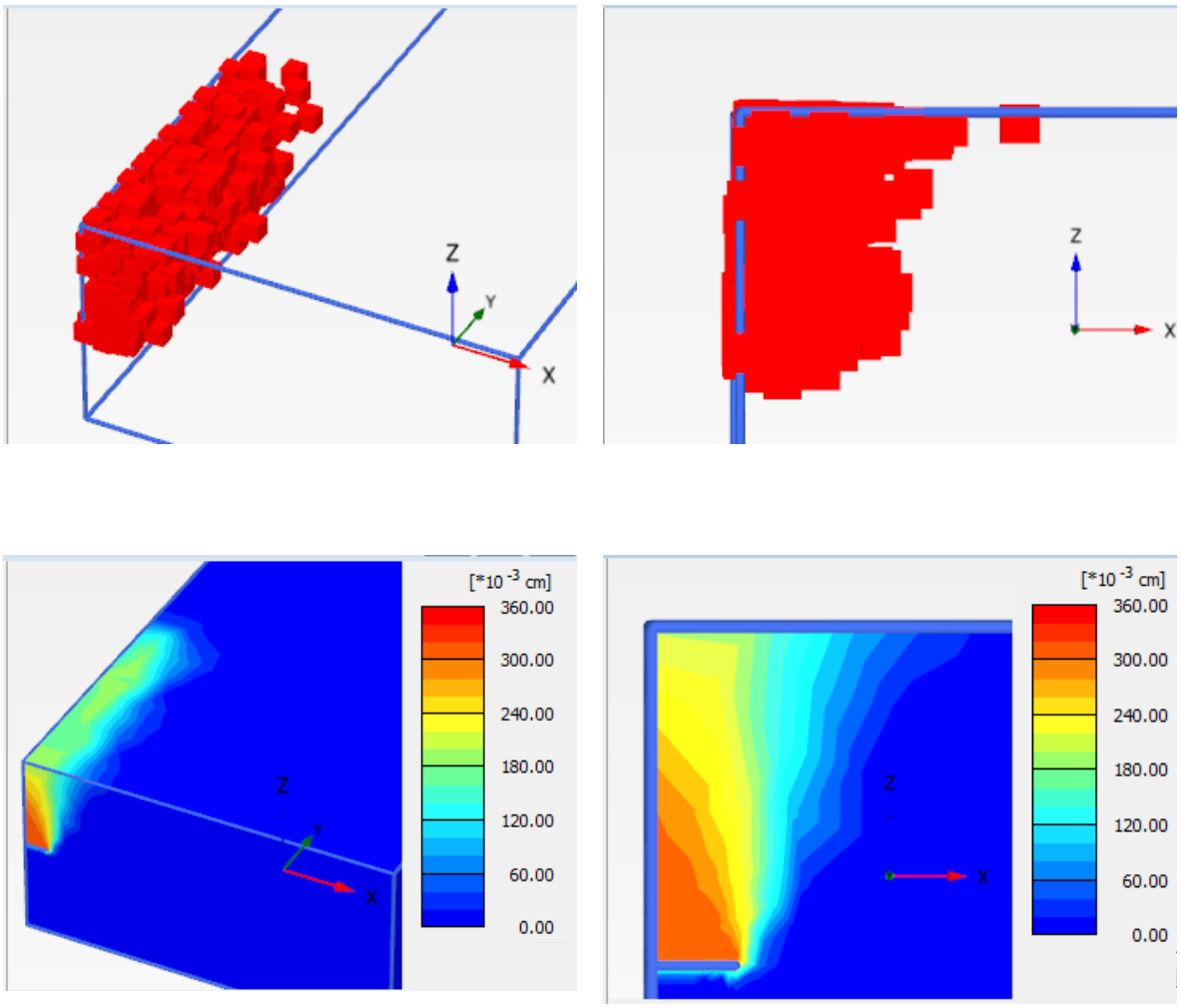
Z
Y
X
Z
X
[*10 -3 cm]
360.00
300.00
240.00
180.00
120.00
60.00
0.00
Z
X
[*10 -3 cm]
360.00
300.00
240.00
180.00
120.00
60.00
0.00
Z
X

(a)

Dense, H/D=2

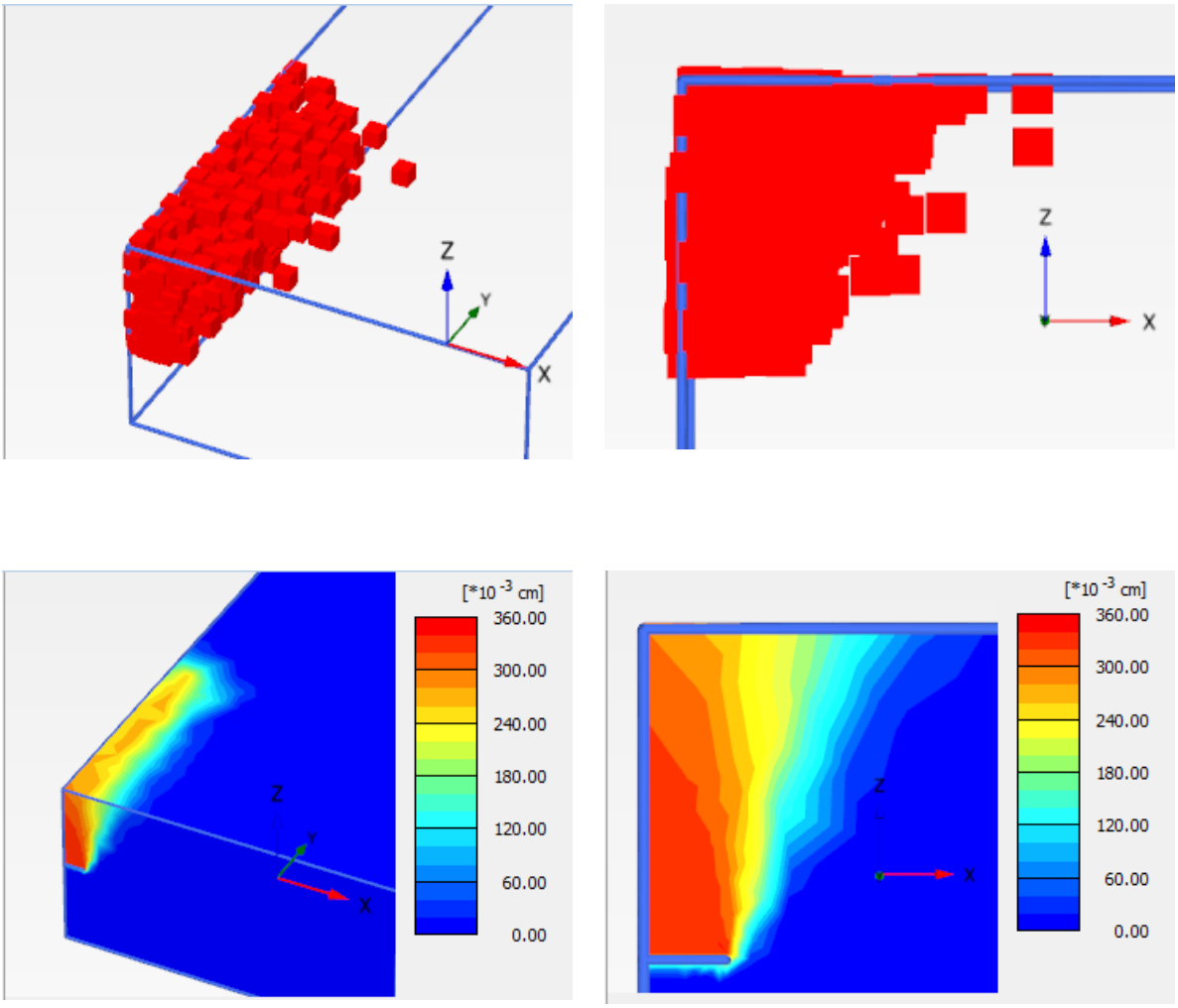

(b)

Figure 5-13 Plastic points and total displacement around the strip plate at H/D=2 (a) loose sand, (b) dense sand

Loose, H/D=6

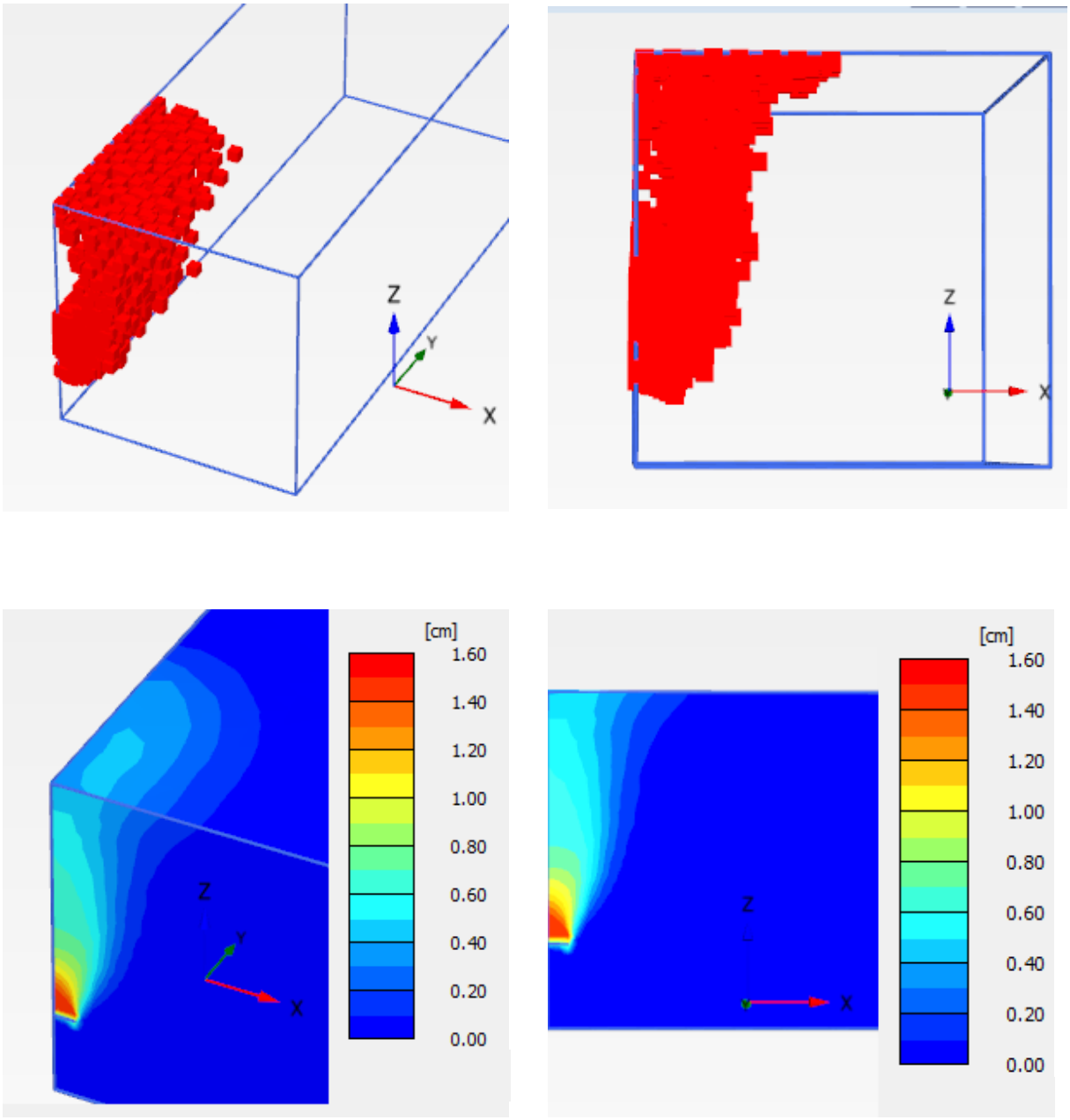
Z
Y
X
Z
X
[cm]
1.60
1.40
1.20
1.00
0.80
0.60
0.40
0.20
0.00
Z
Y
X
[cm]
1.60
1.40
1.20
1.00
0.80
0.60
0.40
0.20
0.00
Z
X

(a)

Dense, H/D=6

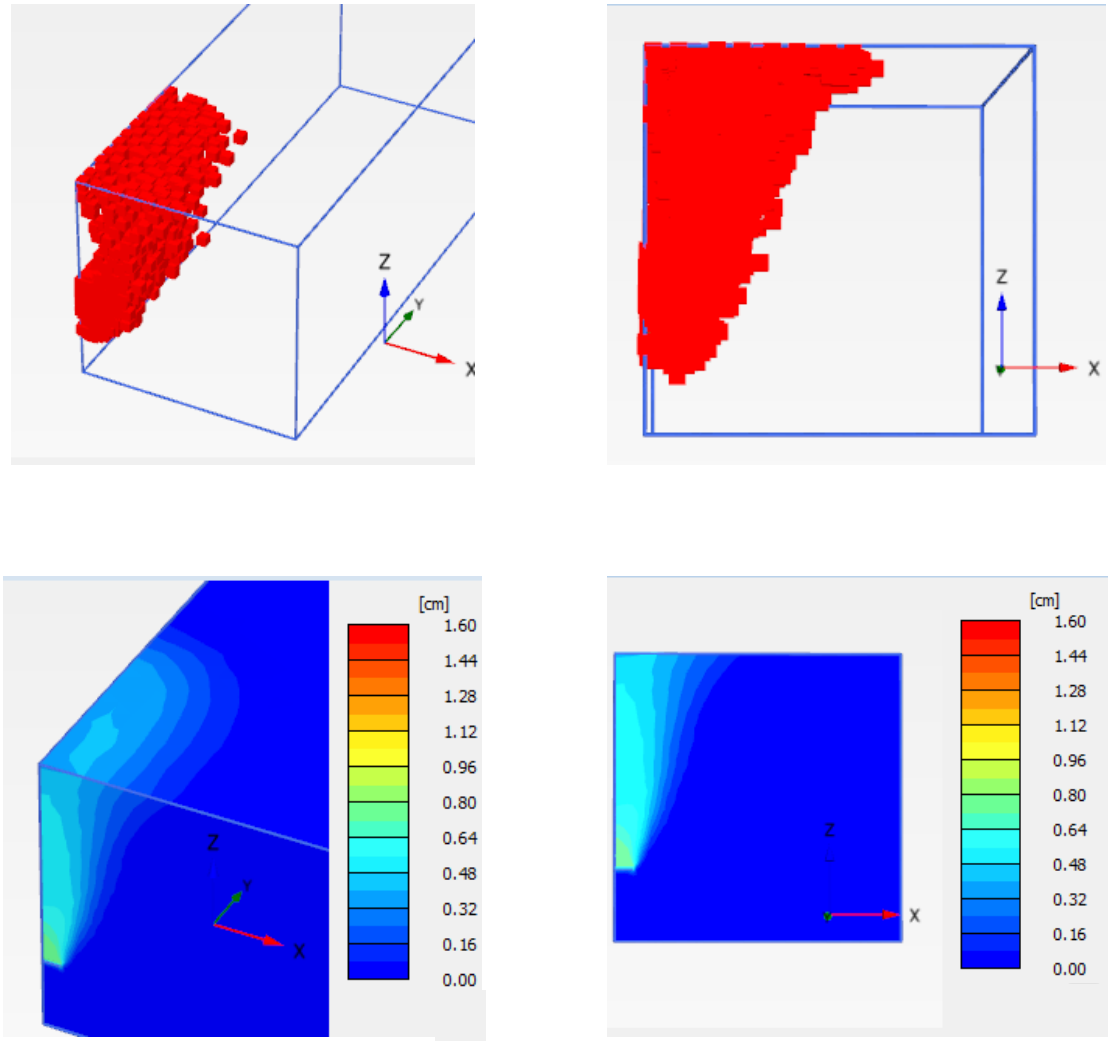

(b)

Figure 5-14 Plastic points and displacement around the strip plate anchor plate at H/D=6 (a) loose sand, (b) dense sand

Another analysis at H/D=12 for strip plate at the loose sand is performed to figure out the shape of the failure mechanism of that at larger depths and is shown in Figure 5-15. It seems that failure mechanism has a complicated U shape in this case. However, as expected the same as other ones at loose sand and deep condition, it is localized to the plate and does not reach the surface of the soil.

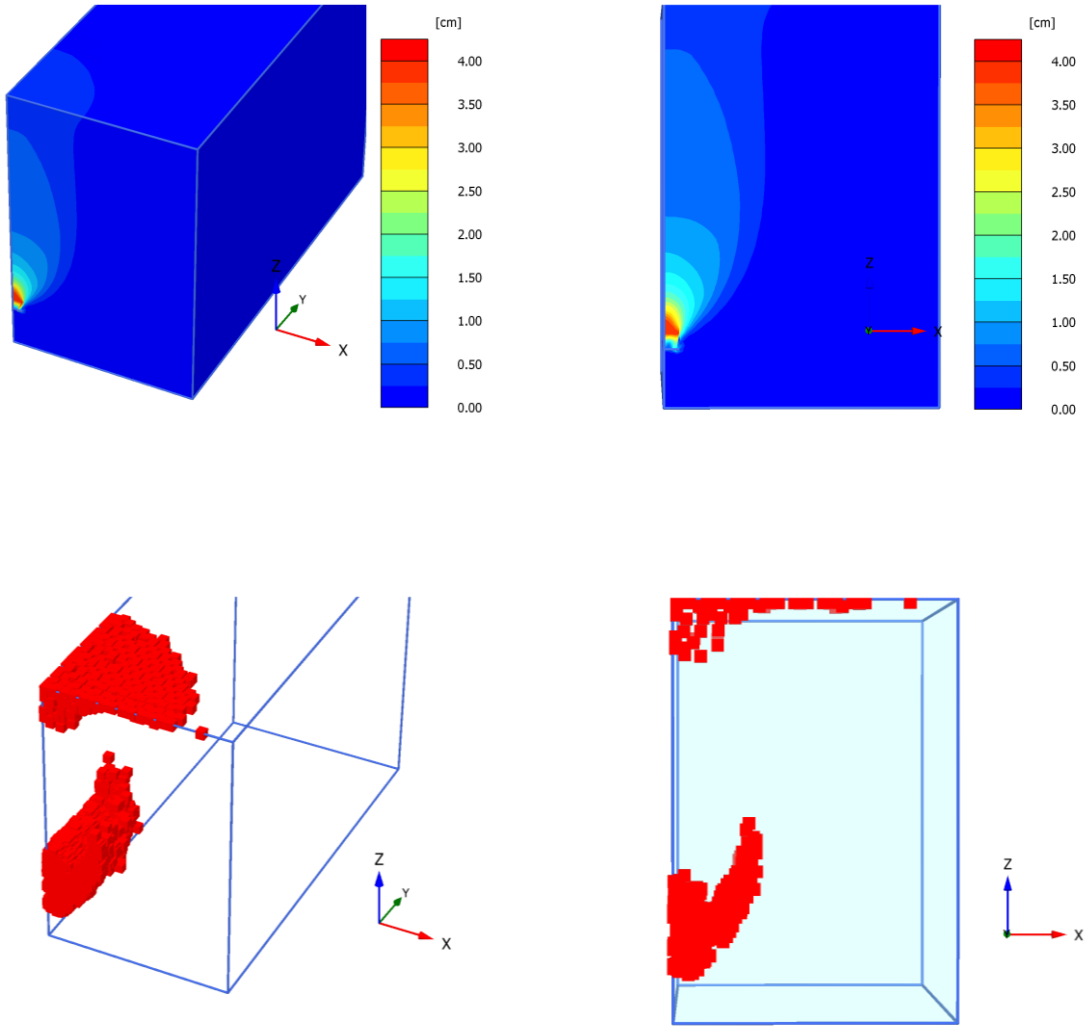

Figure 5-15 Total deformation and plastic points around the strip plate at H/D=12 and loose sand

5.8 A consideration in an Economic Design

The main point in engineering design is, concluding the most efficient and economical solution with considering project's limitations.

Additional comparative analyses for showing the differences between a circular and a square plate with the same area is performed for the case of H/D=2 and dense sand. The equivalent square of a circular with a diameter of 7.5 cm has a dimension equal to B=6.6 cm. for the same embedment ratio (H/D=H/B=2), embedment depth for square plate is equal to 13.2 cm that is smaller than 15 cm (the case for circular). In this case, the equivalent square plate provides 12% lower capacity than the circular plate [Figure 5-16]. However, if the capacity is compared at the same embedment depths, H=15 cm, in this case, the square plate provides 4% higher capacity than square plate [Figure 5-16].

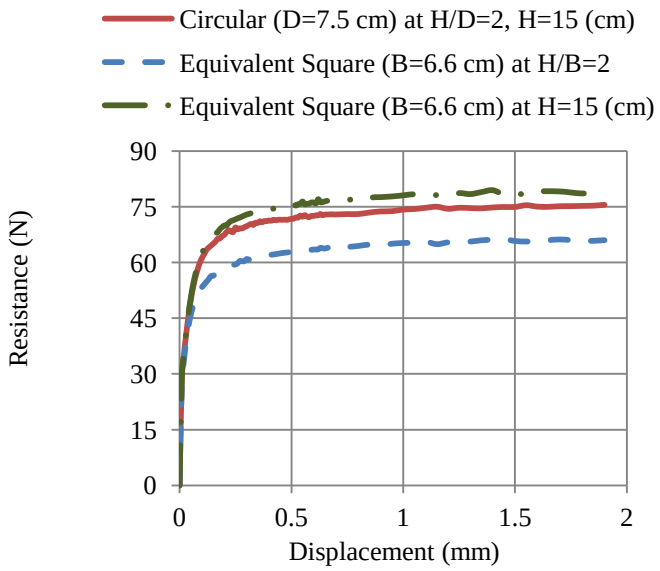

Figure 5-16 Load displacement curve for a circular (D=75 mm) and an equivalent square

At the case of same depth, the square plate provides slightly higher capacity because it has 13% higher embedment ratio (H/B= 2.27). However, if the comparison is made at the same embedment ratio (H/B=H/D), the circular plate is the most efficient one. Figure 5-17

shows that circular plate effects bigger zone than the square plate and has a smaller shear band around its edges at the same embedment ratio (H/B=H/D=2). It means that if in the design there is a limitation regarding embedment depth, at the same depth using the equivalent square plate is more economical option but otherwise (no limitation in the embedment depth) the circular plate is the best option regarding using less amount of steel.

Circular (D=7.5 cm) at H/D=2 Equivalent square (B=6.65 cm) at H/B=2

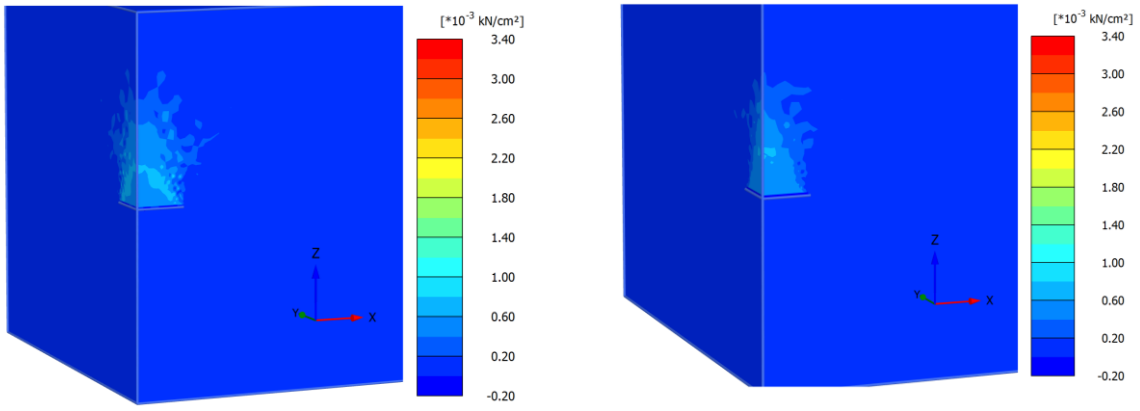

(a)

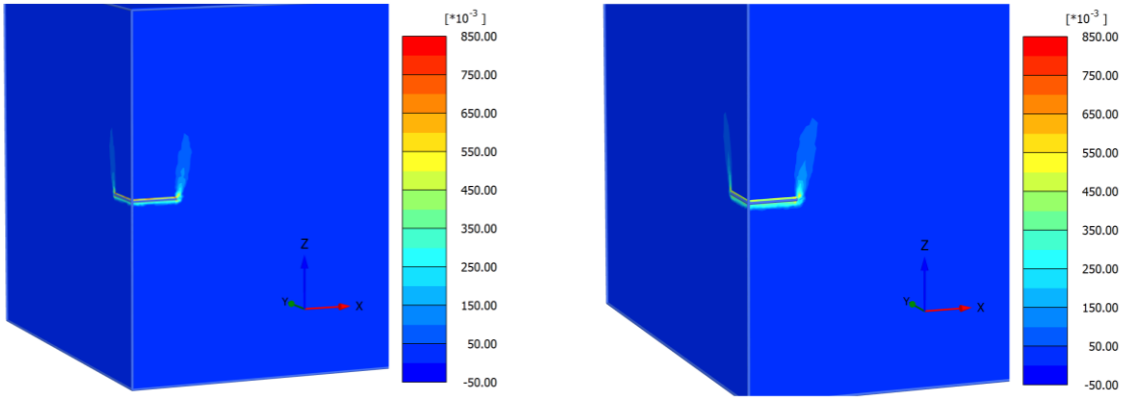

(b)

Figure 5-17 (a) Mobilized shear strength and (b) deviatoric shear strain around the circular and its equivalent square plate

5.9 Comparison of 2D and 3D Modeling

According to the results of the previous section, the shape of the plate has a significant effect on the breakout factor, and 3D analysis is required for the square or rectangular plates. A 3D numerical analysis is a very time consuming and expensive method. In some cases, plane strain and axisymmetric models in the 2D analyses are used to simulate the strip anchor and circular plates. In this section, the results from a 2D analysis are compared with the results from 3D analysis for a circular and strip plates. The same plates (D= 7.5 cm) are simulated using 2D model at dense sands in the shallow and deep embedment rations (H/D= 2, 6). In Figure 5-18 the results are compared. Results show that as expected 3D analysis and axisymmetric 2D analysis provide exactly the same results in the modeling of a circular plate. For the strip plate, 2D plane strain model provides smaller breakout factor than 3D numerical analysis. It can be related to the assumption of 2D plane strain model, which considers L/B equal to infinity while at this 3D model L/B is assumed equal to 10. Comparison, the results of the square and strip plate at the previous section, showed that the square plate provides higher N_q value. Thus in the strip plate smaller L/B provides higher N_q and this differences presented in Figure 5-18(b) seem reasonable.

As a conclusion of two last parts, in the absence of 3D numerical package, 2D axisymmetric analysis of an equivalent circular plate, exactly at the same depth, can be a good representative of a square plate, capacity wise.

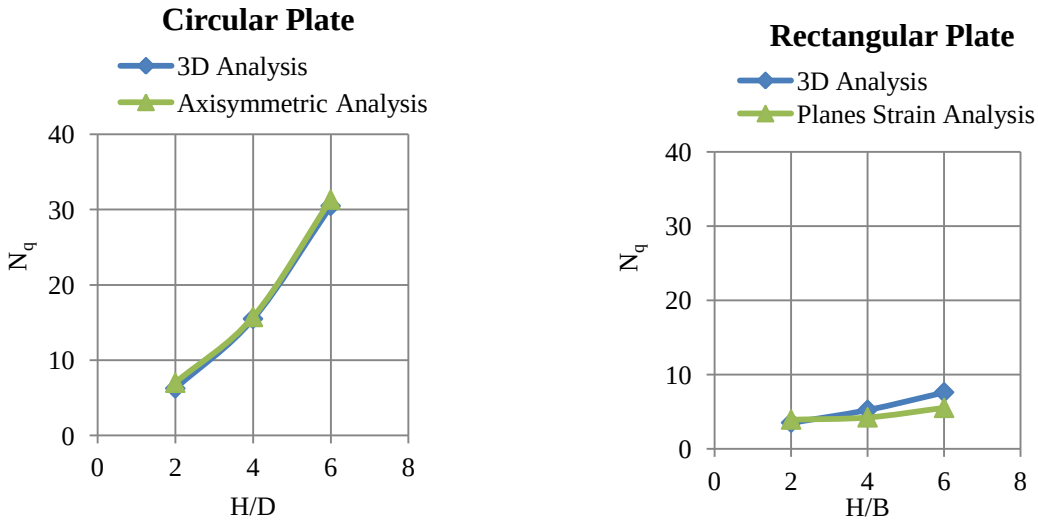

(a) (b)

Figure 5-18 Comparison between 3D and 2D numerical analyses for (a) circular plate and (b) rectangular plate

5.10 Summary and Conclusions

A comprehensive 3D numerical study is performed to investigate the pullout behavior of the plate anchors in dry sands. Different embedment depths and soil properties are considered. The preciseness of 3D numerical model is investigated in capturing the failure mechanism. The shape effect on failure mechanism and breakout factor is investigated by solving the problem for square and strip plates. The results of 3D numerical modeling are compared with the 2D axisymmetric and plane strain models, and the effectiveness of the 2D simplifications are investigated. The following results are conducted:

- 3D numerical modeling provides a very good estimation of the breakout factor in the loose and dense packing sands in comparison with experimental data.

- 3D numerical model is capable of predicting the failure mechanism. Failure mechanism of the plate anchors in the sands is depending on the soil properties, embedment depths and shape of the plate.
- The breakout factor of the square plate presents very good agreement with the breakout factor of the circular plates at the shallow embedment depths (H/D=2), when the width of the square plate is equal to the diameter of the circular plate. The circular plate provides 20% higher breakout factor at the H/D=6.
- The circular plate provides much higher breakout factor than same width strip plate. The shape factor of the strip plate at H/D=2 is equal to 1.8 and increases with the depth of embedment such that this value at H/D=6 is almost equal to 4.
- The shape factor is independent of soil properties, and it is almost the same for dense and loose densities.
- The breakout factor of the circular plate anchor is higher than a square plate with the same width. The breakout factor of the square plates is higher than that from a same width strip plate. The reason of that can be related to the mobilized shear stress zone around the plate's edges in comparison with the area of the plate. This influence or efficiency factor is biggest in the circular plate in comparison with those from square and strip plate.
- The circular plate provides higher capacity than an equivalent square plate with the same area at the same embedment ratio (H/D=H/B). But if there is a limitation for embedment depth, at the same depth (H), the equivalent square plate provides slightly higher capacity than circular one and is more economical option regarding using less amount of steel.

- The results of the axisymmetric models have a very good agreement with the 3D numerical analysis in the simulation of the circular plate anchors. The plane strain simulation provides very good agreement with the 3D numeral analysis of the strip plates (L/B=10) at the shallow embedment depths (H/D=2). The results come from these two analyses deviates slightly at the deeper embedment depths such that at the H/D=6, the 3D numerical analysis provides 27% higer break out factor. It can be

related to the fact that in the plane strain model the L/B is considered infinity and by increasing the L/B the breakout factor is decreasing.

- In the absence of 3D numerical package, 2D axisymmetric analysis of an equivalent circular plate with the same area, exactly at the same depth, can be a good representative of a square plate, capacity wise.

5.11 References

Andreadis, A., and Harvey, R.C. (1981). "A design procedure for embedded anchors". *Applied Ocean Research, 3(4): 171–182.*

Balla, A. (1961). "The resistance to breaking out of mushroom foundations for pylons". *In Proceedings of the 5th International Conference on Soil Mechanics and Foundation Engineering, Paris, France, Vol. 1, pp. 569–576.*

Brinkgreve, R. B. J. and Vermeer, P. A. (1997). Plaxis finite element code for soil and rock analysis- Version 7. Balkema, Rotterdam.

Brinkgreve, R. B. J. (2005). "Selection of soil models and parameters for geotechnical engineering application." *In: Yamamuro, JA and Kaliakin, VN, editors. Geotechnical Special Publication No.128, ACSE, pg 69-98.*

Brinkgreve, RBJ. Engin, E. Engin, H.K. (2010). "Validation of empirical formulas to derive model parameters for sands" *Numerical Methods in Geotechnical Engineering – Benz & Nordal (eds)*

© 2010 Taylor & Francis Group, London, ISBN 978-0-415-59239-0.

Dickin, E, A (1988). "Uplift behavior of horizontal anchor plate in sand". *Journal of Geotechnical Engineering, Vol.114, No.11.*

Dickin, E.A. and Laman, M. (2007). "Uplift response of strip anchors in cohesion less soil." Advances in Engineering Software, 1(38), 618-625 (2007).

Dickin. Edward A. (1989). "Uplift behavior of horizontal anchor plates in sand." Journal of Geotechnical Engineering, Vol.114, No.11.

Downs D.I. and Chieurzzi, R. (1966) "Transmission tower foundations" *Journal of Power Div., ASCE, Vol. 88, No. 2, 91-114.*

Fityus, S. G. Yu, S. and Pearce, A.G. (2000). "Failure mechanisms of vertically loaded plate anchors in sand" ISRM International Symposium, International Society for Rock Mechanics, 19-24 November, Melbourne, Australia.

Ilamparuthi, K. Dickin, E.A. and Muthukrisnaiah, K. (2002). " Experimental investigation of the uplift behavior of circular plate anchors embedded in sand". *Can. Geotech. J. 39: 648-664.*

Koutsabeloulis, N. C., and Griffiths, D.V. (1989). "Numerical modeling of the trap door problem." *Geotechnique, 39(1): 77-89.*

Liu, J., Liu, M., and Zhu, Z. (2012) "Sand Deformation around an Uplift Plate Anchor. " *Journal of Geotechnical and Geoenvironmental Engineering, Vol. 138, No. 6, June 1, 2012.*

Majer, J. (1955). "Zur berechnung von zugfundamenten." *Osterreichister Bauzeitschift, 10(5), 85–90 (in German).*

Mariupol'skii, L.G., (1965) "The bearing capacity of anchor foundations" *Osnovaniya fundamenty i Meckanika Gruntor, Vol. 3, No. 1, pp 26-32.*

Meyerhof, G. G., and Adams, J.I. (1968) "The ultimate uplift capacity of foundations." *Canadian Geotechnical Journal, 5(4): 225-244.*

Murray, E.J and Geddes, J.D. (1987) "Uplift of anchor plate in sand" *Journal of Geotechnical Engineering, Vol.113, No.3.*

Niroumand, H. Kassim, k.A. and Nazir, R. (2013) "The influence of soil reinforcement on the uplift response of symmetrical anchor plate embedded in sand" *Measurement: Journal of the International Measurement Confederation, 46: 2608-2629.*

PLAXIS 2D Manuals (2012), PLAXIS BV, Delft, The Netherlands

Rowe, R. K and Davis, E. H. (1982) ‘‘The behavior of anchor plates in sand” *Geotechnique, Vol.32, pp. 25-41.*

Chapter 6 SEPLA Keying Effect

This chapter will be submitted to a conference, as a technical note. The authours are Zahra Aghazadeh Ardebili, S.M.ASCE[1]; M.A. Gabr, F.ASCE[2]; M.S. Rahman[3]

6.1 Abstract

Suction Embedded Plate Anchor (SEPLA) has been used as an economical and efficient foundation system in deep waters to response the oil and energy development on seabed resources. In the majority of earlier research for SEPLA, an ideal keying procedure is assumed. During the ideal keying procedure, a plate anchors rotate until to become perpendicular to the pull out direction. In this situation, the maximum soil resistance is mobilized. In the reality, reaching to this ideal condition is not feasible always. During an imperfect keying process, plates are not completely perpendicular to the pullout direction and have an inclination with an angle of (θ) toward the ideal direction. It is important to know the effect of imperfect keying based on (θ) on the capacity, in considering a proper safety factor in the design of these kinds of foundations. In this study, the effect of imperfect keying is investigating by using a 3D numerical analysis. SEPLA with a vertical pull out load is studied, and the inclination of the plate toward the ideal situation is considered between 5 to 30 degrees. The reductions in the breakout factor in comparison with the ideal one are presented at different inclinations.

Key Words: Suction embedded Plate Anchors; 3D Finite element analysis; Clays, Bed keying.

[1] Graduate Research Assistant, North Carolina State Univ., Campus Box 7908, Raleigh, NC 27695 (corresponding author). E-mail: zaghaza@ncsu.edu
[2] Alumni Distinguished Undergraduate Professor, North Carolina State Univ., Campus Box 7908, Raleigh, NC 27695.E-mail: gabr@ncsu.edu
[3] Professor, North Carolina State Univ., Campus Box 7908, Raleigh, NC 27695.E-mail: rahman@ncsu.edu

6.2 Introduction

Suction Embedded Plate Anchor (SEPLA) is a plate anchor installed on the seabed by using a suction caisson. Since 1988 SEPLA has been used as an economical and efficient foundation system in deep waters (>2000m) to response the oil and energy development on seabed resources. SEPLA uses the advantage of suction piles (known penetration depth and geographical location) and vertically loaded anchors (VLA) (lower cost and efficiency) while it avoids their disadvantages (large, heavy and costly to handle suction caissons and imprecise positioning for VLAs) (Brown 2011).

In this mooring system, a suction caisson, which is slotted vertically into its base, is used to embed a plate anchor in the seabed. The plate is placed vertically in the soil, and then a mooring chain attached to the plate is tensioned causing plate anchor to move and rotate until to be perpendicular to the pullout direction. This process is called installation or keying. The procedure is shown in Figure 6-1. The installation of the plate anchor is one of the essential aspects of the performance and efficiency of SEPLA. During the keying, anchor loses some of its embedment depth for decreasing this loss; a flap that is another rectangular plate anchor and can rotate is added to the plate anchor. Padeye for propose of connection with chain and shank are added to the fluke or rectangular plate anchor. The configuration of SEPLA is shown in Figure 6-2 and Figure 6-3.

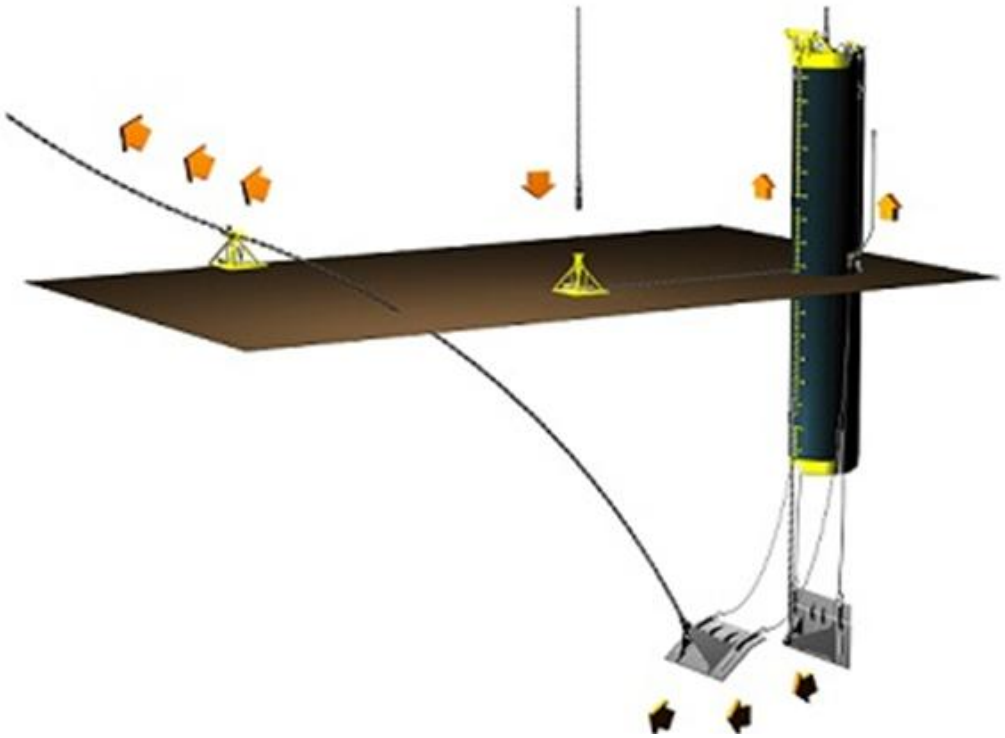

Figure 6-1 SEPLA concept suction installations, caisson retrieval, anchor keying, and mobilized anchor. (InterMoor)

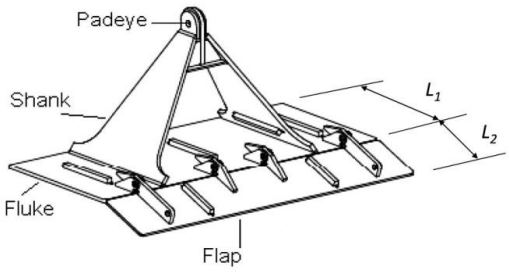

Figure 6-2 Configuration of SEPLA (Yang, et al. 2012)

Figure 6-3 Typical SEPLA (Brown, et al. 2011)

6.3 Previous Research on SEPLA

A couple of full-scale tests, small-scale, and centrifuge tests are done on SEPLA to investigate its efficiency and behavior during keying. Wilde et al. (2001) performed full and reduced scale onshore and offshore testing on SEPLA. Their results showed that SEPLA can be used confidently as anchor points for temporary mooring systems. El-Sherbiny (2005) performed laboratory scaled model test by normally consolidated and lightly overconsolidated clays. He found that for getting the maximum capacity the caisson should be loaded at a depth between two-thirds and three-quarter of the embedment depth. On the other hand, the excess pore pressure and the failure mechanism are a function of the position of the load application. Gaudin, et al. (2006) performed a series of centrifuge tests investigating the influence of the installation process on the capacity of SEPLA. A good agreement was observed between the normalized anchor capacity and theoretical solutions. They found that the loss of embedment during the keying is dependent on load inclination at the anchor padeye. Brown et al. (2011) published the results of performing and monitoring of full-scale offshore tests of SEPLA and they developed a simple analytical method to predict SEPLA keying using the geometry of the anchor and local in-situ vane shear test's results.

Song (2009) and Yang (2012) performed a numerical analysis of SEPLA in clay. Song et al. (2009) investigated the trajectory of SEPLA using large deformation analysis for the strip plate anchor. They performed some centrifuge model test on a square anchor in uniform and consolidated transparent soil with anchor pull out angle varying from 30° to 90° also. They found that the loss in anchor embedment during anchor keying can be function of a dimensionless anchor geometry factor, the eccentricity of the padeye, angle of loading, and the net moment applied to the anchor. The loss in anchor embedment decreases linearly with decreasing pullout angle. They proposed a simple formula and design procedures to estimate the loss in anchor embedment during keying. Yang et al. (2012) also conducted an analytical model for predicting the behavior of SEPLA during the anchor rotation from its initial position to become perpendicular to the loading direction. They used a generalized plastic limit analysis to estimate the trajectories and corresponding capacities of SEPLAs under different loading conditions investigated the effect of flap theoretically.

6.4 Aim of This Study

In the majority of earlier studies on SEPLA, an ideal keying procedure is assumed. During the ideal keying procedure, a plate an anchor rotates until becomes perpendicular to the pull out direction. In this situation, the maximum soil resistance is mobilized. In the reality, reaching to this ideal condition is not feasible always. In a bad keying; plates are not completely perpendicular to the pullout direction and have an inclination with an angle of (θ). Therefore, it is important to know the effect of bad keying based on (θ) on the capacity. This study helps to consider a proper safety factor in the design of these kinds of foundations. The importance of this study comes from the rapidly developing offshore energy industries.

In this study, a bad keying effect is investigated for SEPLA at saturated clay in the case of vertical pull out. In the ideal keying the plate rotates and becomes horizontal (θ=0) such that ultimate pullout load direction is perpendicular to the plate's surface [Figure 6-4]. The 3D numerical analyses are conducted to figure out the effect of bad keying when plate does not rotate enough and needs more rotation (θ°). On the other hand, plate anchor stops at a state, which has an inclination angle (θ°) with the ideal position (horizontal in this case). This bad keying inclination angle (θ°) is considered between 5 to 30 degree and break out factors are calculated and compared with that in the ideal situation (θ=0). The reduction in the breakout factor is presented in a table for each bad keying inclination angle (θ°). These results can help to consider a realistic factor of safety in the design of SEPLA.

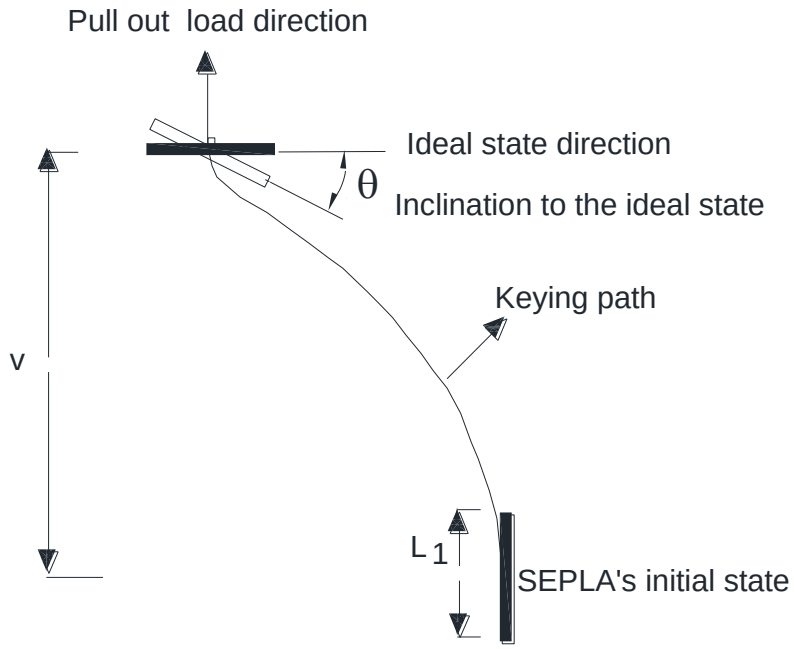

Figure 6-4 Trajectory of SEPLA, when pull out direction is vertical

6.5 Assumed Parameters and Finite Element Model

A 3D finite element model is developed in PLAXIS for analyzing SEPLA in saturated clay. For the simplicity, just the fluke without the shank and flap is modeled, and the result is compared with Yang, et al. (2012)'s results for SEPLA without shank and flap. A rectangular plate (representing fluke) with a dimension of 3m*7.3m*0.15m and stiffness of steel (200 Gpa) is assumed (Yang, et al. 2012). The domain is assumed big enough such that the failure points do not reach the boundaries. The convergence analysis is conducted, and the medium mesh with finer elements around the plate with a coarseness ratio of 0.1 is applied. In Figure 6-5 model domains and the applied mesh are shown for horizontal case.

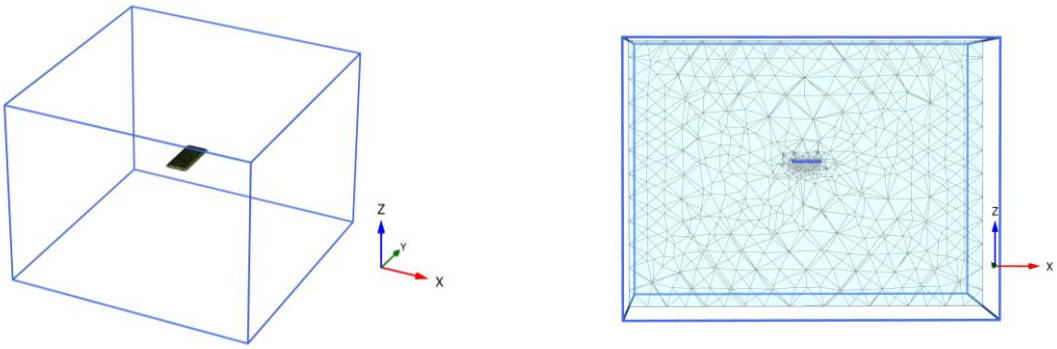

Figure 6-5 Model domain and applied mesh for the horizontal case

Mohr-Coulomb model is used modeling undrained clay. The soil properties are considered the same as Yang, et al. (2012), [related to his Test 4] and presented in Table 6-1. Where, γ_{sat} , S_u and E_u , are saturated density, undrained shear strength and undrained Young's modulus. $\varphi(°)$ and $\psi(°)$ are friction and dilatancy angles.

Table 6-1 Assumed Parameters for Saturated Clay

γ_{sat} *(kN/m³)*	Soil strength Su (*kN/m²*) at Depth z(m)	E_u *(kN/m²)*	$\varphi(°)$	$\psi(°)$
18.5	$S_u = 3.5 + 0.9z$	$500 * S_u$	0	0

Yang, et al. (2012) assumed the embedment ratio equal (H/L_1) to 5 and predicted the loss during the keying and the ultimate capacity for the different pull out inclination. In this study, the embedment ratio is considered equal to 5 minus the predicted embedment loss (v). Embedment loss ratio at this case according to Yang, et al. (2012) is $v / L_1 = 0.95$. Therefore, embedment depth is calculated by the following equation and is assumed equal to 13.7 m.

$$H = (5 - \frac{v}{L_1}) * L_1 \qquad \text{Equation 6-1}$$

The analysis is displacement control in which a series of prescribed displacement is applied uniformly to the plate, and corresponding resistance on the plate is monitored. The load-displacement curve is developed, and the capacity is considered equal to the ultimate load where the load-displacement curve becomes plateau. The dimensionless breakout factor is calculated by using Equation 6-2.

$$N_c = \frac{F}{A.S_u}$$ Equation 6-2

Where, S_u is the undrained shear strength at the middle of plate's face at the initial situation.

The capacity is calculated for the ideal case when the plate rotates enough to be perpendicular to the pull out direction. Dimensionless breakout factor, in this case, equal to 12.79. This amount is 9.6% higher than Yang, et al. (2012)'s result (11.67) at this situation (Type 90 degrees). This amount of overprediction is reasonable since Mohr-Coulomb model overpredicts the capacity in the undrained analysis. According Aghazadeh, et al. (2015), soils experience a decrease in the mean effective stress during shearing while Mohr-Coulomb model considers a constant mean effective in this state. Therefore, Mohr-Coulomb model reaches to the failure line at higher shear stress and over predicts N_c. This issue is discussed completely by Aghazadeh, et al. (2015). Since this study compares the bad keying with the ideal keying the precise estimation of the capacity is not the case, and all of the other analyses, which will be compared with the horizontal case, are modeled with Mohr-Coulomb.

The analysis is repeated when a bad keying situation causes the plate dose not rotate enough and is not completely perpendicular to the pull out direction. This inclination is considered equal to 5 to 30 degree. The load-displacement curve for each case is presented in Figure 6-6.

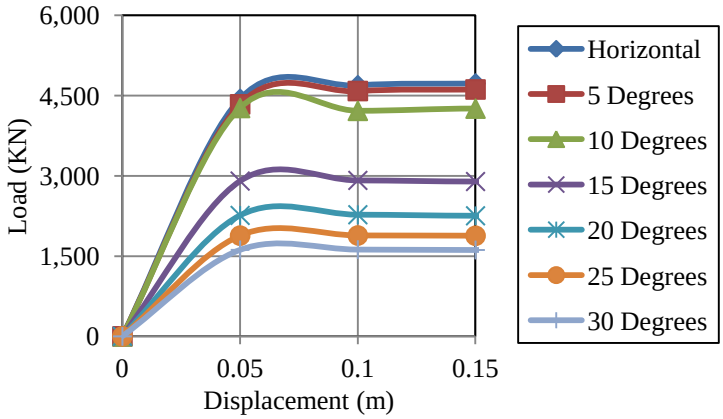

Figure 6-6 Load displacement curves for different plate inclination

The dimensionless breakout factor for the different situation of bad keying, in this case, is presented in Figure 6-7. The breakout factor decreases dramatically with the plate's inclination increases, such that when the plate is rotated only 60 degrees (θ=30), N_c value is decreased 66%. In Table 6-2 the reduction of N_c is presented based on the required angle toward the ideal case.

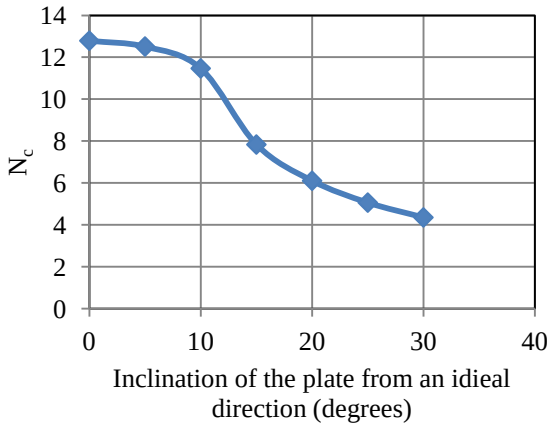

Figure 6-7 Vertical dimension-less breakout factor based on plate's inclination

Table 6-2 Reduction in the Breakout Factor Based on Plate's Inclination

$\theta(^\circ)$	0	5	10	15	20	25	30
N_c	12.8	12.5	11.5	7.8	6.1	5.1	4.4
$\frac{N_{c\ ideal} - N_{c\ incomplete}}{N_{c\ ideal}} * 100$	0.0	2.2%	10.3%	38.7%	52.3%	60.4%	65.9%

The reductions for small angles (5 and 10 degrees) are small, but it dramatically increases by increasing the inclination. Canizal, et al. (2014), explained the reason of that. They explained that for a small amount of the inclination of the plate, the failure is because of pull out failure but by increasing the angle of plates inclination sliding failure becomes dominant. Therefore, break out factor decreases dramatically.

In Figure 6-9 and Figure 6-9 the mobilized shear strength around the plate anchor with inclination equal to 0 and 30 degrees are shown at its highest resistance. S_u for the soil at this depth is equal to 17 (kN/m^2). The soil around the inclined plate has reached to this ultimate shear amount before developing a pullout failure wedge.

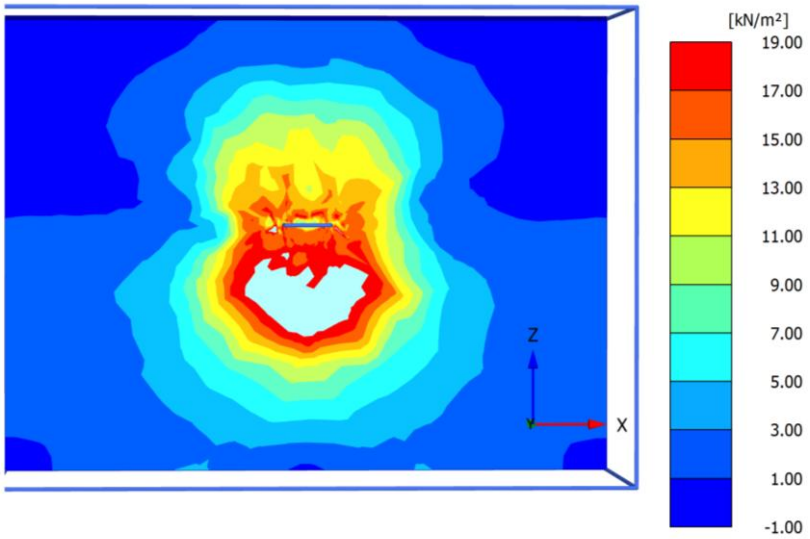

Figure 6-8 Mobilized shear strength around the horizontal plate

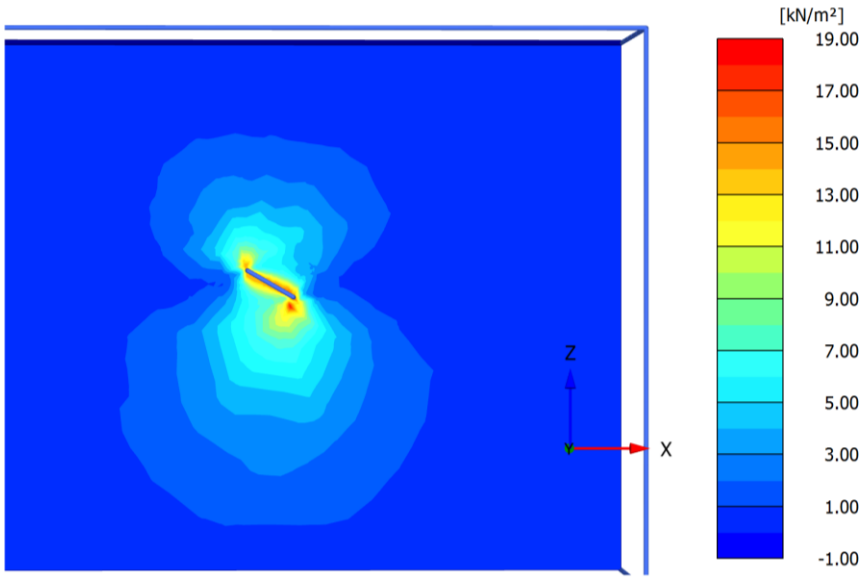

Figure 6-9 Mobilized shear strength around the plate with an inclination equal to 30 degree

6.6 Summary

By using the 3D numerical modeling, the effect of a bad keying for a vertically loaded SEPLA is investigated. The ultimate breakout factor for the ideal situation ($\theta=0$) is calculated. At this situation, plate anchor is rotated completely and becomes perpendicular to the vertical direction. As a bad keying effect, an inclined plate with a vertical pull out load is considered such that the inclination of the plate toward the horizontal direction (ideal state) is considered between 5 to 30 degrees. The capacity for each inclination is calculated, and the reduction amount of that in comparison with the ideal case is calculated and presented. The reduction of breakout factor is increased by the inclination of the plate. For example, at inclination equal to 5 degrees, the reduction is equal to 2.2% while in the inclination equal to 30 degrees it is equal to 66%. This bad keying effect needs to be considered in the safety factor and design of these kinds of foundations.

6.7 References

Brown. R.P, Wong. P.C, Audibert. J.M (2011). "SEPLA keying prediction method based on full-scale offshore tests", *Frontiers in Offshore Geotechnics II – Gourvenec & White (eds) © 2011 Taylor & Francis Group, London, ISBN 978-0-415-58480-7.*

Canizal, F., Canizal, j., Castro, J., Costa A. da, and Sagasera, C., (2014). "Ultimate pullout resistance of late anchors buried in sandy seabed", *Numerical methods in geotechnical engineering – Hicks, Brinkgreve & Rohe (EDS) @ 2014 Taylor & Francis Group, London, 978-1-138-00146-6.*

Gaudin, C., O'Loughlin, C. D., Randolph, M. F.,(2006) " Centrifuge tests on suction embedded plate anchors" , *Taylor & Francis Group plc, London, UK.*

Gaudin, C., O'Loughlin, C. D., Randolph, M. F., and Lowmass, A. C. (2006). "Influence of the installation process on the performance of suction embedded plate anchors", *Geotechnique, 56(6), 381–391.*

Song, Z., Hu, Y., O'Loughlin, C., and Randolph, M. F. (2009). "Loss in anchor embedment during plate anchor keying in clay", *J. Geotech. Geoenviron. Eng., 135(10), 1475–1485.*

Wilde, B. (2005). "Program of centrifuge and field tests on the suction embedded plate anchor", *Rep. to SEPLA Joint Industry Project, Inter Moor, Houston.*

Wilde, B., Treu, H., and Fulton, T. (2001). "Field testing of suction embedded plate anchors", *Proc., 11th Int. Offshore and Polar Engineering Conf., Int. Society of Offshore and Polar Engineers, Mountain View, CA, 544–551.*

Yang. Ming, Aubeny. Charles P, Murff. James D. (2012) "Behavior of Suction Embedded Plate Anchors during Keying Process", *Journal of geotechnical and geoenvironmental engineering. Vol. 138, No. 2, February 1, 2012.*

Chapter 7 Conclusions and Future Work

7.1 Introduction

This dissertation presents 2D and 3D numerical analyses of the vertically loaded plate anchors, using different constitutive models. The purpose of this study was to (i) reaching to a better estimation of plate anchors capacity and behaviour by application of different constitutive models, identifying the best constitutive model for simulation of clay, and optimizing of an available design method; (ii) comparing the results from a conventional elastic perfectly plastic model with a hardening model in capturing sands behavior, and investigating the size and dilatancy effect at different embedment depths and soil properties; (3) investigating the shape effect on the breakout factor and failure mechanism in sands along with considering different geometry and soil properties; (4) investigating the bad keying effect of suction embedded plate anchors.

The dissertation consists of the following major components: (1) plate anchors in clays, (2) plate anchors in sands, (3) plate's shape effect, 4) SEPLA keying. The following sections present the main conclusions of each component and the suggestions for future study.

7.2 Summary and Conclusions

7.2.1 Plate Anchors in Clay

In this study, effective stress analyses for the uplift capacity of plate anchors are performed while utilizing Mohr- Coulomb (MC), Modified Cam-Clay (MCC) and Soft Soil (SS) constitutive models, for both plane strain and axisymmetric conditions. The capacities of plate anchors are assessed through the application of a displacement control approach, and equivalent input parameters are used for the three different models. A series of finite element analyses are performed using the computer program PLAXIS. The results show that the use of MC model in the analysis yielded a higher estimated pullout capacity in comparison with those from the SS and MCC models. The SS and MCC models provide predictions that are in a good agreement with each other as well as experimental data, especially for the axisymmetric condition. The effective stress parameters are correlated with the undrained

shear strength and the ultimate dimensionless breakout factors from the three constitutive models are compared to each other and to the lower bound solution by Merifield et al. (2003). Based on the soil properties and plate dimensions assumed in this study, the following conclusions are advanced:

- Based on the total stress analysis, results using Mohr-Coulomb model provided a good agreement with Tresca, which was used by Merifield (2003). As expected Mohr-Coulomb and Tresca are the same when dilation angle is zero.
- Results based on the use of MC model over predicted. In this case, the stress paths (p′ - q graphs) show that in the effective stress analysis for the undrained material, MC model considers a constant mean effective stress during shearing while soils experience a decrease in the mean effective stress in this state.
- SS and MCC models provide closer results to the experimental data in comparison with MC.
- Results based on using the MCC yield a higher deviatoric strain in the final state. The reason of higher deviatoric strain in MCC is related to its failure criterion. At MCC model failure occurs when the internal friction is fully mobilized, and the soil is in the state of the critical void ratio. At this state, no volume change occurs, and the deviatoric strain goes to infinity.
- In the case of the shallow plates, the failure surface extends into the soil surface, which causes the movement of soil above the plate. The uplift resistance of the plate in this situation includes the soil's effective weight and the mobilized shear strength along the failure surface. The amount of soil moved by plate depends on the failure mechanism. Therefore, it is reasonable that in shallow depths (less that critical depth) the estimates of the breakout factors in this study are higher than values for weightless soil reported in the literature and the differences is be equal or less than $\gamma' H / S_u$.
- It is proposed that the ultimate breakout factor in Merifield et al. (2003)'s equations be modified to 7.65 for strip plates and 10.84 for circular plate anchors. Such a

modification will provide a better estimation of capacity, especially for large H/D ratios.

- The use of Mohr-Coulomb constitutive model is common, and perhaps a higher factor of safety criterion should be considered during the design phase if such a model is used.

7.2.2 Plate Anchors in Sands

In this study, the pullout capacity of a horizontal circular plate anchor in sand is investigated using numerical analyses to study the influence of stress-dependent modulus, friction angle dilation, and the size of the plate on the pullout capacity of plate anchors. The capacities of plate anchors are assessed through the application of displacement control approach. A series of large deformation analyses are performed using Hardening Soil (HS) model in dry sands, and the results are compared with available experimental data. The drained large deformation analyses are conducted in the saturated sands using two different constitutive models (MC and HS models) and the results are presented and discussed. The effects of dilatancy angle and size of the plate in saturated sands at different embedment depths are investigated. The main conclusions from this study are summarized in the following:

- The results of the large deformation analyses using HS Model are in good agreement with existing experimental data for the dry loosely packed sands at shallow embedment depths (H/D<6). For higher embedment depths (H/D>6), this analysis overpredicts the experimental data. It can be related to the assumed dilatancy angle. Assuming the higher amount of the dilatancy angle results a higher capacity especially at the deep embedment depths.
- The results of the large deformation analyses using HS Model are in an encouraging agreement with existing experimental data for the dry densely packed sands at embedment ratio, between1 to 10.
- In saturated sands, the results show that although MC cannot explain the softening behavior of the sands. However, a very good agreement is found with a hardening soil model such as HS model at the shallow depths ($H/D \leq 4$). The advantage of using

MC model over HS model is obviously fewer model parameters. MC model requires just five parameters while HS model needs ten. At larger depths, MC model provides lower capacities.

- MC has a failure surface fixed in stress space and a stress independent stiffness. HS model has a confining stress dependent stiffness. Stresses and consequently modulus intensely increase, locally around the plate by applying a prescribed displacement at HS model. HS model by having expanding failure surface and stress dependent stiffness provides higher capacity than MC model at saturated sands. This difference becomes significant at larger depths with higher initial stresses.
- The ultimate residual capacity in the saturated sands is the same for MC and HS models.
- The increase in dilatancy angle increases the capacity in the saturated sands by extending the failure zone. The effect of dilatancy angle in the shallow embedment depths and loose sands are negligible. However, this effect becomes significant at larger embedment depths and dense sands. For a dense saturated sand with relative density of 80% and a dilatancy angle equal to 8 degrees, capacity increases by more than 40% at a $H/D=7$ while this increase is just 10% at a $H/D=1$.
- The size effect in different embedment depths is investigated in the dense saturated sands. Analyses are conducted by using plate anchors with diameters equal to 1 and 5 m at embedment depths ($H/D=3,4$). The results show that the size effect is negligible in this range of assumed data when the friction angle is independent of stress level. When friction angle is changing (decreasing) by increasing the stress level, the bigger plate provides smaller breakout factor.

7.2.3 Plate's Shape Effect in Sands

A comprehensive 3D numerical study is performed to investigate the pullout behavior of the plate anchors in dry sands. Different embedment depths and soil properties are considered. The accuracy of 3D numerical model is investigated in capturing the failure mechanism. The shape effect on failure mechanism and break out factor is investigated by solving the problem for square and strip plates. The results of 3D numerical modeling are

compared with the 2D axisymmetric and plane strain models, and the effectiveness of the 2D simplifications are investigated. The following results are conducted:

- 3D numerical modeling provides a very good estimation of the breakout factor in the loose and dense packing sands in comparison with experimental data.
- 3D numerical model is capable of predicting the failure mechanism. Failure mechanism of the plate anchors in the sands is depending on the soil properties, embedment depths and shape of the plate.
- The breakout factor of the square plate presents very good agreement with the breakout factor of the circular plates at the shallow embedment depths (H/D=2), when the width of the square plate is equal to the diameter of the circular plate. The circular plate provides 20% higher breakout factor at deeper depth (H/D=6).
- The circular plate provides much higher breakout factor than same width strip plate. The shape factor of the strip plate at H/D=2 is equal to 1.8 and increases with the depth of embedment such that this value at H/D=6 is almost equal to 4.
- The shape factor is independent of soil properties, and it is almost the same for dense and loose densities.
- The breakout factor of the circular plate anchor at a given embedment ratio is higher than a square plate with the same width. The breakout factor of the square plates at a given embedment ratio is higher than that from a same width strip plate. The reason of that can be related to the mobilized shear stress zone around the plate's edges in comparison with the area of the plate. This influence or efficiency factor is biggest in the circular plate in comparison with those from square and strip plate.
- The circular plate provides higher capacity than an equivalent square plate with the same area at the same embedment ratio (H/D=H/B). But if there is a limitation for embedment depth, at the same depth (H), the equivalent square plate provides slightly higher capacity than circular one and is more economical option regarding using less amount of steel.
- The results of the axisymmetric models have a very good agreement with the 3D numerical analysis in the simulation of the circular plate anchors. The plane strain simulation provides very good agreement with the 3D numeral analysis of the strip

plates (L/B=10) at the shallow embedment depths (H/D=2). The results come from these two analyses deviates slightly at the deeper embedment depths such that at the H/D=6 the 3D numerical analysis provides 27% higer break out factor. It can be related to the fact that in the plane strain model the L/B is considered infinity and by increasing the L/B the breakout factor is decreasing.

- In the absence of 3D numerical package, 2D axisymmetric analysis of an equivalent circular plate (with the same area), exactly at the same depth, can be a good representative of a square plate, capacity wise.

7.2.4 SEPLA Keying

By using the 3D numerical modeling, the effect of a bad keying for a vertically loaded SEPLA is investigated. The ultimate breakout factor for the ideal situation (θ=0) is calculated. At this situation, plate anchor is rotated completely and becomes perpendicular to the vertical direction. As a bad keying effect, an inclined plate with a vertical pull out load is considered such that the inclination of the plate toward the horizontal direction (ideal state) is considered between 5 to 30 degrees. The capacity for each inclination is calculated, and the reduction amount of that in comparison with the ideal case is calculated and presented. The reduction of breakout factor is increased by the inclination of the plate. For example, at inclination equal to 5 degrees, the reduction is equal to 2.2% while in the inclination equal to 30 degrees it is equal to 66%. This bad keying effect needs to be considered in the safety factor and design of these kinds of foundations.

7.3 Suggestions for Future Work

Some of the researchers reported that anchors geometry (diameter of anchors) has a significant effect on the breakout factor. Ovesen (1981), Dickin (1988), Sakai and Tanaka (1998), and Niroumand et al. (2013) have reported an influence of size effect on the breakout factor in sands based on their theoretical and experimental works. It has been reported that N_q value decreases by increasing the plate's diameter at a constant H/D value. This has been attributed to a decrease of the mobilized friction angle due to increase in confining

pressure (Khatri and Kumar 2011) and progressive failure and larger shear banding around the larger plate (Sakai and Tanaka 1998). On the other hand, Ilamparuthi et al. (2002) studied the uplift behavior of relatively large-scale model circular plates in loose, medium dense and dense dry sand. They used circular plate anchors with diameters equal to 100, 150, 200, 300, 400(mm). They concluded that for a given density of soil, break out factor depends only on H/D and is not affected by plates size (D Because of the size effect, the bigger plate provides smaller breakout factor at the same embedment ratio. One of the reasons of size effect is related to the variable friction angle. In the dense sands, friction angle decreases by increasing the mean effective stress, but it may not be the case for the loose sands. An experimental study to compare the size effect at loose and dense sands is suggested to clarify the size effect at sands with different properties.

The efficiency of SEPLA in deep waters (>1500 m), suggests the idea of using SEPLA in shallower waters. SEPLA could provide an efficient and an economic foundation system for the wave energy industry. The wave energy industry operates in shallow water (<100m) where sands, are more common. No numerical or analytical research has been done so far to study SEPLA in the sand. The feasibility of application of SEPLA in sands needs to be investigated experimentally and numerically. A 3D-large deformation numerical analysis is needed to investigate SEPLA's trajectory. Yang et al. (2012) used a generalized plastic limit analysis to estimate the trajectory and corresponding capacity of SEPLA in undrained clay. They assumed that the plastic potential surface is the same as the yield function because of the flow rule criteria, and there are no volume changes during the loading and failure. This method is not applicable to sand. Normality and associated flow rule are not applicable for cohesionless soils, and the plastic potential surface is not always the same as the yield function in sands. Also, the analysis in the sand is in a drained condition, and a volume change is expected. Soil will be detached from the beneath of anchor due to a large deformation before the failure in the sand. Therefore using a 3D numerical finite element analysis is needed. Plaxis 3D is not able to tolerate the intense distortion around the plate during the keying process. Using another 3D package like ABAQUS, which can model the large deformation analysis, is recommended.

The general shapes of failure mechanisms for different plate's shapes, embedment depths and soil densities are presented at this study. Translation of the failure shapes from the numerical modeling into limit equilibrium analyses equations is another suggestion for future work.